

TRANSMISSION LINE FAULT LOCATION USING INTEROPERABILITY AND  
INTEGRATION OF DATA AND MODEL

A Dissertation

by

PAPIYA DUTTA

Submitted to the Office of Graduate and Professional Studies of  
Texas A&M University  
in partial fulfillment of the requirements for the degree of

DOCTOR OF PHILOSOPHY

Chair of Committee,	Mladen Kezunovic
Committee Members,	Garng M. Huang
	Shankar P. Bhattacharyya
	Salih Yurttas
Head of Department,	Chanan Singh

May 2014

Major Subject: Electrical Engineering

Copyright 2014 Papiya Dutta

## ABSTRACT

This dissertation proposes selective scheme of transmission line fault location by choosing between two different types of fault location algorithms depending on the availability of measurements.

The first type is an accurate method to detect, classify and locate transmission line faults using synchronous samples of voltages and currents captured during fault transients from both ends of the transmission line of interest. The method is tested for several faults simulated on IEEE 118 bus test system and it has been concluded that it can detect and classify a fault using pre and post fault recorded samples within  $\frac{1}{2}$  of nominal frequency cycle of fault inception and locate fault with 3% accuracy. This time response performance is highly desirable since with the increasing use of modern circuit breakers which can open the faulty line in less than two cycles, the time window of the fault waveforms is significantly reduced due to the unavailability of measurement signals after breakers open.

The second type is a sparse measurement based fault location scheme using phasor measurements from different substations located in the vicinity where the fault has occurred and can be applied if the measurements are not available from any of the line ends. Fault resistance is one of the major sources of uncertainty in this type of transmission line fault location estimation. A correction scheme to reduce impact of fault resistance on sparse measurement method is proposed.

Both of the proposed schemes require power system model information, and in each case field captured measurements at different substations need to be integrated with

SCADA data recorded by remote terminal units to implement a system level transmission line fault location scheme. This requires a data processing solution which will correlate data and power system models expressed in different formats but having similar descriptions seamlessly, extract useful information from them automatically, and use such information in proposed fault location applications efficiently.

A third contribution of this dissertation work is development of a unified representation of data and model, which allows seamless information exchange between different power system models and between data and models, thereby achieving interoperability and integration. This approach allows easy implementation of future fault location schemes with the same data used for the proposed schemes, as well as an easy addition of data from new intelligent electronic devices that may be used for the same algorithms in the future.

## DEDICATION

To my baby Ujjayini Gupta.

## ACKNOWLEDGEMENTS

First of all, I would like to express my earnest gratitude to my graduate studies advisor, Dr. Mladen Kezunovic, for his guidance and support providing me direction and insight on numerous occasions during the course of this research. Without his guidance, inspiration, and support throughout the course of my research, this work would not be complete. I also would like to thank Dr. Huang, Dr. Bhattacharyya, and Dr. Yurttas for serving as my committee members.

I have been lucky for working at Power Systems Control and Protection Laboratory, Texas A&M University and being able to interact with all the brilliant people that work there. I would like to thank my colleagues Ms. Maja Knezev, Dr. Satish Natti, Dr. Chengzong Pang, Dr. Jinfeng Ren, Dr. Saeed Lotfifard, Ms. Chenyan Guo, Mr. Noah Badayos, Dr. Ce Zheng, Dr. Yimai Dong, Dr. Yufan Guan, Dr. Vuk Malbasa, Ms. Biljana Matic Cuka, Ms. Qin Yan, Ms. Bei Zhang, Mr. Po-Chen Chen, Mr. Ahad Esmaeilian, Mr. Ahmad Abdullah, Mr. Payman Dehghanian, Mr. Mohammad Tasdighi, Ms. Tatjana Dokic for their help and support throughout my graduate study. Thanks to the department faculty and staffs, in particular Ms. Tammy Carda and Ms. Nancy Reichart.

My research was mainly funded by financial resources from five projects. Three were funded by NSF I/UCRC Power System Engineering Research Center (PSERC): “Integration of Substation IED Information into EMS Functionality,” “PHEVs as Dynamically Configurable Dispersed Energy Storage,” “The Smart Grid Needs: Model and Data Interoperability, and Unified Generalized State Estimator”. Another one was

funded by U.S. Department of Energy (DOE): “Synchronized Sampling Uses for Real Time Monitoring and Control”. The fifth one was funded by ARPA-E to develop “Robust Adaptive Topology Control (RATC)” solution under GENI contract 0473-1510. I would like to acknowledge the financial supports from all the sponsors.

I want to thank my parents and brother and sister for their unconditional love and support from the very first day of my life. Finally, thanks to my husband Kashyap Gupta and little daughter Ujjayini for their love and encouragement.

Last, but certainly not least, I would like to thank my friends for their support over the years.

## NOMENCLATURE

ATP	Alternative Transients Program
CIM	Common Information Model
COMTRADE	Common Format for Transient Data Exchange
DFR	Digital Fault Recorder
DPR	Digital Protective Relay
EMS	Energy management system
FERC	Federal Energy Regulatory Commission
GPS	Global Positioning System
GWAC	GridWise® Architecture Council
IEC	International Electrotechnical Commission
IED	Intelligent Electronic Device
IEEE	Institute of Electrical and Electronics Engineers
ISO	Independent System Operator
NERC	North American Electric Reliability Corporation
NIST	National Institute of Standards and Technology
PDC	Phasor Data Concentrator
PMU	Phasor Measurement Unit
PSS/E	Power System Simulator for Engineering
PUC	Public Utility Commission
RTU	Remote Terminal Unit

SCADA	Supervisory Control and Data Acquisition System
SCL	Substation Configuration Language
SER	Sequence of Event Recorder
SGIP	Smart Grid Interoperability Panel
UML	Unified Modeling Language
XML	eXtensible Markup Language



## TABLE OF CONTENTS

	Page
ABSTRACT .....	ii
DEDICATION .....	iv
ACKNOWLEDGEMENTS .....	v
NOMENCLATURE .....	vii
TABLE OF CONTENTS .....	ix
LIST OF FIGURES .....	xi
LIST OF TABLES .....	xiv
1. INTRODUCTION .....	1
1.1. Background .....	1
1.2. Proposed research.....	6
1.3. Organization of the dissertation .....	8
1.4. Conclusions .....	9
2. FAULT LOCATION WITH FULL DATA: TWO END SYNCHRONIZED SAMPLING METHOD .....	10
2.1. Background .....	10
2.2. Fault detection and classification .....	12
2.3. Fault location.....	29
2.4. Implementation.....	33
2.5. Test results.....	35
2.6. Conclusions .....	40
3. FAULT LOCATION WITH LIMITED DATA: SPARSE MEASUREMENT METHOD .....	42
3.1. Background .....	42
3.2. Sparse measurement based fault location method.....	44
3.3. Fault resistance compensation correction scheme [48].....	47
3.4. Implementation.....	52
3.5. Case study .....	57
3.6. Conclusions .....	59

4.	INTEROPERABILITY AND INTEGRATION OF DATA AND MODEL FOR TRANSMISSION LINE FAULT LOCATION .....	60
4.1.	Background .....	60
4.2.	Power substation data.....	64
4.3.	Power system models.....	65
4.4.	Integration of data and model.....	65
4.5.	Standards used to describe data and model.....	67
4.6.	Conclusions.....	74
5.	UNIFIED REPRESENTATION OF DATA AND MODEL FOR TRANSMISSION LINE FAULT LOCATION .....	75
5.1.	Background .....	75
5.2.	Unified representation of data and model .....	78
5.3.	Illustration of unified representation.....	81
5.4.	Conclusions.....	92
6.	CONCLUSIONS .....	94
6.1.	Contributions.....	94
6.2.	Conclusions.....	95
	REFERENCES.....	98
	APPENDIX A .....	110
	APPENDIX B .....	112

## LIST OF FIGURES

	Page
Figure 1.1 Transmission line fault location scheme .....	8
Figure 2.1 Transmission line with two-end measurements .....	14
Figure 2.2 (a-c): $P_1(t)$ and $P_2(t)$ with respect to time for 'ag' fault; (d-f): $P_{sgn}(t)$ with respect to time for 'ag' fault .....	17
Figure 2.3 (a-c): $P_1(t)$ and $P_2(t)$ with respect to time for 'ab' fault; (d-f): $P_{sgn}(t)$ with respect to time for 'ab' fault .....	18
Figure 2.4 (a-c): $P_1(t)$ and $P_2(t)$ with respect to time for 'abg' fault; (d-f): $P_{sgn}(t)$ with respect to time for 'abg' fault .....	20
Figure 2.5 (a-c): Zero sequence current factors for 'ab' fault; (d-f): Zero sequence current factors for 'abg' fault .....	21
Figure 2.6 (a-c): $P_1(t)$ and $P_2(t)$ with respect to time for 'abc' fault; (d-f): $P_{sgn}(t)$ with respect to time for 'abc' fault .....	22
Figure 2.7 (a-c): $P_1(t)$ and $P_2(t)$ with respect to time for load level change; (d-f): $P_{sgn}(t)$ with respect to time for load level change .....	23
Figure 2.8 (a-c): $P_1(t)$ and $P_2(t)$ with respect to time for adjacent line; (d-f): $P_{sgn}(t)$ with respect to time for adjacent line .....	24
Figure 2.9 (a-c): $P_1(t)$ and $P_2(t)$ with respect to time for weak infeed case; (d-f): $P_{sgn}(t)$ with respect to time for weak infeed case .....	25
Figure 2.10 Parallel transmission line .....	26
Figure 2.11 (a-c): $P_{sgn}(t)$ with respect to time for 'ag' fault on line-1; (d-f): $P_{sgn}(t)$ with respect to time for 'ag' fault on line-2 .....	26
Figure 2.12 Transmission line with 3 end measurements .....	27
Figure 2.13 (a-c): $P_1(t)$ and $P_2(t)$ with respect to time for 'abg' fault on line-3-4; (d-f): $P_{sgn}(t)$ with respect to time for 'abg' fault on line-3-4 .....	28
Figure 2.14 Transmission line segment of length $\Delta x$ .....	29

Figure 2.15 Set of ordinary differential equations in $(x, t)$ plane.....	31
Figure 2.16 Flowchart of the proposed fault detection, classification and location scheme.....	34
Figure 3.1 Faulted circuit model. ....	44
Figure 3.2 Flowchart of sparse measurement algorithm. ....	47
Figure 3.3 Flowchart of corrected sparse measurement algorithm. ....	48
Figure 3.4 Solution architecture. ....	53
Figure 3.5 Faulty network. ....	58
Figure 3.6 $R_F$ vs. $x$ plot. ....	58
Figure 4.1 GWAC Interoperability Stack.....	61
Figure 4.2 GWAC Stack with data and information flow (part of the picture adopted from [56]).....	63
Figure 4.3 Functional diagram for substation data flow.....	66
Figure 4.4 GWAC Stack with related standards. ....	70
Figure 5.1 Data and information flow for fault disturbance monitoring.....	77
Figure 5.2 Unified representation of data and model. ....	79
Figure 5.3 Node-breaker representation of small power network [83]. ....	81
Figure 5.4 Bus-branch representation of small power network. ....	82
Figure 5.5 Node breaker representation of Substation-1.....	83
Figure 5.6 Node-breaker representation with terminals and connectivity nodes .....	86
Figure 5.7 Bus-branch representation with topological nodes .....	86
Figure 5.8 Substation object in CIM .....	88
Figure 5.9 Substation object in SCL.....	88
Figure 5.10 ThermalGeneratingUnit object in CIM.....	89

Figure 5.11 PowerTransformer object in CIM .....	90
Figure 5.12 PowerTransformer object in SCL .....	90
Figure 5.13 Part of SCL corresponding to triggered IED .....	92

## LIST OF TABLES

	Page
Table 2.1 Lines considered for fault scenarios: IEEE 118 bus test system .....	35
Table 2.2 Summary of fault detection & classification with varying fault distance and fault resistance (IEEE 118 system: Case 1) .....	36
Table 2.3 Summary of fault detection & classification for high fault resistance (IEEE 118 system: Case 1) .....	38
Table 2.4 Summary of fault detection and classification with varying fault inception angle (IEEE 118 bus test system: Case 1) .....	39
Table 3.1 Sensitivity to $R_F$ for different $R_F$ ranges .....	59
Table 4.1 Standards to describe data and model interpretation and exchange .....	68
Table 4.2 Packages of common information model .....	71
Table 4.3 Contents of substation configuration language .....	73

# 1. INTRODUCTION

## **1.1. Background**

### *1.1.1. Transmission line fault location*

Transmission lines are generally exposed to several types of faults which are usually caused by random and unpredictable events such as lightning, short circuits, overloading, equipment failure, aging, animal/tree contact with the line, human intended or unintended actions, lack of maintenance etc. Protective relays, placed at both ends of a transmission line sense the fault immediately and isolate the faulted line by opening the associated circuit breakers. Faults may be temporary (fault is cleared after breaker re-closing) or permanent (fault is not cleared even after several re-closing attempts). To restore service after permanent fault, an accurate location of the fault is highly desirable to help the maintenance crew find and repair the faulted line section as soon as possible.

Though distance relays typically already have algorithms for fault location embedded in their design, and can determine the location in the fast and reliable ways, they cannot meet the need of accurate fault location under all circumstances. They may over-reach or under-reach due to several unknown parameters, such as pre-fault loading, fault resistance, remote infeed etc.

### *1.1.2. Survey of transmission line fault location methods*

Transmission line faults may be calculated either using power frequency components of voltage and current or higher frequency transients generated by the fault [1]-[3]. Phasor based methods use fundamental frequency component of the signal and

lumped parameter model of the line while time-domain based methods use transient components of the signal and distributed parameter model of the line. Both of these methods can be subdivided into another two broad classes within each category: a) one-end methods [4]-[9] where data from only one terminal of the transmission line is available and b) two-end methods [10]-[19] where data from both (or multiple) ends of the transmission line can be used. Two ended methods can use synchronized or unsynchronized phasor measurements, as well as synchronized or unsynchronized samples.

Travelling wave based fault location approaches [20]-[22] use transient signals generated by the fault. They are based on the correlation between the forward and backward travelling waves along a line or direct detection of the arrival time of the waves at terminals.

Impedance based methods, either phasor or time domain based, generally estimate the distance to fault as a function of total line impedance (considering transmission line as being homogeneous) using voltage and current measurements from single or multiple ends.

One ended, impedance-based fault location methods are simple, fast and require only local measurement data. The simplest approach is a reactance-based method which measures the apparent impedance ignoring fault resistance and effect of load current. In this method the apparent impedance of the line is measured. This method works well for homogeneous systems subject to faults not involving significant fault resistance and load current. Large errors are introduced by remote-end current feed, load impedance, power transmission angle, and angle difference between line and source impedances. Algorithms reported in [4]-[7] extend simple reactance method by making assumptions to eliminate



effect of remote in feed and fault resistance. Algorithms reported in [8]-[9] estimate fault location for parallel transmission lines using data from one end.

Two-end methods work on equalizing voltage of fault point from both ends of the line and fundamentally are more accurate than one end methods [10]. The calculations may be based on unsynchronized measurements from two ends [10]-[16]. References [11]-[13] use phasors and lumped parameter line model to compute location of fault. Reference [14] uses distributed parameter model of the line implementing the same approach as described in [11]. While all two end methods are essentially accurate they need extra communication for data synchronization. This can be overcome by fully utilizing the advantages of modern digital technologies and signal processing to estimate the synchronizing difference between both ends using nonlinear mathematical optimization [15]-[16]. Synchronized measurements were utilized in [17]-[19] making them more accurate and can be employed with current data capturing capability of IEDs.

Each of the techniques requires very specific measurements from one or both (multiple) ends of the line to produce results with desired accuracy. However, availability of data may be a challenging issue. Digital fault recorders (DFRs) and other IEDs are generally placed in critical substations and therefore in some cases it is not possible to get recorded measurements from both or any end of the faulty line if this source of data is used. Although protective relays exist on every transmission line, some of them may still be electromechanical and they do not have capability to record measurements. Sometimes, not all the DFRs installed may be triggered by a fault. Therefore neither two- nor one-end

methods can always be applied. In such cases some unconventional techniques based on wide area measurements may have to be used [23]-[24].

On the other hand, performance of transmission line fault location algorithms depends on several factors [2] and thus analysis of sensitivity of fault location output with those factors is very crucial to estimate the accuracy of the output.

### *1.1.3. Need for interoperability and integration of data and model used in fault location implementation*

Traditionally, in a substation, remote terminal units (RTUs) acquire analog and digital measurements (bus voltages, branch flows, frequency, breaker status, transformer tap position etc), collectively called supervisory control and data acquisition SCADA measurements, which are sent to the energy management systems (EMS) in every two to ten seconds. With the rapid advancement of technology, other intelligent electronic devices (IEDs) besides RTUs are now widely used in substations. These computer-based devices can record and store a huge amount of data (both operational and non-operational) with a periodicity depending upon the intended purpose of the device. For example, digital fault recorders (DFRs) only capture data during occurrence of a fault whereas phasor measurement units (PMUs) take continuous time-synchronized data with high sampling rates. Such devices are typically characterized with sampling rates much higher than what is found in RTUs and with much higher accuracy. Thus a great amount of data is recorded, which if used properly can become a great benefit for the EMS operators when trying to predict, monitor and post-mortem analyze power system events.

Digital fault recorders (DFRs), generally placed in critical substations will be automatically triggered due to occurrence of an event like fault and will record corresponding current, voltage and status signals. These recorded quantities can be used along with the data collected by SCADA to predict the location of transmission line fault more accurately. But as these IEDs are not placed in ends of every line, in some cases it is not possible to get recorded measurements from both or any end of the faulty line if this source of data is used. Although protective relays exist on every transmission line, some of them may still be electromechanical and they do not have capability to record measurements. Sometimes, not all the DFRs installed may be triggered by a fault. Therefore neither two- nor one-end methods can always be applied. In such cases some unconventional techniques based on wide area measurements may have to be used [23]-[24].

Transmission line fault location requires both power system model information and field data captured at different substations. With rapid deployment of IEDs in most of the substations, the number of data capture points significantly increased which may result in increased information and analytical capabilities if properly used. Presence of different types of models (detailed node-breaker representation vs. less detailed bus-branch representation), different types of data captured (continuous data scans vs. data captured triggered by an event) by different devices of different vendors hinder interoperability and integration of field data with power system model information. Therefore a solution to achieve interoperability of data and model is also required.

## 1.2. Proposed research

Considering all the factors stated, transmission line fault location scheme should have the following characteristics:

- Appropriately choose suitable algorithm depending on the availability of data
- Reduce sensitivity to different factors affecting estimation of distance to fault
- Properly use all available data and model through interoperability and integration

A transmission line fault location scheme is required to deal with the above mentioned characteristics. It should be capable of enhancing fault location estimation accuracy by selecting proper fault location algorithm depending on the availability and location of recorded data as well as network topology and circumstances surrounding faults. It should also be improving the selected algorithm by minimizing sensitivity to several factors. A unified representation of data and model to reduce number of mappings between them and correlate different types of data and model without any user intervention is needed for successful implementation of the scheme.

Therefore the proposed solution needs to first integrate all relevant types of data and model seamlessly and then choose proper algorithm depending on the availability of data (data from two ends will lead to synchronized sampling based fault location while data from one will lead to reduced-accuracy algorithm, and no data from any end will lead to sparse measurement based fault location). A spline interpolation technique may be introduced to improve performance of synchronized sampling based fault location under low sampling frequency and a fault resistance sensitivity correction scheme will be studied to deal with unknown fault resistance in sparse measurement based fault location method.

The objective proposed are:

- Develop a methodology for fault location under limited available data
- Develop a methodology for fault location under fully available data
- Develop a unified representation of data and model for transmission line fault location implementation featuring
  - Integration of synchronous and asynchronous measurements
  - Handling node/breaker and bus/branch models seamlessly

A smart scheme to locate transmission line faults is proposed which is capable of using different fault location algorithms depending on the availability and location of recorded data as well as network topology and circumstances surrounding faults.

The transmission line fault location scheme is shown in the following flowchart (Figure 1.1). The method first accumulates power system model and data information, integrates them and prepares a unified representation of data and model as addressed in section 5 thereby achieving interoperability and integration of huge amount of recorded data by IEDs and SCADA and power system models. Now the method selects an appropriate algorithm depending (described in section 2 and section 3) on availability of measurements.

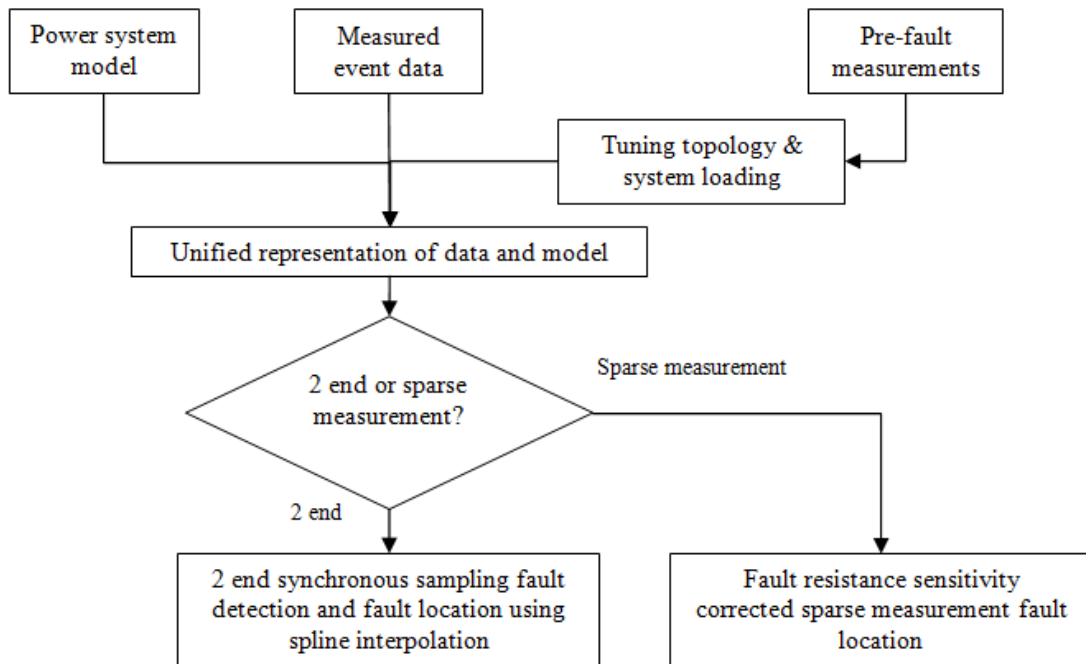


Figure 1.1 Transmission line fault location scheme.

### 1.3. Organization of the dissertation

This dissertation is organized as follows. Section 2 describes transmission line fault detection, classification and location method using synchronous samples of voltage and currents measured at both ends of the line. Under limited availability of measurements a sparse measurement based fault location method which is least sensitive to fault resistance impact is proposed in section 3. Section 4 discusses the need for interoperability and integration of data and model. A unified representation of data and model is proposed in section 5. Section 6 concludes the dissertation.

#### **1.4. Conclusions**

Accurate estimation of transmission line fault location under availability and origin of recorded data and prevailing system conditions is required. An intuitive approach is proposed which can choose between two different algorithms depending on availability of data: (1) two end synchronous sampling based fault location and (2) sparse measurement based fault location with resistance sensitivity correction. Implementation of these methods requires interoperable solution of integrated recorded data and power system model information. To achieve this a unified representation of data and model is proposed.

## 2. FAULT LOCATION WITH FULL DATA: TWO END SYNCHRONIZED SAMPLING METHOD

### 2.1. Background

Nowadays transmission lines are expected to operate close to their power transfer limits, which may increase the number of cascading outages when faults occur during high loading. Quick fault analysis to facilitate timely restoration of service is a desirable self-healing feature. A fault analysis tool should be able to detect, classify and locate fault event by automatically interpreting recorded transients captured during relay trip operation.

Several fault analysis methods either as a complete tool or as separate fault detection, classification and location functions are described in literature.

Early fault detection and classification techniques were based on changes on voltages, currents and impedances with respect to some preset values to identify fault types [25]-[26]. In the last two decades, different Artificial Neural Network (ANN) and Fuzzy based methods were introduced for fault detection and classification [27]-[29]. In general, irrespective of wide range of operating conditions (varying system loading, fault resistance, fault inception instance, etc.), ANN based methods have been successful in detecting and classifying the faults, but they need a huge amount of training cases to achieve a good performance. A combination of fuzzy set and wavelet transform method based on line current [30], while it uses simple fuzzy rules even in case of complex networks, it can't classify all types of faults. In [31], a setting-free two-end method compares the direction of power measured at two ends and detects and classifies fault



using established rules. Though the method is a setting-free one, calculating the average value of power will cause delay in operation of the method, which can be considered as a major drawback if relay operation has to be corrected immediately.

Transmission line fault location methods either use power frequency components of voltage and current or higher frequency transients generated by the fault [1]-[2]. All these methods can be subdivided depending upon the availability of recorded data: one-end methods [5]-[9] where data from only one terminal of the transmission line is available and two-end methods [14]-[18] where data from both (or multiple) ends of the transmission line can be used. Two ended methods can use synchronized or unsynchronized phasor measurements or samples. These methods are suitable for off-line analysis but require better computational performance to be used for on-line analysis.

A typical fault analysis tool [32]-[35] performs fault detection, classification and location as a total package. In [32], fault detection and classification requires some pre-set thresholds and fault location is based on less accurate lumped parameter model. In [33], a method that implements a fault detection and classification based on Fuzzy ART neural network needs significant training beforehand. Fault location approach introduced in [33] is very accurate but requires high sampling rate for input data. Methods introduced in [34]-[35] are based on data captured using phasor measurement unit (PMU) and therefore still depend on phasor calculation, which can cause delay in obtaining results.

An accurate fault analysis tool based on two end synchronous samples is required which is transparent to different types of transmission line configurations, does not require any threshold to detect fault, use a very short span of post fault measurements.

An automated fault analysis tool that overcomes time response and accuracy shortcomings of the previous methods is proposed in this section. It utilizes synchronized samples captured during transients from both ends of the transmission line to detect, classify and locate transmission line faults and hence verify whether the line was healthy or faulty at the time of relay operation. The proposed method is tested for several faults simulated on IEEE 118 bus test system and it has been concluded that it can detect and classify a fault using pre and post fault recorded samples within  $\frac{1}{2}$  of nominal frequency cycle of fault inception and accurately locate fault with 3% accuracy. This time response performance is highly desirable since with the increasing use of modern circuit breakers which can open the faulty line in less than two cycles, the time window of the waveforms is significantly reduced due to the unavailability of measurement signals after breakers open.

## **2.2. Fault detection and classification**

To detect and classify a fault the proposed method compares the change of direction of instantaneous powers on all three phases computed at two ends of a transmission line using synchronized voltage and current samples measured at both ends. The method has a significant advantage over the method proposed in [31] as computing instantaneous power does not need any averaging and therefore the samples captured can be used directly.

In Figure 2.1,  $V_1(t), I_1(t)$  represents voltage and current measured at one end (Bus 1) of the line at instant  $t$ . Similarly  $V_2(t), I_2(t)$  represents voltage and current measured at

other end (Bus 2) of the line at same instant  $t$ . Currents are measured in the assumed direction shown in Figure 2.1. All voltage and currents are single phase quantities.

Voltage and currents at bus 1 are shown in ( 2.1 ) and ( 2.2 ),

$$V_1(t) = V_{1m} \cos \omega t \quad ( 2.1 )$$

$$I_1(t) = I_{1m} \cos(\omega t - \theta_1) \quad ( 2.2 )$$

where

$V_{1m}$  : Maximum value of voltage

$I_{1m}$  : Maximum value of voltage

$\omega$  : Angular frequency

$\theta_1$  : Phase angle between  $V_1(t)$  and  $I_1(t)$

Instantaneous power at bus 1 ( 2.3 ),

$$\begin{aligned} P_1(t) &= V_1(t) \times I_1(t) \\ &= V_{1m} I_{1m} \cos \omega t \cos(\omega t - \theta_1) \\ &= \frac{V_{1m} I_{1m}}{2} [\cos(2\omega t - \theta_1) + \cos \theta_1] \\ &= \frac{V_{1m} I_{1m}}{2} [\cos 2\omega t \cos \theta_1 + \sin 2\omega t \sin \theta_1 + \cos \theta_1] \\ &= P_{1m} (\cos 2\omega t + 1) \cos \theta_1 + P_{1m} \sin 2\omega t \sin \theta_1 \end{aligned} \quad ( 2.3 )$$

Voltage and currents at bus 2 are shown in ( 2.4 ) and ( 2.5 ),

$$V_2(t) = V_{2m} \cos(\omega t - \delta) \quad ( 2.4 )$$

$$I_2(t) = I_{2m} \cos(\omega t - \delta - \theta_2) \quad ( 2.5 )$$

where

$V_{2m}$  : Maximum value of voltage

$I_{2m}$  : Maximum value of voltage

$\theta_2$  : Phase angle between  $V_2(t)$  and  $I_2(t)$

$\delta$  : Phase angle difference between bus 1 and bus 2

Instantaneous power at bus 2 ( 2.6 ),

$$\begin{aligned} P_2(t) &= V_2(t) \times I_2(t) \\ &= V_{2m} I_{2m} \cos(\omega t - \delta) \cos(\omega t - \delta - \theta_2) \\ &= P_{2m} (\cos 2(\omega t - \delta) + 1) \cos \theta_2 + P_{2m} \sin 2(\omega t - \delta) \sin \theta_2 \end{aligned} \quad (2.6)$$

Now with the assumed direction of currents, magnitude of  $I_2(t)$  is negative before fault and positive after fault.

For unfaulted situation instantaneous powers are shown in ( 2.7 ) and ( 2.8 ):

$$P_1^u(t) = P_{1m}^u (\cos 2\omega t + 1) \cos \theta_1^u + P_{1m}^u \sin 2\omega t \sin \theta_1^u \quad (2.7)$$

$$P_2^u(t) = -P_{2m}^u (\cos 2(\omega t - \delta) + 1) \cos \theta_2^u - P_{2m}^u \sin 2(\omega t - \delta) \sin \theta_2^u \quad (2.8)$$

After fault, instantaneous powers are shown in ( 2.9 ) and ( 2.10 ):

$$P_1^f(t) = P_{1m}^f (\cos 2\omega t + 1) \cos \theta_1^f + P_{1m}^f \sin 2\omega t \sin \theta_1^f \quad (2.9)$$

$$P_2^f(t) = P_{2m}^f (\cos 2(\omega t - \delta) + 1) \cos \theta_2^f + P_{2m}^f \sin 2(\omega t - \delta) \sin \theta_2^f \quad (2.10)$$

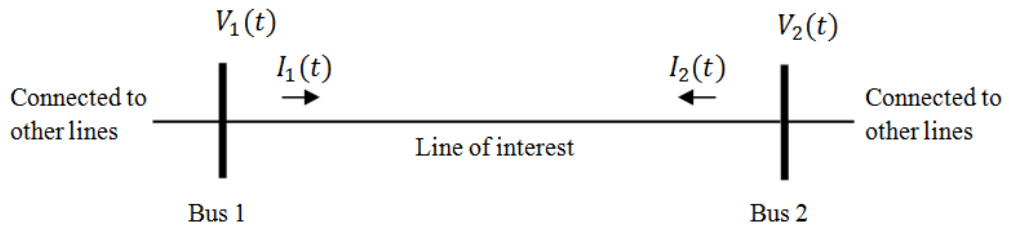


Figure 2.1 Transmission line with two-end measurements.

If both before fault and after fault power factor angles are lagging i.e.  $\theta_1^u > 0, \theta_2^u > 0; \theta_1^f > 0, \theta_2^f > 0$ , then the following inequalities should be satisfied:

( 2.11 ) shows the before fault condition:

$$|P_1^u(t)| > 0, |P_2^u(t)| < 0 \quad (2.11)$$

( 2.12 ) shows the after fault condition:

$$|P_1^f(t)| > 0, |P_2^f(t)| > 0 \quad (2.12)$$

If before fault power factor angles are leading and after fault power factor angles are lagging i.e.  $\theta_1^u < 0, \theta_2^u < 0; \theta_1^f > 0, \theta_2^f > 0$ , then the following inequalities should be satisfied:

( 2.13 ) shows the before fault condition:

$$|P_1^u(t)| > 0 \text{ if } (\cos 2\omega t + 1)\cos \theta_1^u > \sin 2\omega t \sin \theta_1^u \quad (2.13)$$

$$|P_2^u(t)| < 0 \text{ if } (\cos 2(\omega t - \delta) + 1)\cos \theta_2^u > \sin 2(\omega t - \delta)\sin \theta_2^u$$

( 2.14 ) shows the after fault condition:

$$|P_1^f(t)| > 0, |P_2^f(t)| > 0 \quad (2.14)$$

This can be shown in all combinations of lagging and leading power factor angles before and after fault,  $|P_1^u(t)| > 0, |P_2^u(t)| < 0$  and  $|P_1^f(t)| > 0, |P_2^f(t)| > 0$  if one or some of the inequalities ( 2.15 )-( 2.18 ) are true.

$$(\cos 2\omega t + 1)\cos \theta_1^u > \sin 2\omega t \sin \theta_1^u \quad (2.15)$$

$$(\cos 2(\omega t - \delta) + 1)\cos \theta_2^u > \sin 2(\omega t - \delta)\sin \theta_2^u \quad (2.16)$$

$$(\cos 2\omega t + 1)\cos \theta_1^f > \sin 2\omega t \sin \theta_1^f \quad (2.17)$$

$$(\cos 2(\omega t - \delta) + 1)\cos \theta_2^f > \sin 2(\omega t - \delta)\sin \theta_2^f \quad (2.18)$$

Under small values of power factor angles, all of the inequalities ( 2.15 )-( 2.18 ) are satisfied. In general in transmission systems, before fault power factor angles are very small and after fault they are lagging, which is sufficient to conclude  $|P_1''(t)| > 0, |P_2''(t)| < 0$  and  $|P_1^f(t)| > 0, |P_2^f(t)| > 0$ .

Therefore, this is a unique feature of instantaneous power under different types of faults which helps detect and classify faults without using any threshold. This feature is observed only on the faulted phases.

In the following sections how this concept can be used to detect and classify different types of faults will be shown.

### 2.2.1. Single phase to ground fault

In case of single phase to ground fault ('ag'), plot of  $P_1(t)$  and  $P_2(t)$  with respect to time is shown in Figure 2.2(a-c). Right after the fault inception (0.02 sec),  $|P_{1a}^f(t)| > 0, |P_{2a}^f(t)| > 0$  in phase 'a' while for the other two phases  $|P_{1b}^f(t)| > 0, |P_{2b}^f(t)| < 0; |P_{1c}^f(t)| > 0, |P_{2c}^f(t)| < 0$ .

To represent this feature mathematically, signum function is used, which is defined as ( 2.19 ):

$$\text{sgn}(x) = \begin{cases} -1, & x < 0 \\ 0, & x = 0 \\ 1, & x > 0 \end{cases} \quad (2.19)$$

$\text{sgn}(P_1(t))$  and  $\text{sgn}(P_2(t))$  are calculated for each phase and the difference  $P\text{sgn}(t) = \text{sgn}(P_1(t)) - \text{sgn}(P_2(t))$  for each phase are plotted in Figure 2.2(d-f).

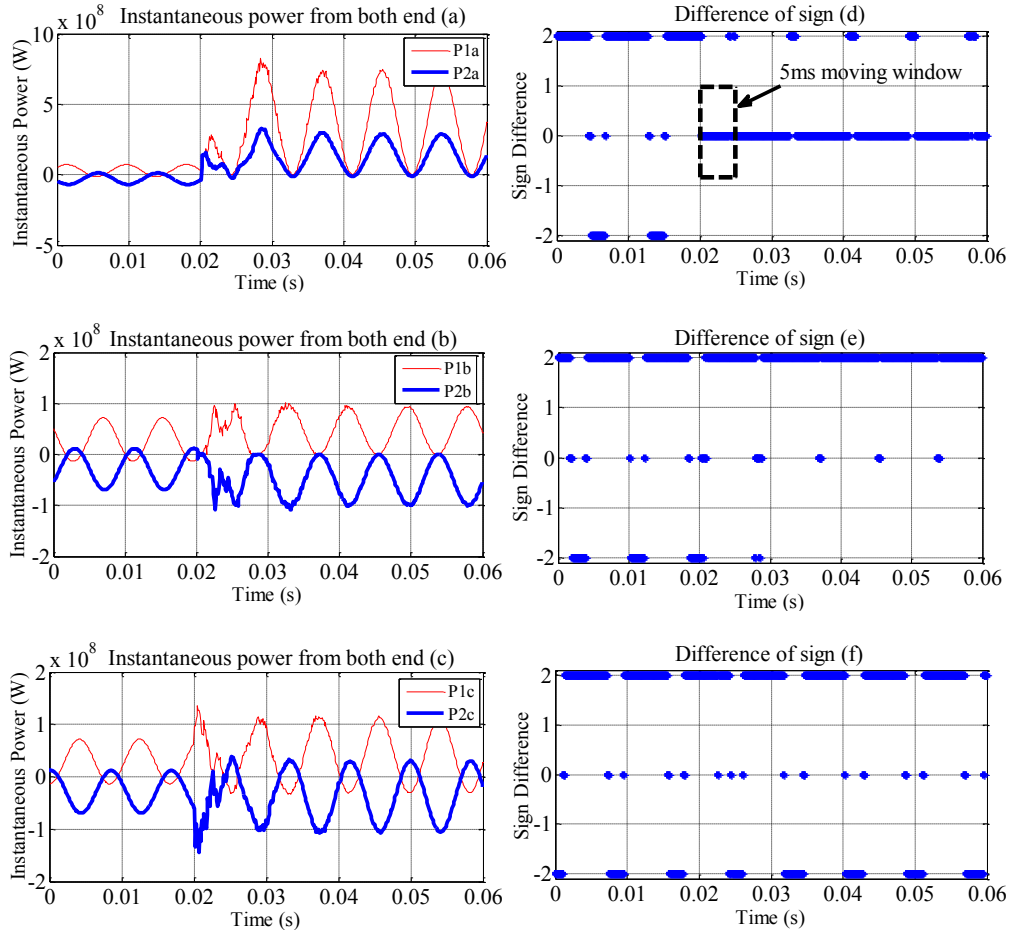


Figure 2.2 (a-c):  $P_1(t)$  and  $P_2(t)$  with respect to time for 'ag' fault; (d-f):  $P_{sgn}(t)$  with respect to time for 'ag' fault.

Theoretically, before fault this difference  $P_{sgn}(t)$  should be  $\pm 2$  and after fault  $P_{sgn}(t)$  should be 0, but due to transients and noise present in the measurements, some outliers are present. It is clear from Figure 2.2(d-f) that on phase 'a'  $P_{sgn}(t)$  becomes almost zero after fault while the other phases remain unchanged. The instant this change occurred is the fault instant. A moving window (5 ms used in this example) is used to

check whether at least 90% (due to presence of outliers) of  $P_{sgn}(t)$  are zero, which indicates the instant faulted phase (phase 'a' here) experienced a fault.

### 2.2.2. Phase faults

#### Phase-to-phase fault

In case of phase-to-phase fault ('ab'), plot of  $P_1(t)$  and  $P_2(t)$  with respect to time is shown in Figure 2.3(a-c).

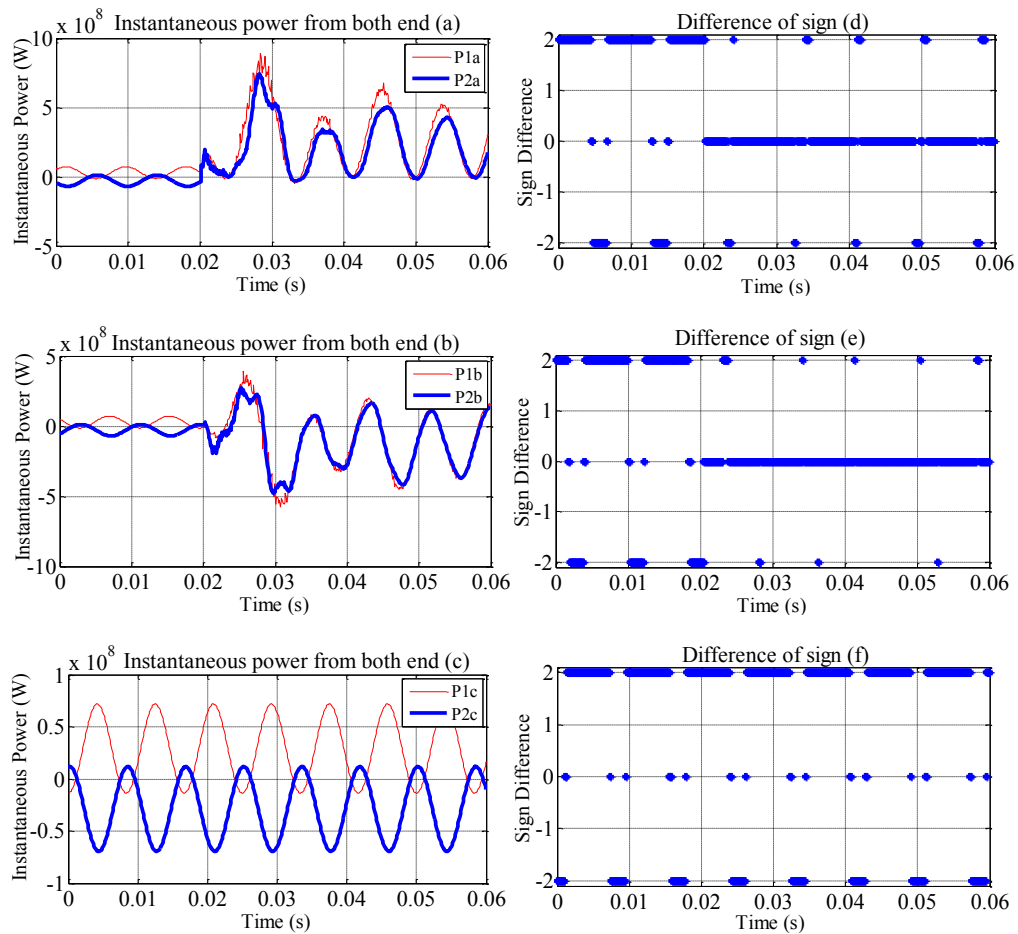


Figure 2.3 (a-c):  $P_1(t)$  and  $P_2(t)$  with respect to time for 'ab' fault; (d-f):  $P_{sgn}(t)$  with respect to time for 'ab' fault.



Right after the fault inception (0.02 sec),  $|P_{1a}^f(t)| > 0, |P_{2a}^f(t)| > 0$  in phase 'a' and  $|P_{1b}^f(t)| > 0, |P_{2b}^f(t)| > 0$  in phase 'b' while  $|P_{1c}^f(t)| > 0, |P_{2c}^f(t)| < 0$  in phase "c". Plot of difference of  $\text{sgn}()$ ,  $P\text{sgn}(t)$  with respect to time is shown in Figure 2.3(d-f). It is clear that after fault,  $P\text{sgn}(t)$  is almost zero for both phases 'a' and 'b'.

Therefore we can use the same logic used for single phase to ground fault to detect fault in phase-to-phase faults.

### ***Phase-to-phase-to-ground fault***

In case of phase-to-phase-to-ground fault ('abg'), plot of  $P_1(t)$  and  $P_2(t)$  with respect to time is shown in Figure 2.4(a-c). Plot of  $P\text{sgn}(t)$  with respect to time is shown in Figure 2.4(d-f). Both of the plots show exactly the similar behavior as of phase-to-phase fault ('ab').

As in phase-to-phase-to-ground fault, significant amount of zero sequence current will be present, it can be used as a classification feature between phase-to-phase and phase-to-phase-to-ground faults.

We define zero sequence current factors for each phase as ( 2.20 )-( 2.22 ):

$$F_a = \frac{3I_0(t)}{I_a(t)} \quad ( 2.20 )$$

$$F_b = \frac{3I_0(t)}{I_b(t)} \quad ( 2.21 )$$

$$F_c = \frac{3I_0(t)}{I_c(t)} \quad ( 2.22 )$$

Where  $3I_0(t) = I_a(t) + I_b(t) + I_c(t)$

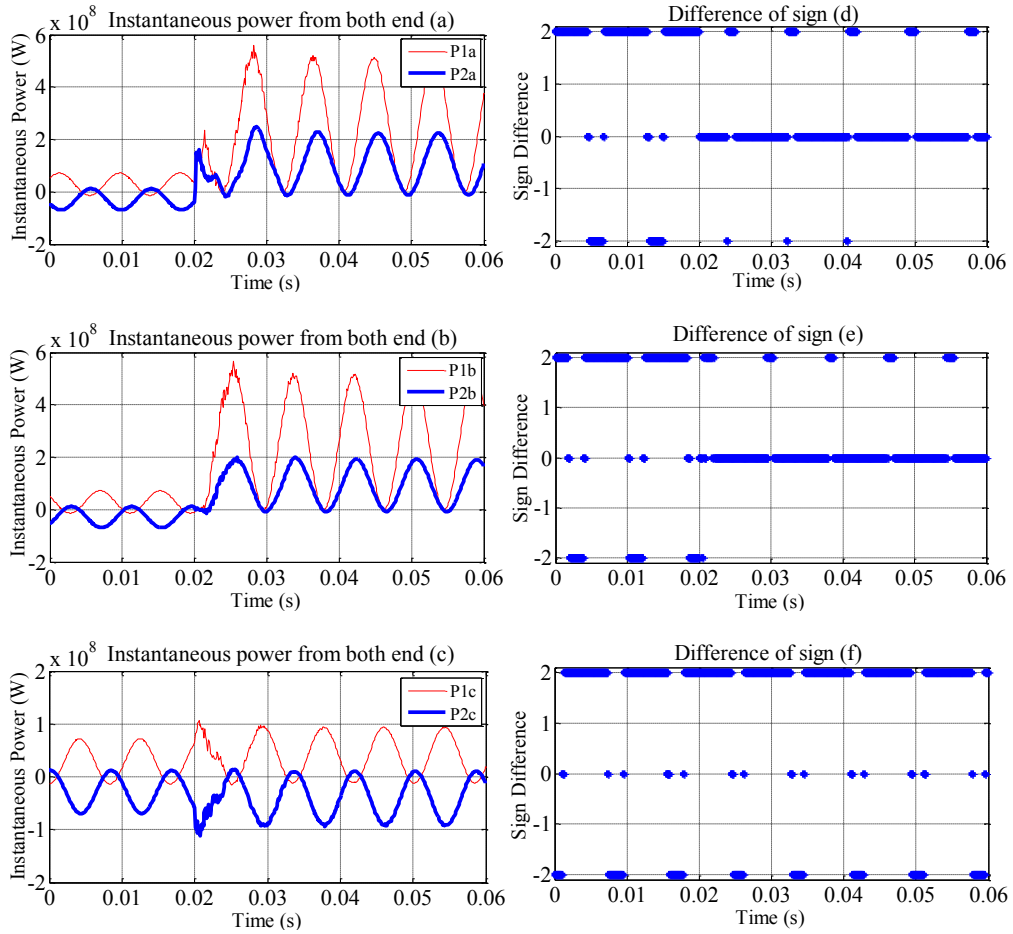


Figure 2.4 (a-c):  $P_1(t)$  and  $P_2(t)$  with respect to time for 'abg' fault; (d-f):  $P_{sgn}(t)$  with respect to time for 'abg' fault.

Figure 2.5(a-c) shows the plot of zero sequence current factors for each phase for 'ab' fault. Figure 2.5(d-f) shows the same for 'abg' fault. It is clear that values of those factors are much higher in case of 'abg' fault. For mathematical implementation we have rounded those factors and they are always zero for 'ab' fault and greater than zero for 'abg' fault. Therefore by investigating these factors, classification between 'ab' and 'abg' fault is possible.

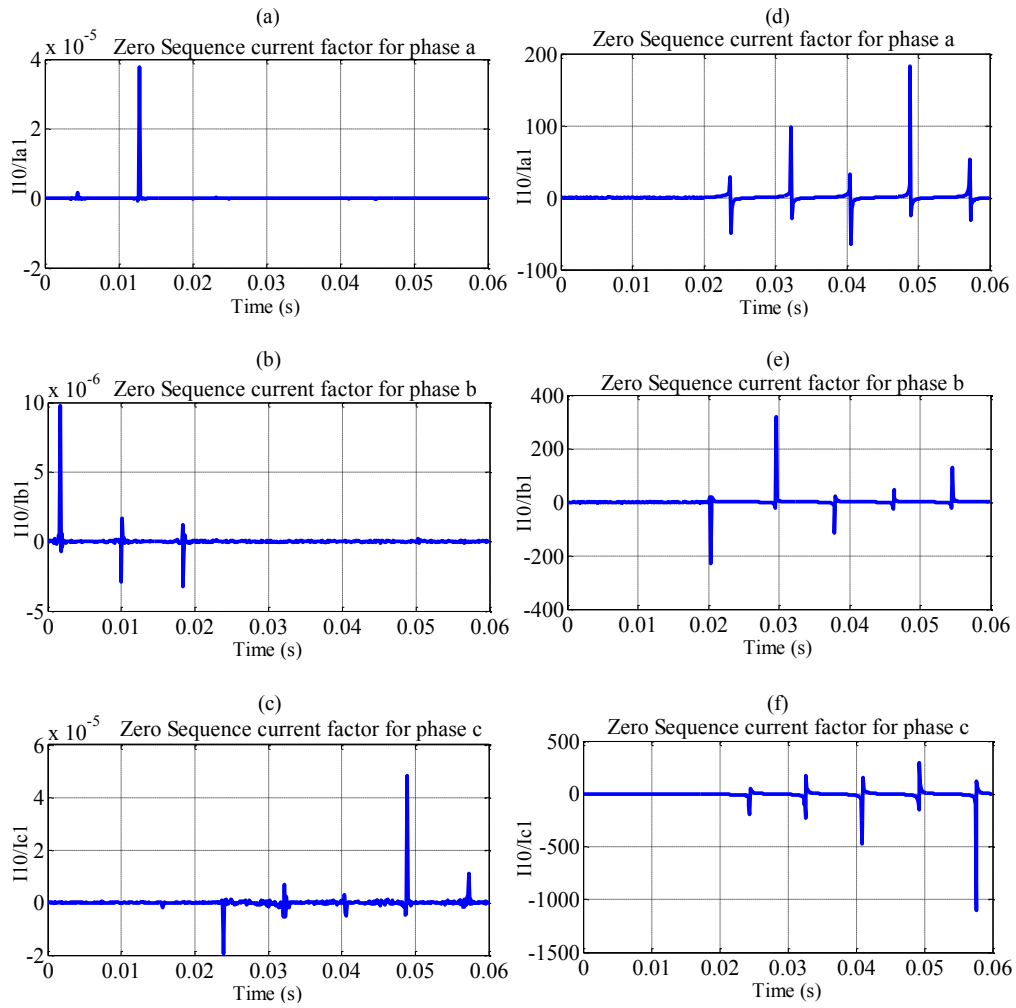


Figure 2.5 (a-c): Zero sequence current factors for 'ab' fault; (d-f): Zero sequence current factors for 'abg' fault.

### 2.2.3. Three phase faults

In case of three phase fault ('abc'), plot of  $P_1(t)$  and  $P_2(t)$  with respect to time is shown in Figure 2.6(a-c). Plot of  $P_{sgn}(t)$  with respect to time is shown in Figure 2.6(d-f).

It is clear that all three phases are faulted as  $|P_{1a}^f(t)| > 0, |P_{2a}^f(t)| > 0, |P_{1b}^f(t)| > 0, |P_{2b}^f(t)| > 0$  and  $|P_{1c}^f(t)| > 0, |P_{2c}^f(t)| > 0$ .

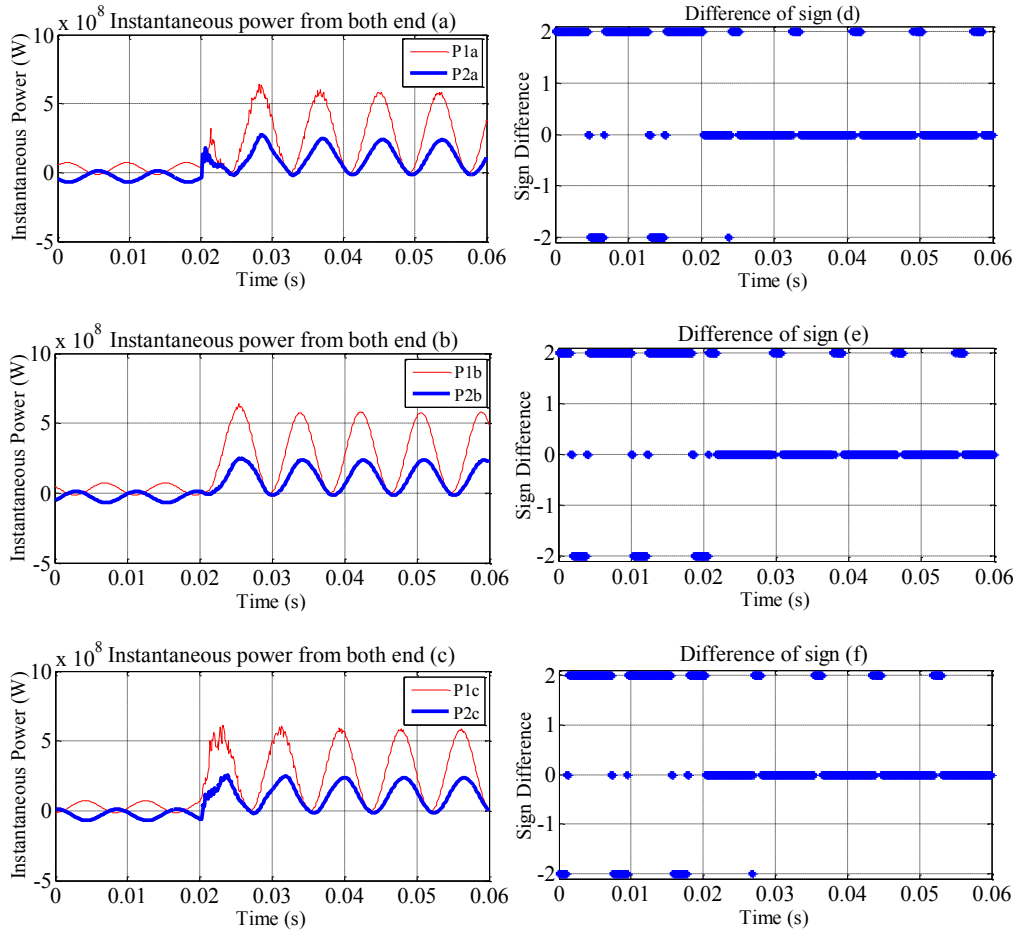


Figure 2.6 (a-c):  $P_1(t)$  and  $P_2(t)$  with respect to time for 'abc' fault; (d-f):  $P_{sgn}(t)$  with respect to time for 'abc' fault.

#### 2.2.4. Load level change

Sometimes relay trips following overload conditions due to sudden change in load. In that case, fault detection method should not detect this change as a fault and warning about relay mis-operation should be issued. In case of load level change (one change of 100% at 0.025 sec and another change of 50% over already increased load at 0.04 sec), plot of  $P_1(t)$  and  $P_2(t)$  with respect to time is shown in Figure 2.7(a-c). Plot of  $P_{sgn}(t)$

with respect to time is shown in Figure 2.7(d-f). From Figure 2.7 it is clear that the line is not faulted.

### 2.2.5. Faults on adjacent line

To verify that the method is not influenced by faults on adjacent line, an 'ag' fault is applied on an adjacent line and plot of  $P_1(t)$  and  $P_2(t)$  with respect to time is shown in Figure 2.8(a-c). Plot of  $P_{sgn}(t)$  with respect to time is shown in Figure 2.8(d-f). From Figure 2.8 it is clear that the line of interest is not influenced by faults on adjacent line.

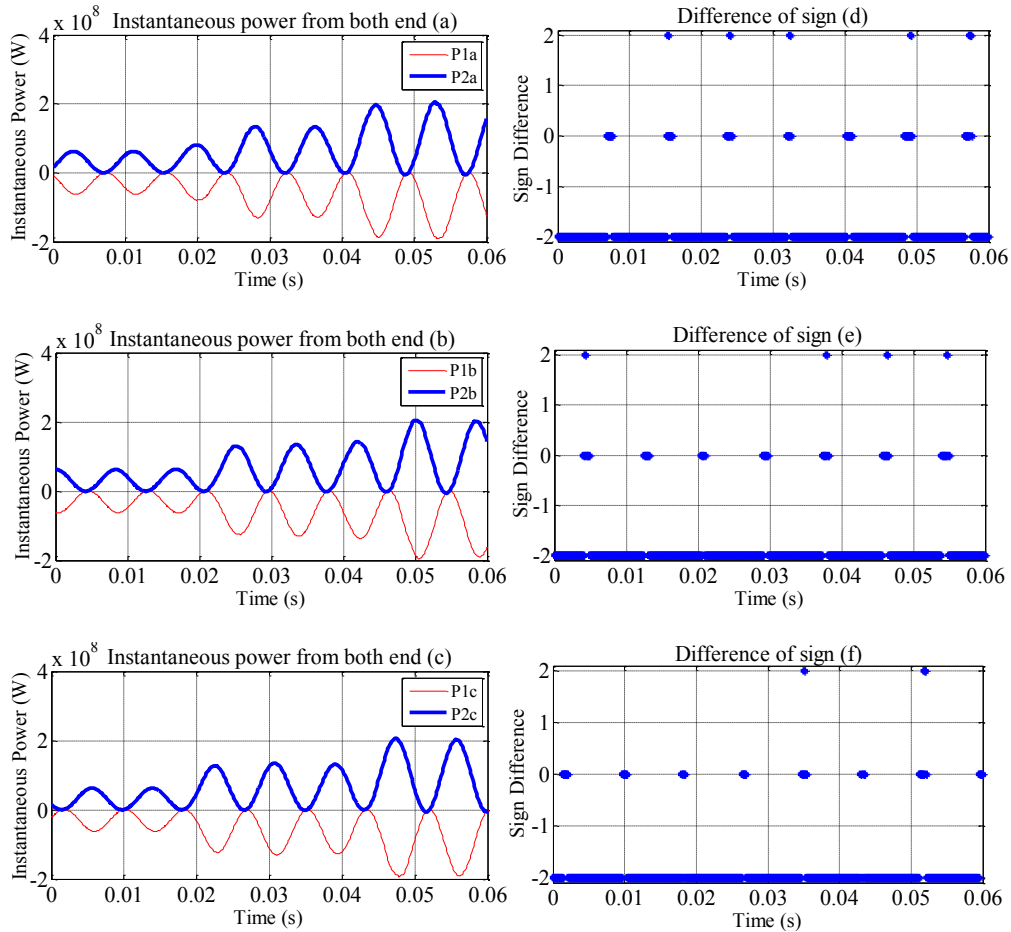


Figure 2.7 (a-c):  $P_1(t)$  and  $P_2(t)$  with respect to time for load level change; (d-f):  $P_{sgn}(t)$  with respect to time for load level change.

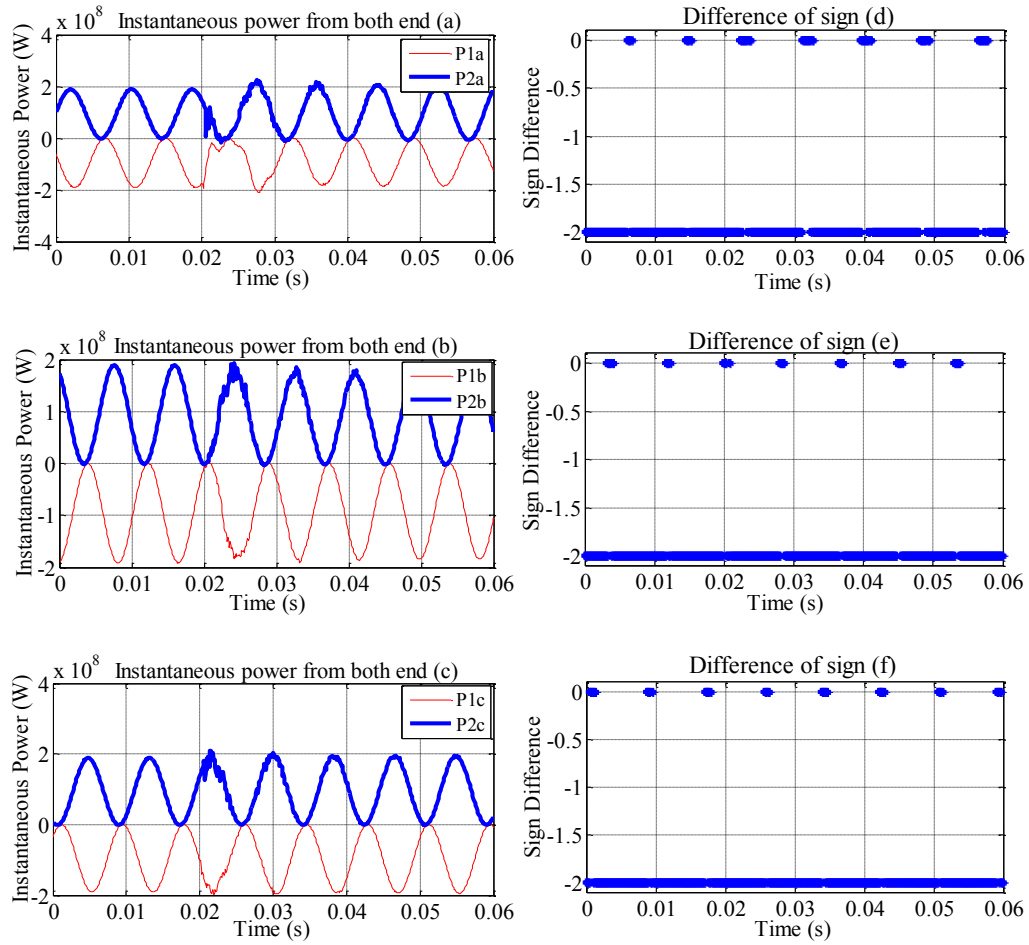


Figure 2.8 (a-c):  $P_1(t)$  and  $P_2(t)$  with respect to time for adjacent line; (d-f):  $P_{sgn}(t)$  with respect to time for adjacent line.

### 2.2.6. Faults under weak infeed

A single phase fault (ag) is applied on a line with weak infeed. Plot of  $P_1(t)$  and  $P_2(t)$  with respect to time is shown in Figure 2.9(a-c). Plot of  $P_{sgn}(t)$  with respect to time is shown in Figure 2.9(d-f). From Figure 2.9 it is clear that the proposed method can detect and classify fault under weak infeed condition. As the proposed method relies on change of

direction, unless the current from weak infeed is exact zero it is applicable. Therefore this method is not applicable to radial distribution systems.

### 2.2.7. Faults on parallel lines

Detection and classification of faults occurring on parallel lines (Figure 2.10) either single line fault or cross-line fault is very difficult due to presence of mutual coupling. If synchronous voltage and current measurements at both ends of the parallel lines are available, we can apply the proposed method to detect and classify fault.

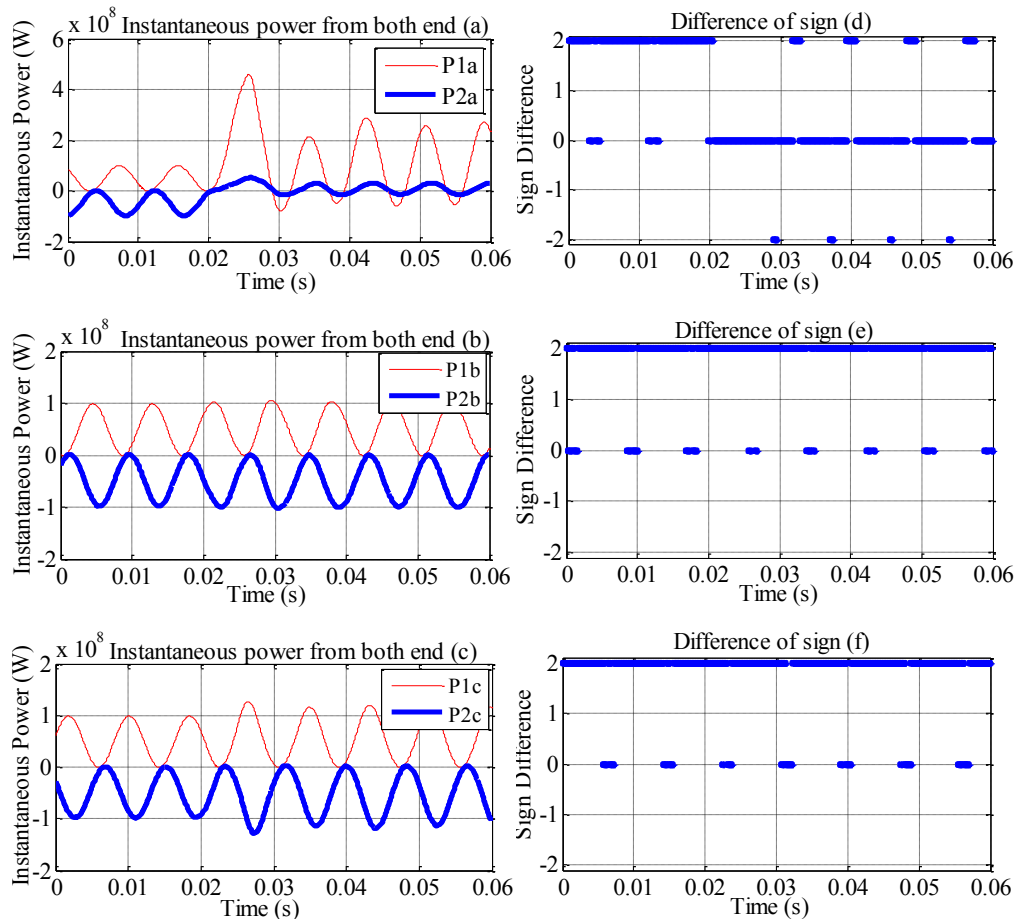


Figure 2.9 (a-c):  $P_1(t)$  and  $P_2(t)$  with respect to time for weak infeed case; (d-f):  $P_{\text{sgn}}(t)$  with respect to time for weak infeed case.

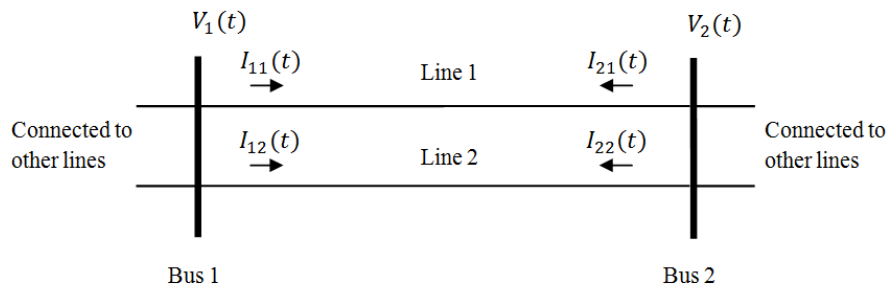


Figure 2.10 Parallel transmission line.

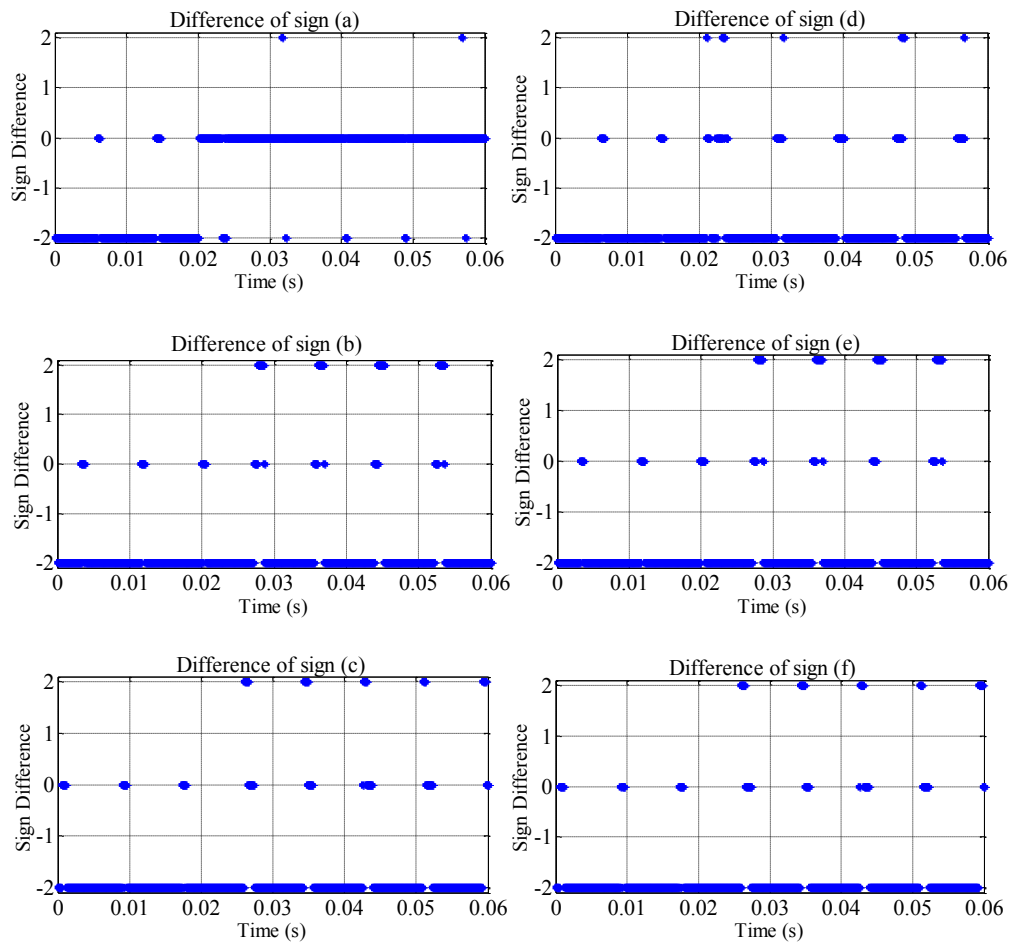


Figure 2.11 (a-c):  $P_{sgn}(t)$  with respect to time for 'ag' fault on line-1; (d-f):  $P_{sgn}(t)$  with respect to time for 'ag' fault on line-2.



Figure 2.11(a-c) shows plot of  $P_{sgn}(t)$  with respect to time for one of the lines (line 1) and Figure 2.11(d-f) shows the same for the other line (line 2) for ag fault on the 1<sup>st</sup> line. It can be concluded that only one line is faulted and the other not and the fault type is 'ag' fault. For cross-line faults, both lines will be detected as faulted.

### 2.2.8. Faults on three terminal lines

A three terminal line configuration application, which is really important from protection and fault detection point of view, is discussed. As demonstrated below, the proposed method is able to identify and classify the faults which occur inside the three terminal lines.

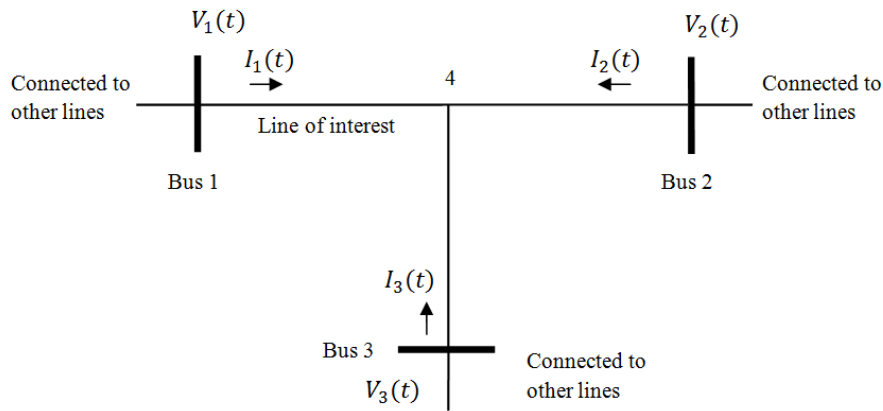


Figure 2.12 Transmission line with 3 end measurements.

According to Figure 2.12, by using only measurements for bus 1 and bus 2, the proposed method successfully detects and classifies the faults which occur inside the three terminal lines. As an example, a phase-to-phase-to-ground fault inserted at the middle of section 3-4 with 20 ohm fault resistance. Plot of  $P_1(t)$  and  $P_2(t)$  with respect to time is

shown in Figure 2.13(a-c). Right after the fault inception (0.02 sec),  $P_1(t)$  and  $P_2(t)$  in both phase 'a' and 'b' are in the same direction while that of c phase remains unchanged. Plot of  $P_{sgn}(t)$  with respect to time is shown in Figure 2.13(d-f). It is clear that after fault  $P_{sgn}(t)$  is almost zero for phase 'a' and 'b'.

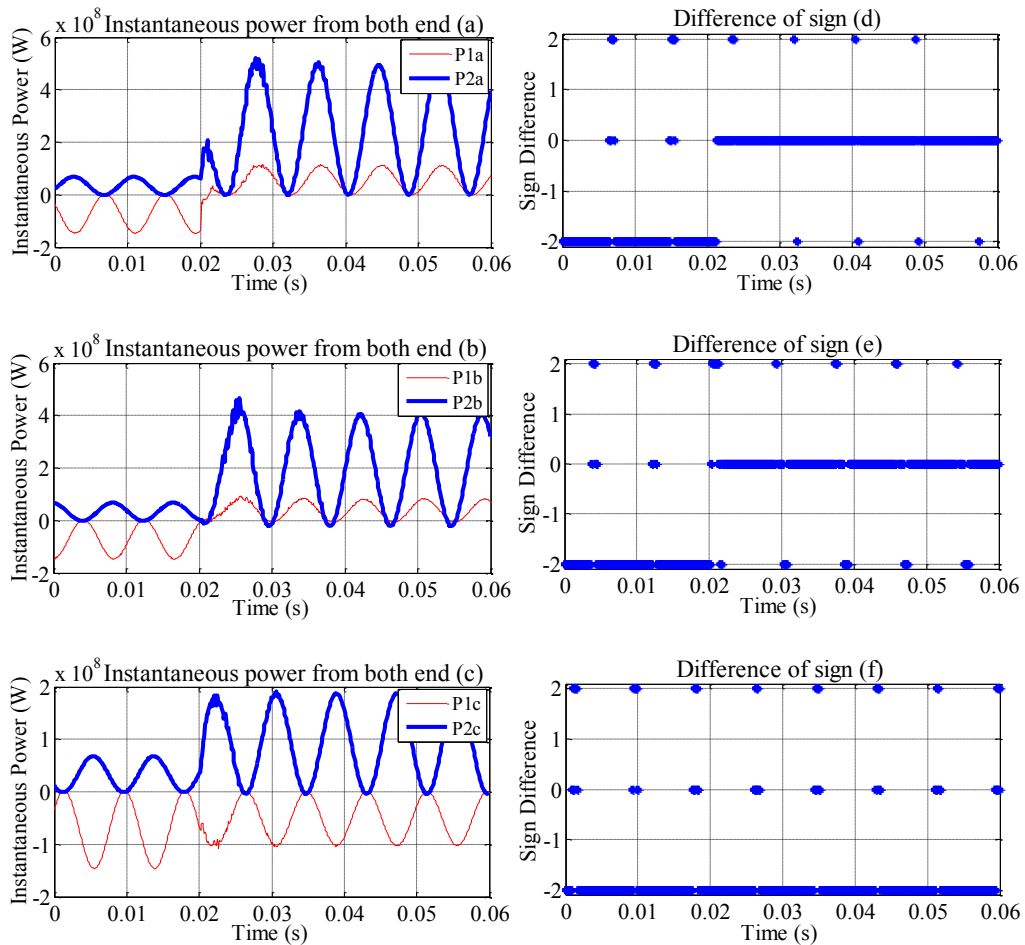


Figure 2.13 (a-c):  $P_1(t)$  and  $P_2(t)$  with respect to time for 'abg' fault on line-3-4; (d-f):  $P_{sgn}(t)$  with respect to time for 'abg' fault on line-3-4.

### 2.3. Fault location

Once fault detection scheme detected a fault in a line, synchronized sampling based fault location scheme, originally proposed in [18] is used to locate exact location of the fault using fault detection and classification outputs. The fault location method in [18] requires high sampling of data and yet the method used for fault detection and classification requires lower sampling rate. A spline interpolation technique [36] is used to introduce samples in between two adjacent samples of original voltage and current waveforms, thereby increasing sampling rate for input data.

A segment  $\Delta x$  of transmission line is shown in Figure 2.14.

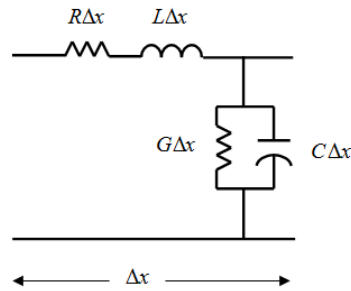


Figure 2.14 Transmission line segment of length  $\Delta x$ .

Transmission line partial differential equations are ( 2.23 )-( 2.24 ):

$$\frac{\partial v(x,t)}{\partial x} = -Ri(x,t) - L \frac{\partial i(x,t)}{\partial t} \quad ( 2.23 )$$

$$\frac{\partial i(x,t)}{\partial x} = -Gv(x,t) - C \frac{\partial v(x,t)}{\partial t} \quad ( 2.24 )$$

$v(x,t)$  and  $i(x,t)$  are the instantaneous voltage and current at any point X along the line, at distance  $x$  from one end of the line.

These hyperbolic partial differential equations are solved using method of characteristics [37]. The transmission line equations are transformed into an equivalent set of ordinary differential equations. These ordinary differential equations apply only in certain directions in the  $(x,t)$  plane, known as characteristic directions.

Let us define Characteristics impedance  $Z_c = \sqrt{\frac{L}{C}}$  and propagation constant  $\gamma = \sqrt{LC}$

Multiplying ( 2.24 ) by  $Z_c$  and adding with ( 2.23 ), ( 2.25 ) is obtained

$$\left( \frac{\partial}{\partial x} + \gamma \frac{\partial}{\partial t} \right) (v + Z_c i) = -Ri - GZ_c v \quad (2.25)$$

Multiplying ( 2.24 ) by  $Z_c$  and subtracting from ( 2.23 ), ( 2.26 ) is obtained

$$\left( \frac{\partial}{\partial x} - \gamma \frac{\partial}{\partial t} \right) (v - Z_c i) = -Ri + GZ_c v \quad (2.26)$$

Considering the function  $f(x,t)$ ,

$$\frac{df}{dx} = \frac{\partial f}{\partial x} + \frac{dt}{dx} \frac{\partial f}{\partial t} = \left( \frac{\partial}{\partial x} + \frac{dt}{dx} \frac{\partial}{\partial t} \right) f \quad (2.27)$$

From ( 2.27 ),  $\left( \frac{\partial}{\partial x} + a \frac{\partial}{\partial t} \right)$  can be treated as a differential operator which gives total

derivative of  $f(x,t)$  with respect to  $x$  in direction of  $\frac{dt}{dx} = a$  in the  $(x,t)$  plane.

Therefore the set of ordinary differential equations are obtained ( 2.28 )-( 2.29 ):

$$\frac{d}{dx}(v + Z_c i) = \frac{dv}{dx} + Z_c \frac{di}{dx} = -Ri - GZ_c v \text{ along } \frac{dt}{dx} = +\gamma \quad (2.28)$$

$$\frac{d}{dx}(v - Z_c i) = \frac{dv}{dx} - Z_c \frac{di}{dx} = -Ri + GZ_c v \text{ along } \frac{dt}{dx} = -\gamma \quad (2.29)$$

Figure 2.15 shows the ordinary differential equations ( 2.28 )-( 2.29 ) in  $(x,t)$  plane.

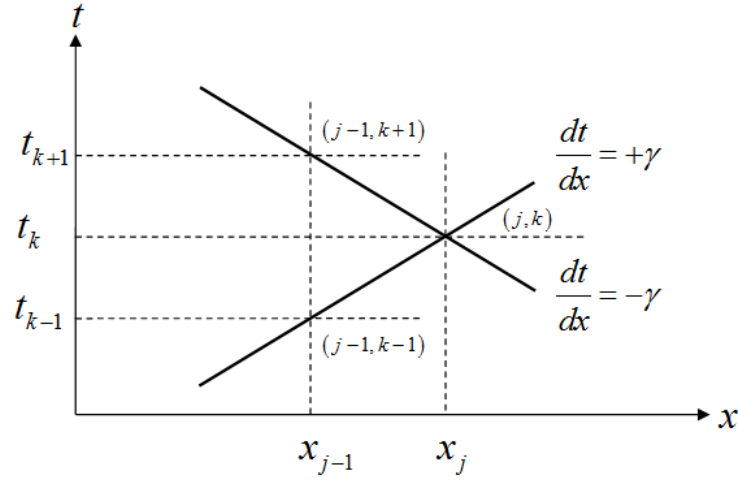


Figure 2.15 Set of ordinary differential equations in  $(x,t)$  plane.

Let us define distance segment,  $\Delta x = x_j - x_{j-1}$  is the distance that the wave travels with a sampling time step,  $\Delta t = t_{k+1} - t_k = t_k - t_{k-1}$  where  $k$  is the present sample point;  $\Delta t = \gamma \Delta x$ .

Points  $p, s, r$  are defined in  $(x,t)$  plane:  $p = (j, k), s = (j-1, k-1), r = (j-1, k+1)$ .

From ( 2.28 )

$$\left(\frac{v(p)-v(s)}{\Delta x}\right)+Z_c\left(\frac{i(p)-i(s)}{\Delta x}\right)=-R\left(\frac{i(p)+i(s)}{2}\right)-GZ_c\left(\frac{v(p)+v(s)}{2}\right) \quad (2.30)$$

From ( 2.29 )

$$\left(\frac{v(r)-v(p)}{\Delta x}\right)-Z_c\left(\frac{i(r)-i(p)}{\Delta x}\right)=-R\left(\frac{i(r)+i(p)}{2}\right)+GZ_c\left(\frac{v(r)+v(p)}{2}\right) \quad (2.31)$$

Adding ( 2.30 ) and ( 2.31 )

$$\left(1+\frac{R\Delta x}{2Z_c}\right)i(p)=\left(\frac{1}{2}-\frac{R\Delta x}{4Z_c}\right)(i(r)+i(s))+\left(\frac{G\Delta x}{4}-\frac{1}{2Z_c}\right)(v(r)-v(s)) \quad (2.32)$$

Subtracting ( 2.31 ) from ( 2.30 )

$$\left(1+\frac{GZ_c\Delta x}{2}\right)v(p)=\left(\frac{R\Delta x}{4}-\frac{Z_c}{2}\right)(i(r)-i(s))+\left(\frac{1}{2}-\frac{GZ_c\Delta x}{4}\right)(v(r)+v(s)) \quad (2.33)$$

Assuming  $G=0$ , equations ( 2.32 ) and ( 2.33 ) can be rewritten as:

$$\begin{aligned} \left(1+\frac{R\Delta x}{2Z_c}\right)i(j,k) &= \left(\frac{1}{2}-\frac{R\Delta x}{4Z_c}\right)(i(j-1,k+1)+i(j-1,k-1)) \\ &- \frac{1}{2Z_c}(v(j-1,k+1)-v(j-1,k-1)) \end{aligned} \quad (2.34)$$

$$\begin{aligned} v(j,k) &= \left(\frac{R\Delta x}{4}-\frac{Z_c}{2}\right)(i(j-1,k+1)-i(j-1,k-1)) \\ &+ \frac{1}{2}(v(j-1,k+1)+v(j-1,k-1)) \end{aligned} \quad (2.35)$$

Since the explicit form of fault location cannot be obtained, an indirect approach is used to calculate the final fault location as described in the following steps:

1. Discretize the line into equal segments with length of  $\Delta x$  and build voltage profile for each point calculating from sending end and receiving end respectively

2. Locate the approximate fault point by finding the point that has the minimum square of voltage difference calculated from both ends
3. Build a short line model surrounding the approximate fault point, and refine fault location using the algorithm based on lumped line parameters.

As the fault location method is based on distributed parameter line model, it requires very high sampling rates for voltage and current signals. Since the fault detection and classification method does not require high sampling rates, spline interpolation technique is used between input samples to achieve higher sampling rate appearance for fault location application.

#### **2.4. Implementation**

Flowchart for the proposed method is shown in Figure 2.16. The method is initiated after a relay trips a line. Synchronized voltage and current measurements from both ends of the line are gathered. Depending on the configuration of the line (single or parallel), instantaneous powers at both ends and  $P_{sgn}(t)$  are calculated for all the phases for the single line or both of the parallel lines. If for parallel lines  $P_{sgn}(t) \approx 0$  in  $\frac{1}{2}$  of nominal frequency cycle moving window for both the lines then it is cross-line or inter-circuit fault, if  $P_{sgn}(t) \approx 0$  for only one line of the parallel lines, fault is single-line fault, and if  $P_{sgn}(t) \neq 0$  there is no fault. If there is any fault on parallel lines, classification procedure will be same as single line case. For single line, if  $P_{sgn}(t) \approx 0$  for all phases, fault type is three phase fault, else if  $P_{sgn}(t) \approx 0$  for two phases, we check for phase-phase-to-ground fault by computing zero sequence current factors and if those factors are much more than zero, then the fault is double-phase-to-ground fault. Otherwise it is phase-to-phase fault. If

$P_{sgn}(t) \approx 0$  for only one phase, then fault type is single-phase-to-ground fault and otherwise there is no fault.

After fault is detected and classified, fault location subroutine is performed as described in section 2.3.

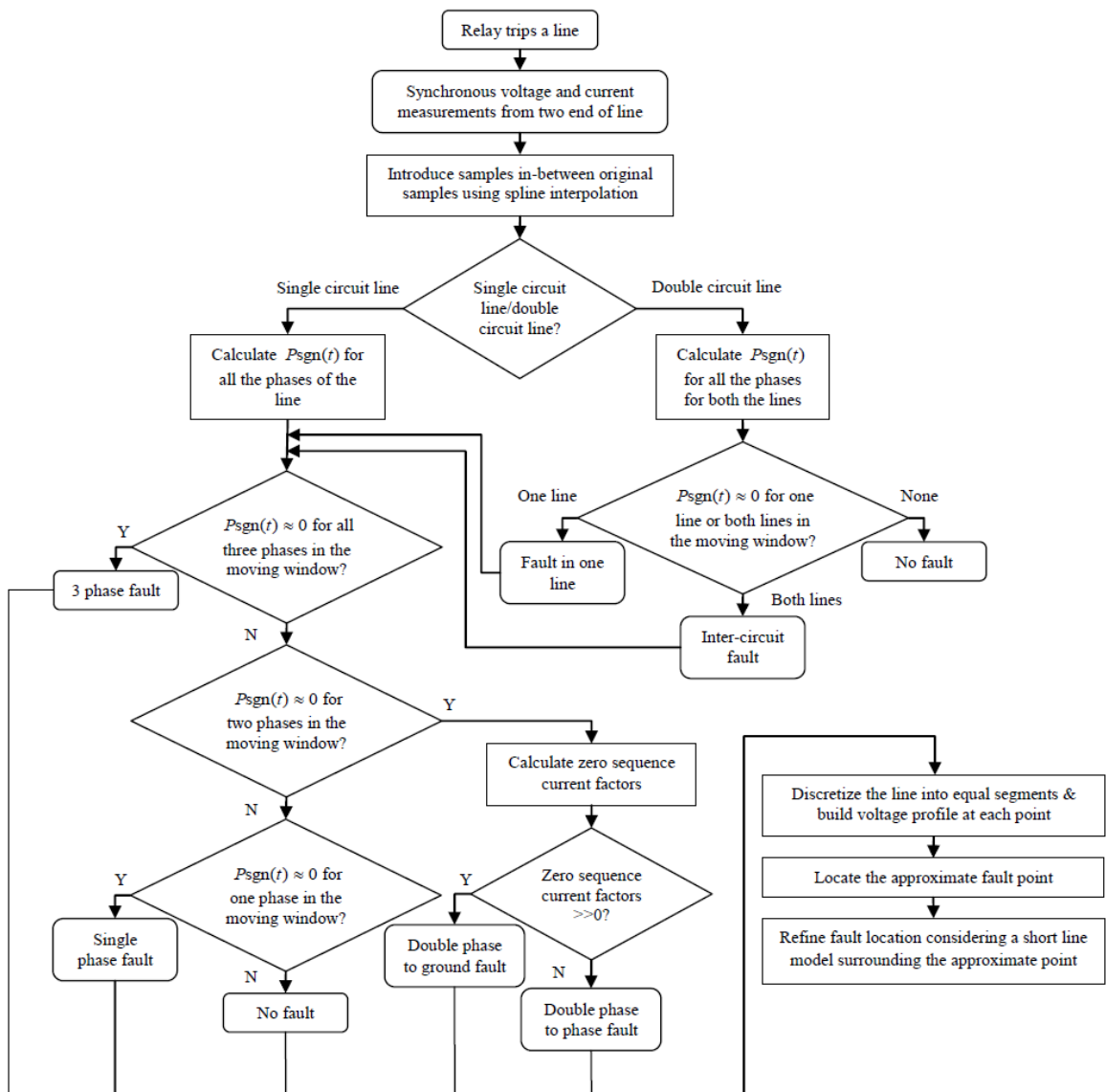


Figure 2.16 Flowchart of the proposed fault detection, classification and location scheme.



## 2.5. Test results

### 2.5.1. Fault scenarios

The IEEE 118 bus test system is modeled in ATP [38] and different types of faults under different conditions are simulated and synchronized voltage and current signal samples pre and post fault at both ends of the line are used to verify the algorithm. The sampling rate for voltage and current measurements is 1 kHz. COMTRADE files generated from ATP are used to verify the developed methods. The transmission lines considered for different fault scenarios creation are shown in Table 2.1.

Fault location error is defined as: Percentage error in fault location estimate based on the total line length:  $e$  (error) = (instrument reading – exact distance to the fault) / total line length. Instrument reading corresponds to the calculated location here.

Table 2.1 Lines considered for fault scenarios: IEEE 118 bus test system

Case #	From Bus	To Bus	Length (miles)	Voltage (kV)
1	30	38	165	345
2	54	49	124	138
3	16	12	36	138
4	82	83	17	138
5	8	30	154	345

### 2.5.2. Results for IEEE 118 bus test system

Results from the fault detection simulation on line 30-38 of the IEEE 118 bus system (case 1 in Table 2.1), are presented below. Results of remaining cases are provided in Appendix B (case 2 in Table B.1, case 3 in Table B. 2, case 4 in Table B.3 and case 5 in Table B.4).

### ***Changing fault distance and fault resistance***

Distance to fault from one end of a line is changed to 5%, 20% and 50% of the line length with fault resistance changes  $0\Omega$ ,  $20\Omega$  and  $100\Omega$ . Table 2.2 provides the summary of the results for different types of fault under varying fault distance and resistance. The proposed method detects and classifies fault using  $\frac{1}{2}$  of nominal frequency cycle data window after fault inception on the post fault data. Fault location accuracy is within 3% except for one case.

Table 2.2 Summary of fault detection & classification with varying fault distance and fault resistance (IEEE 118 system: Case 1)

<b>Fault Type</b>	<b>Fault Location (mi)</b>	<b>Fault Resistance (<math>\Omega</math>)</b>	<b>Fault Inception Angle (degree)</b>	<b>Actual Fault Inception Time (s)</b>	<b>Detected Fault Type</b>	<b>Calculated Fault Inception Time (s)</b>	<b>Time to detect (ms)</b>	<b>Calculated Fault Location (mi)</b>	<b>Fault Location % Error</b>
ag	8.28 (5%)	0	0	0.02	ag	0.022	2	-	-
	33.13 (20%)				ag	0.022	2	33.84	0.43
	82.84 (50%)				ag	0.022	2	82.70	0.09
	8.28 (5%)	20	0	0.02	ag	0.022	2	-	-
	33.13 (20%)				ag	0.024	4	33.84	0.43
	82.84 (50%)				ag	0.022	2	82.70	0.09
	8.28 (5%)	100	0	0.02	ag	0.022	2	9.14	0.52
	33.13 (20%)				ag	0.022	2	33.82	0.41
	82.84 (50%)				ag	0.022	2	82.70	0.09
ab	8.28 (5%)	0	0	0.02	ab	0.027	7	12.02	2.26
	33.13 (20%)				ab	0.023	3	33.26	0.08
	82.84 (50%)				ab	0.023	3	82.52	0.19

Table 2.2 Continued

Fault Type	Fault Location (mi)	Fault Resistance ( $\Omega$ )	Fault Inception Angle (degree)	Actual Fault Inception Time (s)	Detected Fault Type	Calculated Fault Inception Time (s)	Time to detect (ms)	Calculated Fault Location (mi)	Fault Location % Error
abg	8.28 (5%)	0	0	0.02	abg	0.027	7	12.02	2.26
	33.13 (20%)				abg	0.023	3	33.26	0.08
	82.84 (50%)				abg	0.023	3	82.52	0.19
	8.28 (5%)	20	0	0.02	abg	0.023	3	10.06	1.08
	33.13 (20%)				abg	0.023	3	33.54	0.24
	82.84 (50%)				abg	0.023	3	82.54	0.18
	8.28 (5%)	100	0	0.02	abg	0.023	3	10.73	1.48
	33.13 (20%)				abg	0.023	3	33.06	0.05
	82.84 (50%)				abg	0.023	3	82.46	0.23
abc	8.28 (5%)	0	0	0.02	abc	0.024	4	-	-
	33.13 (20%)				abc	0.024	4	37.62	2.71
	82.84 (50%)				abc	0.023	3	83.90	0.64
	8.28 (5%)	20	0	0.02	abc	0.023	3	8.07	0.13
	33.13 (20%)				abc	0.023	3	38.01	2.94
	82.84 (50%)				abc	0.023	3	82.83	0.004
	8.28 (5%)	100	0	0.02	abc	0.023	3	13.12	2.92
	33.13 (20%)				abc	0.023	3	45.03	7.18
	82.84 (50%)				abc	0.023	3	82.61	0.14

***Under high fault resistance***

Table 2.3 shows the summary of the results of single line to ground faults under very high fault resistance. High resistance fault cases are extremely rare for other fault types.

Table 2.3 Summary of fault detection & classification for high fault resistance (IEEE 118 system: Case 1)

Fault Location (mi)	Fault Resistance ( $\Omega$ )	Actual Fault Inception Time (s)	Calculated Fault Inception Time (s)	Time to detect (ms)	Calculated Fault Location (mi)	Fault Location % Error
8.28 (5%)	200	0.02	0.024	4	9.09	0.49
33.13 (20%)			0.024	4	33.79	0.4
82.84 (50%)			0.024	4	82.71	0.08
8.28 (5%)	500	0.02	0.023	3	9.02	0.45
33.13 (20%)			0.024	4	33.73	0.36
82.84 (50%)			0.024	4	82.74	0.06
8.28 (5%)	1000	0.02	0.022	2	8.98	0.42
33.13 (20%)			0.022	2	33.66	0.31
82.84 (50%)			0.022	2	82.78	0.04
8.28 (5%)	10000	0.02	0.022	2	8.93	0.39
33.13 (20%)			0.022	2	33.38	0.15
82.84 (50%)			0.022	2	82.79	0.03

### *Changing fault inception angle*

Fault inception angle in degrees is changed to 0°, 40°, 80°, 120° and 160°. Table 2.4 provides the summary of the results for different types of fault under varying fault inception angle. Proposed method detects and classifies faults within ½ of nominal frequency cycle for all types of fault. Fault location accuracy is within 3%.

Table 2.4 Summary of fault detection and classification with varying fault inception angle (IEEE 118 bus test system: Case 1)

Fault Type	Fault Location (mi)	Fault Resistance ( $\Omega$ )	Fault Inception Angle (degree)	Actual Fault Inception Time (s)	Detected Fault Type	Calculated Fault Inception Time (s)	Time to detect (ms)	Calculated Fault Location (mi)	Fault Location % Error
ag	33.13 (20%)	20	0	0.02	ag	0.024	4	33.84	0.43
			40	0.0218	ag	0.025	3.1	34.57	0.87
			80	0.0237	ag	0.03	6.2	35.59	1.48
			120	0.0255	ag	0.03	4.5	35.44	1.39
			160	0.0274	ag	0.033	5.6	34.54	0.85
	82.84 (50%)	20	0	0.02	ag	0.024	4	82.70	0.09
			40	0.0218	ag	0.025	3.1	82.64	0.12
			80	0.0237	ag	0.028	4.2	82.62	0.13
			120	0.0255	ag	0.03	4.5	82.56	0.17
			160	0.0274	ag	0.033	5.6	82.69	0.09
ab	33.13 (20%)	0	0	0.02	ab	0.023	3	34.16	0.62
			40	0.0218	ab	0.025	3.2	36.47	2.02
			80	0.0237	ab	0.029	5.3	32.71	0.26
			120	0.0255	ab	0.031	5.5	32.29	0.51
			160	0.0274	ab	0.031	3.6	32.84	0.18
	82.84 (50%)	0	0	0.02	ab	0.023	3	82.94	0.06
			40	0.0218	ab	0.025	3.2	82.80	0.02
			80	0.0237	ab	0.028	4.3	82.08	0.46
			120	0.0255	ab	0.03	4.5	82.78	0.04
			160	0.0274	ab	0.031	3.6	82.93	0.05
abg	33.13 (20%)	20	0	0.02	abg	0.023	3	33.54	0.24
			40	0.0218	abg	0.025	3.2	34.00	0.52
			80	0.0237	abg	0.03	6.3	34.05	0.55
			120	0.0255	abg	0.031	5.5	34.75	0.98
			160	0.0274	abg	0.031	3.6	35.14	1.21
	82.84 (50%)	20	0	0.02	abg	0.023	3	82.54	0.18
			40	0.0218	abg	0.025	3.2	82.70	0.08
			80	0.0237	abg	0.028	4.3	82.66	0.11
			120	0.0255	abg	0.031	5.5	82.94	0.06
			160	0.0274	abg	0.031	3.6	82.56	0.17

Table 2.4 Continued

Fault Type	Fault Location (mi)	Fault Resistance ( $\Omega$ )	Fault Inception Angle (degree)	Actual Fault Inception Time (s)	Detected Fault Type	Calculated Fault Inception Time (s)	Time to detect (ms)	Calculated Fault Location (mi)	Fault Location % Error
abc	33.13 (20%)	20	0	0.02	abc	0.023	3	38.01	2.94
			40	0.0218	abc	0.025	3.2	33.53	0.24
			80	0.0237	abc	0.028	4.3	30.23	1.75
			120	0.0255	abc	0.029	3.5	32.40	0.44
			160	0.0274	abc	0.031	3.6	31.26	1.13
	82.84 (50%)	20	0	0.02	abc	0.023	3	82.83	0.00
			40	0.0218	abc	0.025	3.2	82.55	0.18
			80	0.0237	abc	0.028	4.3	82.67	0.10
			120	0.0255	abc	0.029	3.5	82.96	0.07
			160	0.0274	abc	0.031	3.6	83.40	0.34

## 2.6. Conclusions

An accurate fault analysis method which uses synchronized samples of voltages and currents measured at both ends of transmission line is proposed. The unique fault detection and classification works on comparing the change of direction of instantaneous power computed at two ends of the line. The proposed fault location method is based on solving transmission line partial differential equations in time domain. The proposed method is tested for several faults simulated on IEEE 118 bus test system and it has been concluded that it can detect and classify a fault using pre and post fault recorded samples within  $\frac{1}{2}$  of the fundamental frequency cycle of fault inception and accurately locate fault with 3% accuracy. This time response performance is highly desirable since with the increasing use of modern circuit breakers which can open the faulty line in less than two cycles, the time window of the captured fault waveforms is significantly reduced due to the

unavailability of measurement signals after breakers open. The proposed method can detect, classify and locate fault very accurately even if the sampling rate for voltage and current measurements are 1 kHz which is feasible using present day digital relays and IEDs. This method is setting-free and transparent to the impact of fault resistance. It can be applied in case of very high resistance faults. The only drawback is obtaining time-synchronized samples of measurements, which is now feasible at a relatively low cost with GPS enabled IEDs. A very accurate fault detection, classification and location scheme is achieved, which is applicable to different transmission line layouts, setting free, independent of fault resistance impact, applicable to high resistance faults, and still using moderate rate (1 kHz) of input sampling.

### 3. FAULT LOCATION WITH LIMITED DATA: SPARSE MEASUREMENT METHOD

#### 3.1. Background

Traditional transmission line fault location methods require measurements from at least one end of the faulted line. Measurements from all the ends of the faulted line are desirable but not always available. Under these circumstances sparse measurement based fault location scheme [24] using phasor measurements from different substations located in the vicinity where the fault has occurred can be applied if the measurements are not available from any of the line ends.

Fault may occur between transmission line phases or have a ground return path. When a phase-to-phase fault occurs, the fault current flows through arc resistance and if the fault is a ground fault the current path includes earth resistance (consists of tower resistance, tower footing resistance and ground return path) also. Fault resistance is the combined resistance which appears in the fault current path. This is an uncertain parameter as both the arc resistance and earth resistance depend on many parameters that are sometimes very hard to predict.

Distance relay algorithm selectivity may suffer from the combined effect of fault resistance and load current which is known as *reactance effect* [2]. Such algorithms assume that the fault current is in phase with measured current. Presence of remote infeed complicates the situation. Takagi et al. [4]-[5] decomposed the faulted network to pre-fault and pure-fault network and take some assumptions to eliminate fault resistance part from



the circuit equation. Another one-end method using quadratic formula to eliminate fault resistance is introduced in [6] yielding much more accurate result. Using one-end data to estimate fault resistance by modeling the arc is discussed in [39]-[40]. [14] is based on equalizing voltage of fault point from both ends of the line based on measurements from both ends and thus eliminates the impact of fault resistance. A settings free fault location method using synchronized samples from both ends of the line is completely independent of fault resistance, which is not used to develop the algorithm [41].

Typically digital fault recorders (DFRs) or digital protective relays (DPRs) are present in substations and they record current, voltage and status signals on occurrence of an event like fault. Due to the lack of measurement transformers in certain transmission line configurations such as tapped lines availability of measurements from at least one end of the line becomes a problem. If the measurements from other ends are not available, some unconventional fault location techniques based on system-wide sparse measurements may have to be used [23]-[24]. In this case, fault location is estimated by using measurements recorded from IEDs installed in the substations close to the faulted line (but not from the ends of the line) and also using SCADA measurements from all the substations near the fault.

Performance of the system-wide sparse measurement based fault location algorithms depend on fault resistance. The analysis of the impact of the fault resistance on the sensitivity of fault location output is crucial for estimating an accuracy of the output. In [42]-[43] sensitivity of one-end fault location methods is analyzed to determine most contributing uncertainty factors and interaction of uncertainty factors.

This section explains how accuracy of system wide sparse measurement based fault location can be impacted by fault resistance. An intuitive scheme to choose proper fault resistance range is also proposed.

### 3.2. Sparse measurement based fault location method

The basic idea of transmission line fault location is to estimate the distance of the fault point from any one end of the line.

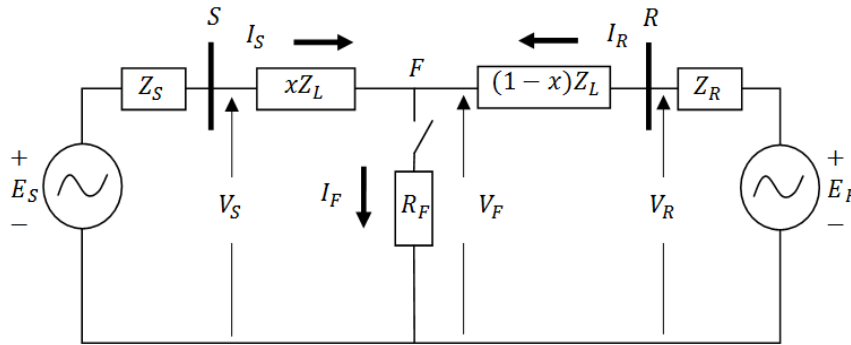


Figure 3.1 Faulted circuit model.

In Figure 3.1 a fault with resistance  $R_F$  has occurred on point  $F$  between two ends ( $S$  and  $R$ ) of a line section  $S$ - $R$ . Considering a homogeneous line, the distance can be expressed as a function of the impedance measured from one end,  $xZ_L$ . The above circuit can be solved accurately if voltage and current measurements from both ends are available.

Installing recording devices (DFRs in our case) on the ends of all the transmission lines is not economical. Although protective relays exist on every transmission line, most of them may still be electromechanical and they do not have capability to record measurements. As a result, in some cases it may happen that there are no recordings at all

available at line ends close to a fault. System-wide sparse measurement based fault location method can be applied in such instances [23]-[24].

In sparse measurement based fault location method, phasor measurements from different substations located in the region where the fault has occurred are used. The measurements are sparse, i.e. they may come from only some of so many transmission line ends (substations) in the region. This method requires synchronization of the measurements, which may be obtained by using DFRs connected to Global Positioning System (GPS) receivers [44]. Besides the sparse measurements, the technique also uses short circuit program, which is initialized and tuned with SCADA PI Historian [45], power system model data and measurements associated with the time of the fault occurrence.

The method uses waveform matching technique between the current and voltage phasors calculated from the waveforms recorded in a substation (nearby the faulted line) and phasors simulated using short circuit simulation of possible fault locations. A commercial short circuit program tool PSS/E<sup>TM</sup> 27 is used for short circuit calculation [46]. The calculated and simulated phasors are compared while the location of the fault is changed in the short circuit program. This process is repeated automatically until the difference between measured and simulated values reaches global optimum (minimum), which indicates that the fault location used in the short circuit program is the actual one in the field. The criteria for the minimal difference are based on a global optimization technique that uses Genetic Algorithm [47].

In this approach field-recorded waveforms are used to calculate phasors and they are in turn matched with the phasors obtained using short circuit study.

The matching degree between the recorded and the simulated waveforms can be formulated as [23] in ( 3.1 ):

$$f_c(x, R_F) = \sum_{k=1}^{N_V} r_{kV} |V_{ks} - V_{kr}| + \sum_{k=1}^{N_I} r_{kI} |I_{ks} - I_{kr}| \quad (3.1)$$

Where,

$f_c(x, R_F)$ : The cost function using phasors for matching

$x, R_F$ : The fault location and fault resistance

$r_{kV}, r_{kI}$ : Weights for the errors of the voltages and currents respectively

$V_{ks}, V_{kr}$ : Simulated and calculated from measurements during-fault voltages respectively

$I_{ks}, I_{kr}$ : Simulated and calculated from measurements during-fault currents respectively

$N_V, N_I$ : Total number of voltage and current phasors to be matched respectively

$k$ : The index of voltage or current phasors

Ideally when the simulated phasors and phasor calculated from the recorded waveforms match completely, the cost function should become zero. In practical solution, the cost function is not zero and should be minimized using some mathematical optimization method. To obtain good phasor matching the fault search range should be extensive. All possible faulty branches and fault resistance should be included in the search range which makes the search two-dimensional and exhaustive. For a large system, multiple searches should be run in parallel which can be achieved using population based

optimization methods such as Genetic Algorithm (GA) [47]. The flowchart of this method is shown in Figure 3.2.

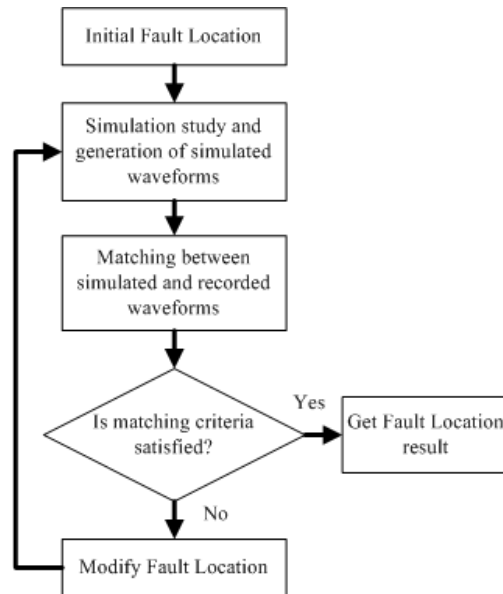


Figure 3.2 Flowchart of sparse measurement algorithm.

### 3.3. Fault resistance compensation correction scheme [48]

Since fault resistance is the most uncertain parameter, a correction scheme to compensate the effect of fault resistance can be proposed.

The correction scheme (shown in Figure 3.3) compensate the effect of fault resistance by using an optimization scheme over the sparse measurement method which selects the fault location and fault resistance pair that cause the output to be least sensitive to fault resistance variation.

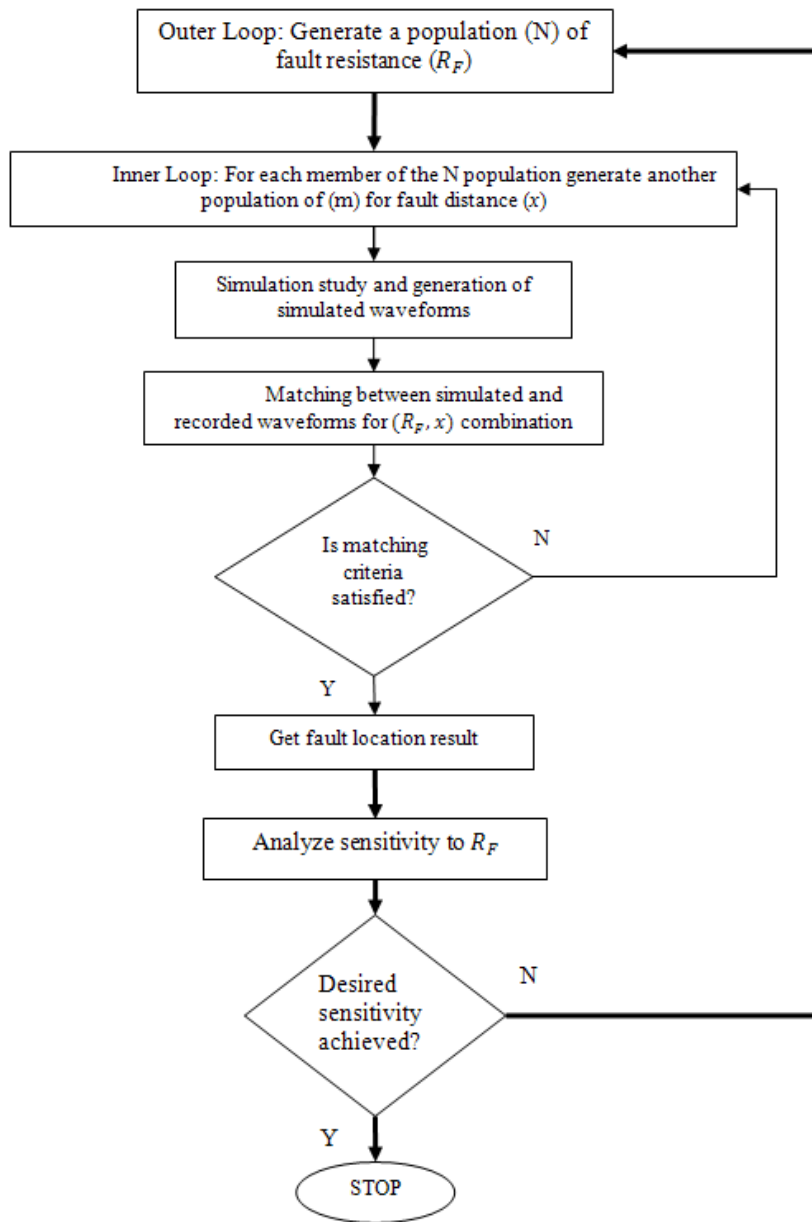


Figure 3.3 Flowchart of corrected sparse measurement algorithm.

The proposed corrected sparse measurement algorithm can be explained in the following step by step method:

**Step 1: Initialization:** Generate a population of fault resistance values  $R_F$  (1 to  $N$ )

**Step 2: Sparse measurement based fault location:** For each  $R_F$ , perform original sparse measurement algorithm and get fault location  $x$  (1 to  $N$ ). Therefore a pair of  $(x, R_F)$  is obtained for  $N$  number of cases.

**Step 3: Estimation of unknown function  $g$  by non-parametric method:**

We have  $N$  pairs of observations  $(x_i, R_{F_i})$  for  $i=1:N$  which are used to estimate the unknown regression function  $g(R_F)$  where fault location is expressed as a function of fault resistance ( 3.2 ):

$$x = g(R_F) + \varepsilon \quad (3.2)$$

$\varepsilon$  is assumed to be zero mean error

Therefore; expected value of  $x$  given  $R_F$  is expressed in ( 3.3 ):

$$E(x/R_F) = g(R_F) \quad (3.3)$$

We can approximate the true function  $g$  by  $\hat{g}$  using traditional non-parametric regression method [49].

**Step 4: Calculate sensitivity to  $R_F$  :**

The variance based global sensitivity analysis method (ANOVA decomposition) is used [50]. The method is summarized below:

If we consider a deterministic model  $Z = f(y)$

Where

$y$  is a vector of input variables  $y = (y_1, y_2, \dots, y_k)$

$Z$  is the model output

We can decompose  $Z = f(y)$  into main effects and interactions in ( 3.4 )

$$f(y) = f_0 + \sum_{i=1}^k f_i(y_i) + \sum_i \sum_{j>i} f_{ij}(y_i, y_j) + \dots + f_{1,2,\dots,k}(y_1, y_2, \dots, y_k) \quad (3.4)$$

If each term is chosen with zero mean

$$\int_0^1 f_i(y_i) dy_i = 0, \forall y_i, i = 1, 2, \dots, k \quad (3.5)$$

$$\int_0^1 \int_0^1 f_{ij}(y_i, y_j) dy_i dy_j = 0, \forall y_i, y_j, i < j \quad (3.6)$$

$$\int_{\Omega} f_{1,2,\dots,k}(y_1, y_2, \dots, y_k) dy_1 dy_2 \dots dy_k = 0 \quad (3.7)$$

Therefore

$$\int_{\Omega} f(y) dy = f_0 \quad (3.8)$$

So we can write

$$Z - E(Z) = f_0 + \sum_{i=1}^k f_i(y_i) + \sum_i \sum_{j>i} f_{ij}(y_i, y_j) + \dots + f_{1,2,\dots,k}(y_1, y_2, \dots, y_k) \quad (3.9)$$

As terms orthogonal, we can square and integrate ( 3.9 ) over  $\Omega$  and decompose the variance of  $f(y)$  into terms of increasing dimensionality

$$\sigma_Z^2 = \sum_{i=1}^k \sigma_{E(Z/y_i)}^2 + \sum_i \sum_j \sigma_{E(Z/y_i, y_j)}^2 + \dots + \sum_i \sum_j \sum_k \sigma_{E(Z/y_i, y_j, y_k)}^2 \quad (3.10)$$

Now we can define sensitivity indices as:

$S_i = \sigma_{E(Z/y_i)}^2 / \sigma_Z^2$  : First order index. Corresponds to main effect of  $y_i$



$S_{ij} = \sigma_{E(Z/y_i, y_j)}^2 / \sigma_Z^2$  : Second order index. It measures the effect of pure interaction

between any pair of factors on the output

And so on.

So ( 3.10 ) becomes ( 3.11 )

$$1 = \sum_{i=1}^k S_i + \sum_i \sum_j S_{ij} + \dots + S_{1,2,\dots,k} \quad (3.11)$$

Therefore in our case, Sensitivity of  $x$  with respect to  $R_F$  (first order index) is given by ( 3.12 ):

$$S_{R_F} = \sigma_{E(x/R_F)}^2 / \sigma_x^2 \quad (3.12)$$

Now  $\sigma_{E(x/R_F)}^2$  and  $\sigma_x^2$  are unknown parameters which can be estimated from the pair of observations generated.

Now  $\sigma_x^2$  is estimated by its unbiased estimator ( 3.13 )

$$S_x^2 = \frac{1}{(N-1)} \sum_i (x_i - \bar{x})^2 \quad (3.13)$$

which is also known as sample variance of  $x$

And  $\sigma_{E(x/R_F)}^2$  is equal to  $\sigma_{g(R_F)}^2$  which can be estimated by its unbiased estimator ( 3.14 )

$$S_{E(x/R_F)}^2 = \frac{1}{(N-1)} \sum_i (g_i - \bar{g})^2 \quad (3.14)$$

Where  $g_i = g(R_{F_i})$

Here we don't know the true  $g$  but we can obtain its estimate  $\hat{g}$  by the traditional non-parametric regression method.

Hence we can estimate  $\sigma_{E(x/R_F)}^2$  by ( 3.15 )

$$S_{E(x/R_F)}^2 = \frac{1}{(N-1)} \sum_i (\hat{g}_i - \bar{\hat{g}})^2 \quad ( 3.15 )$$

Where  $\hat{g}_i = \hat{g}(R_{F_i})$

Now we can segment the range of  $R_F$  in some sub-ranges and also determine the sensitivity in those individual sub-ranges.

**Step 5: Determine optimal pair of  $(x, R_F)$  :**

From the different sensitivity indices in different sub-ranges of  $R_F$ , we can choose the sub-range of  $R_F$  that corresponds to least sensitivity. Now the optimal pair of  $(x, R_F)$  should be the pair that corresponds to minimum of mismatch computed using ( 3.1 ).

### 3.4. Implementation

The architecture of the fault location scheme is shown in Figure 3.4.

Several commercial packages are used to implement this solution. The static power system is modeled using PSS/E<sup>TM</sup> 27 [46]. To tune the power grid with pre-fault data, SCADA PI-Historian [45] data is used.

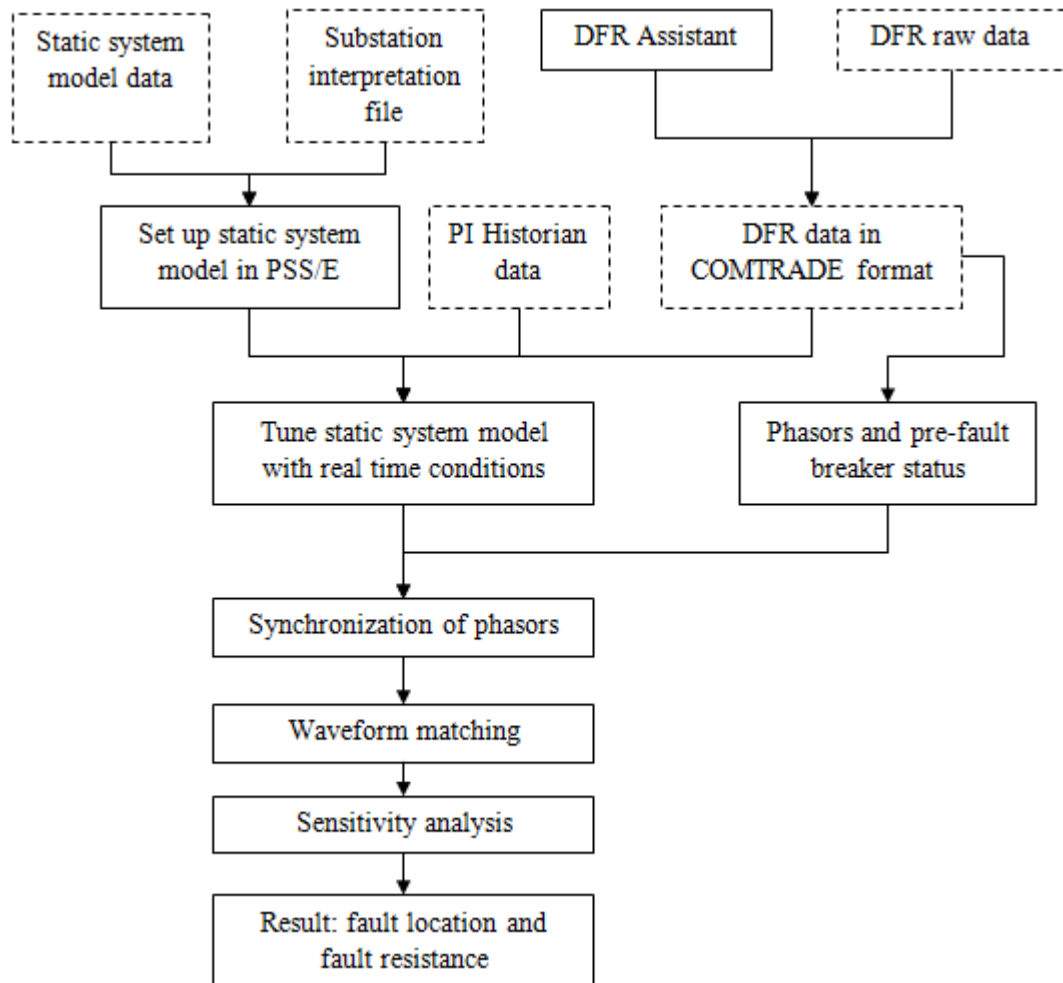


Figure 3.4 Solution architecture.

The detailed data requirements for the implementation are:

- Static system model data: These include power flow system specification data for the establishment of a static system model (in \*.raw format). Power system model data can also be used in saved case format (\*.sav) which is used to extract \*.raw data.

- Event data: These include event data captured by recording devices (DFRs here) after occurrence of a fault. The raw DFR data is converted to COMTRADE format [51] using DFR Assistant software [52] which can generate an analysis report (containing the type of fault and a possible faulted line) in addition to generating the COMTRADE files. The COMTRADE files contain:
  - Configuration files(\*.cfg): information for interpreting the allocation of measured data to the equipment (input channels) for a specific substation
  - Data files (\*.dat): analog and digital sample values for all input channels (described in configuration file) in substation
- SCADA PI Historian data: This data reflects real time changes in power system including the latest load, branch and generator data to tune the static system model with the actual pre and post fault conditions.

The nomenclature of power system components in all three types of data is different. Correlation between all three types of data is required. Substation interpretation files are prepared to correlate the nomenclature used in DFR files and the one used in PSS/E file and PI Historian data. The interpretation files should be modified as frequently as needed to reflect the DFR configuration or system model changes.

Implementation of fault location software is a four step procedure:

#### *3.4.1. System initialization*

This is a onetime procedure used to set up the system. Power system static model data (in \*.raw format) is used to extract all the components and construct topology which will be used later.

#### *3.4.2. Pre-processing event data*

The event data captured by DFRs should be pre-processed to obtain required information to be integrated with power system model data.

The pre-fault phasor can be calculated using first cycle of the recorded waveform. The during-fault phasor can be calculated using any fault cycle following the fault inception and prior to fault clearance. The fault inception moment is determined from waveforms recorded by DFR.

For a typical fault case, several DFRs may be triggered and the phasors calculated from the recorded waveforms may lack time synchronism which will introduce phase angle difference among phasors. Thus time synchronization of the phasors obtained from different DFRs is necessary. The phasors calculated from each DFR recording are synchronized by rotating them in reference to the phasors obtained by the load flow study assuming the angle difference between the pre- and during-fault phasor, for the corresponding recorded current or voltage, is fixed. This way, all recorded pre- and post-fault phasors are synchronized using the same reference.

### 3.4.3. *Tuning with real time data*

The static system model may not reflect the operating conditions of the system when an event is recorded. A tuning with real-time power systems is required. The tuning procedure is done in two steps:

Tuning topology: The topology update is performed using information of the pre-fault breaker status and the pre-fault current magnitudes of the monitored branches derived from the DFR data. It is assumed that a zero magnitude (or smaller than 0.01 p.u.) of the current through a monitored branch indicates an out-of service status of the branch.

Tuning generation and load data: The SCADA PI Historian data is load, branch and generator data scan (typically 10 sec interval) in a period before and after fault for each substation where DFRs triggered. These data were used to update the system load and generation.

The updated model is saved in a new saved case data (\*.sav) which is used for further simulation.

### 3.4.4. *Estimating fault location and evaluating sensitivity to $R_F$*

The fault location solution using GA is performed in the following steps. The outer loop optimization requires iterations with different  $R_F$  in a pre-determined range. The initial population for the inner loop optimization is chosen randomly for this one dimensional (i.e. with one variable  $x$ ) optimization problem. Fault location variable can be chosen from a range of zero to the length of the possible faulted line. Short circuit studies are carried out using PSS/E and the mismatch value from (1) is evaluated for each of the possible fault locations. Now by using three GA operators (selection, crossover and

mutation) fault posing for next iteration is obtained. By iteratively posing faults, running short circuit simulations, evaluating the fitness value, and updating the fault location and resistance, the GA based search engine guides the search process for a globally optimal solution for a given value of  $R_F$ . Now the variance based sensitivity analysis method is used to determine sensitivity of fault location with respect to the fault resistance in the partitioned sub-ranges of  $R_F$ . The sub-range corresponding to least sensitivity is chosen and the minimum mismatch in that range corresponds to the optimal pair of  $(x, R_F)$  for that fault.

### **3.5. Case study**

An actual utility case study is presented here. In the faulted network shown in Figure 3.5, a DFR installed on bus 1 is triggered upon the occurrence of the fault and DFR report indicates the fault is on the line section 1-5 while actually the fault was reported to be 3 miles from bus 8. With our algorithm, the fault is recognized as being either in line section 6-5 or in line section 7-9.

Our software yields much more accurate fault location estimation than what is feasible using other techniques.

Fault resistance range is chosen as 0 per unit to 0.8 per unit and. Fault resistance is changed within its range by increasing its value by 0.008 per unit in each iteration.

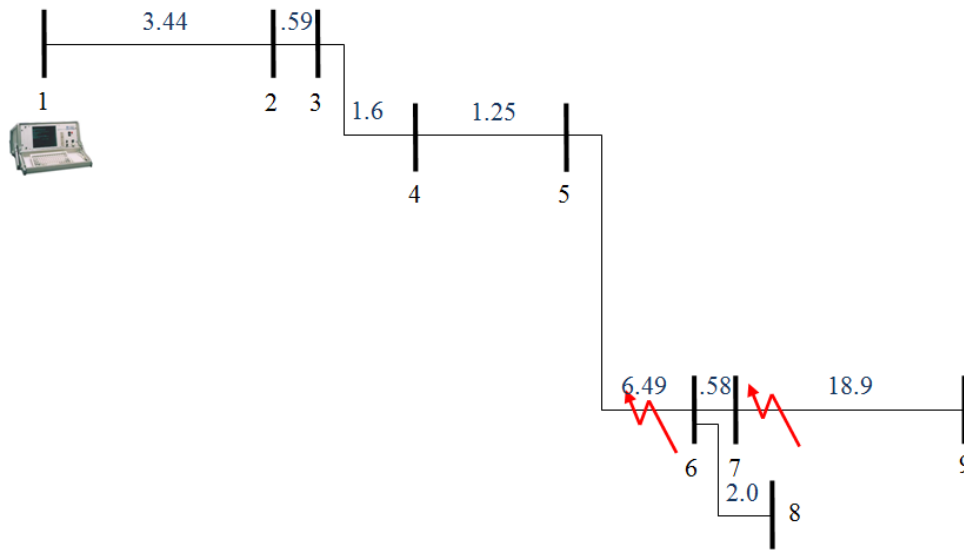


Figure 3.5 Faulty network.

Fault resistance vs. fault location is plotted in Figure 3.6 Sensitivity analysis with respect to fault resistance is performed for several iteration runs and the sensitivity indices corresponding to different sub-ranges of  $R_F$  are presented in Table 3.1.

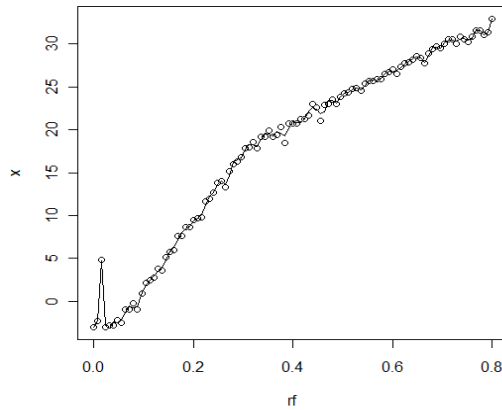


Figure 3.6  $R_F$  vs.  $x$  plot.



This reflects that for fault resistance in the range of 0-0.1 per unit, the sparse measurement based fault location method yields accurate result but after that the algorithm becomes sensitive to the choice of fault resistance.

Table 3.1 Sensitivity to  $R_F$  for different  $R_F$  ranges

Sensitivity to $R_F$ ( $S_{R_F}$ )	Range of $R_F$ (per unit)							
	<i>0-0.1</i>	<i>0.1-0.2</i>	<i>0.2-0.3</i>	<i>0.3-0.4</i>	<i>0.4-0.5</i>	<i>0.5-0.6</i>	<i>0.6-0.7</i>	<i>0.7-0.8</i>
<i>Run 1</i>	0.04	0.98	0.99	0.65	0.71	0.95	0.99	0.99
<i>Run 2</i>	0.02	0.88	0.97	0.94	0.85	0.99	0.84	0.69

### 3.6. Conclusions

Sparse measurement based fault location method is applicable when none of the transmission line ends recorded measurements. The accuracy of this method is influenced by the fault resistance. An intuitive scheme to reduce sensitivity of sparse measurement based fault location with respect to fault resistance is proposed in this section. The proposed fault resistance correction scheme estimates least sensitive pair of fault resistance and fault location using variance based sensitivity analysis. An actual utility case study is reported to show effectiveness of the proposed method. This method can work while measurements from any end of the transmission line is unavailable and it is transparent to fault resistance impact.

## 4. INTEROPERABILITY AND INTEGRATION OF DATA AND MODEL FOR TRANSMISSION LINE FAULT LOCATION

### 4.1. Background

IEEE's definition of *interoperability* is the ability of two or more systems or components to exchange information and to use the information that has been exchanged [53]. According to Grid Wise Architecture Council [54], *interoperability* is the capability of systems or units to provide and receive services and information between each other, and to use the services and information exchanged to operate effectively together in predictable ways without significant user intervention.

Interoperability is a basic building block in the smart grid while standards are key to achieve interoperability. To be interoperable in the context of data and models, a system should plug and play data and models expressed in different formats but having similar descriptions seamlessly, extract useful information from them automatically, and use such information in all power system applications consistently.

The Grid Wise Architecture Council (GWAC) proposed a context-setting interoperability framework (GWAC Stack) [55] to address interoperability requirements (to enable automated information sharing within and between different power system applications) in eight levels of interoperability categories. The interoperability levels with the relevant cross-cutting issues (must be resolved across all the levels to achieve interoperability) are shown in Figure 4.1.

These layers can again be sub-grouped into three major categories:

- **Technical:** Deals with syntax/format and communication of exchanged data
- **Informational:** Deals with semantics of exchanged data
- **Organizational:** Deals with pragmatic aspects of interoperability between organizations or their units.

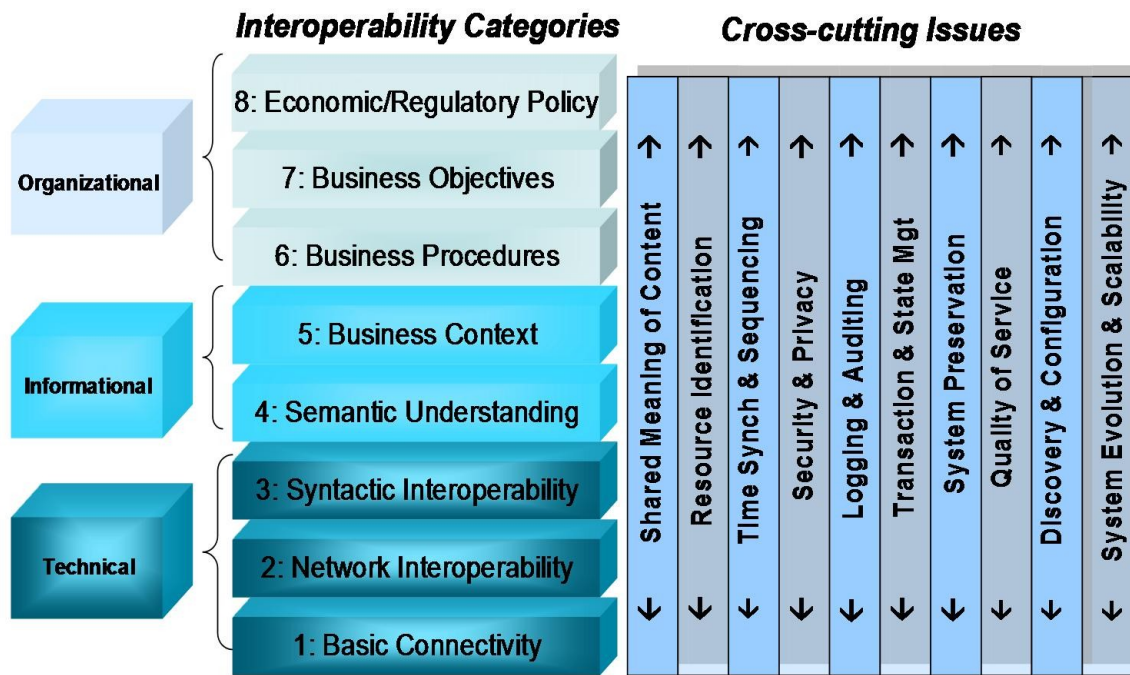


Figure 4.1 GWAC Interoperability Stack.

The interoperability levels from the bottom to the top are:

- **Basic Connectivity:** Mechanism to Establish Physical and Logical Connections of Systems
- **Network Interoperability:** Exchange Messages between Systems across a Variety of Networks

- **Syntactic Interoperability:** Understanding of Data Structure in Messages Exchanged between Systems
- **Semantic Understanding:** Understanding of the Concepts Contained in the Message Data Structures
- **Business Context:** Relevant Business Knowledge that Applies Semantics with Process Workflow
- **Business Procedures:** Alignment between Operational Business Processes and Procedures
- **Business Objectives:** Strategic and Tactical Objectives Shared between Businesses
- **Economic/Regulatory Policy:** Political and Economic Objectives as Embodied in Policy and Regulation

The lower two layers of GWAC stack deal with defining connections and exchanging messages through networks, thereby providing capability of system or units to provide and receive information between each other. Layers 3-4 enable seamless data exchange by understanding the syntax and meaning of the data exchanged. Upper layers 5-8 focus on utilizing information within an application and between several applications. Figure 4.2 shows how data and information flows between all layers.

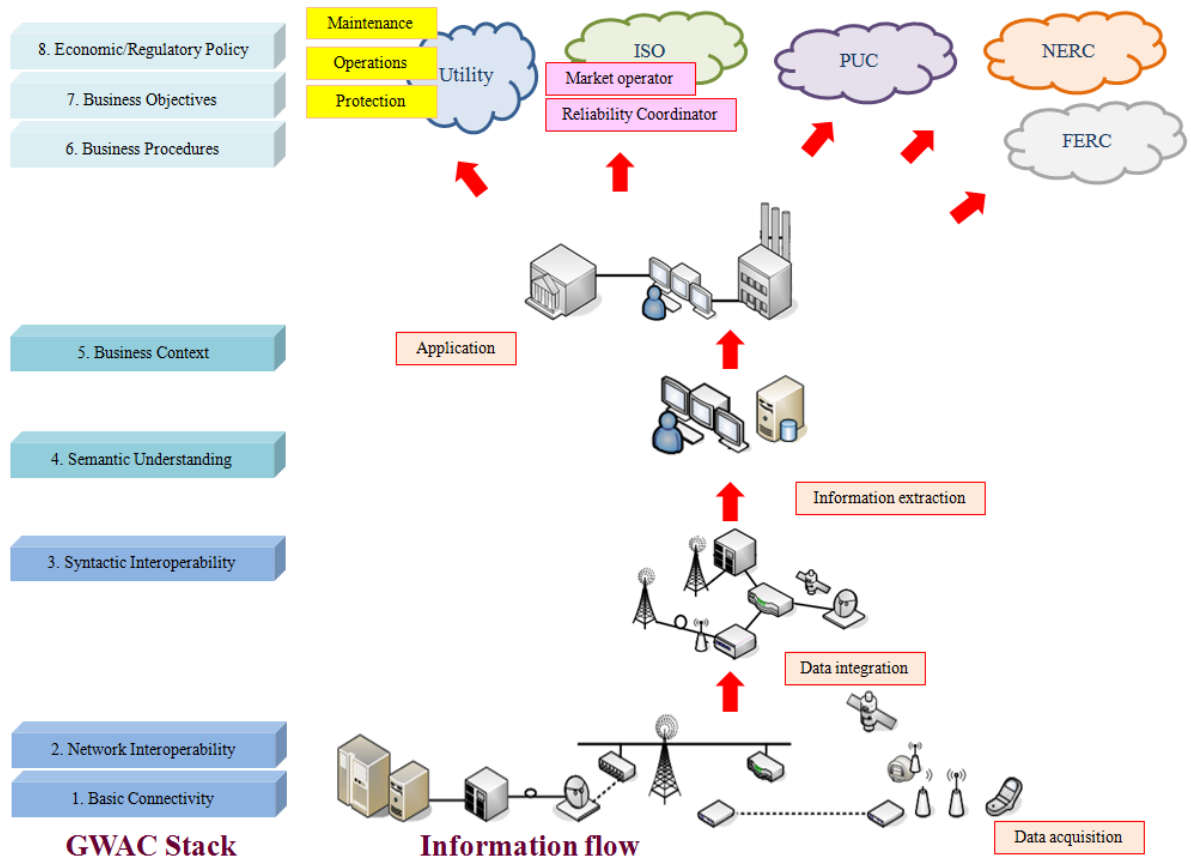


Figure 4.2 GWAC Stack with data and information flow (part of the picture adopted from [56]).

To identify and resolve interoperability within power system models and measured/recorded data in implementing smart grid applications, we are interested in layers 3-4 (Syntactic interoperability to ensure data exchange in a proper syntax and Semantic understanding to interpret exchanged data) of GWAC Stack to consider unified data and information flow across different databases and applications.

Understanding the data structure of the information exchanged and interpreting the information so exchanged, is required by all databases and applications if interoperability is to be achieved. This can be achieved by adopting standardized representation of data and

models. The different types of data and model used in smart grid applications implementation and their standardized representation will be discussed in this section.

## **4.2. Power substation data**

Power system applications use different types of data (measurements) captured and processed in a substation. In this section, we will briefly discuss the different types of data captured/recorded in different devices.

### *4.2.1. Measured data*

Traditionally in a substation, Remote Terminal Units (RTUs) acquire analog measurements such as bus voltages, flows (amps, MW, MVAR), frequency, transformer tap position etc. and status (breaker switching state) signals and send them to the energy management systems (EMS) in every two to ten seconds. These are called supervisory control and data acquisition system (SCADA) scans and those measurements are gathered in a SCADA database in a centralized location.

With the rapid advancement of technology, large scale deployment of intelligent electronic devices (IEDs) became a reality. Different types of IEDs are used in practice: DPR (Digital protective relay), DFR (Digital fault recorder), SER (Sequence of event recorder), etc. When triggered by an event, these computer-based devices can record a huge amount of data (both analog and status) with a much higher sampling rate than SCADA scans. The substation analog signals at high power level are measured and transformed to instrumentation level using current and voltage instrument transformers. The signals are then filtered, digitized, and processed in IEDs. Finally, the measurement data is extracted and supplied in digital computer words as output of these devices. This is

the typical measurement chain for the data acquisition. Various databases are used to store these data and make it available for further processing.

The third type of data acquisition devices, phasor measurement units (PMUs) continuously calculate time-synchronized phasors with high sampling rates. Phasor data concentrators (PDC) gather PMU measurements from all the substations to a centralized location.

#### *4.2.2. Configuration data*

Substation data captured also consists of a configuration data which is the syntactic meaning of what is contained in the captured data fields. This file lists the input channel names and numeric designations and type and unit of data (voltage, current, status) corresponding to the actual data file. This file also contains information regarding the sampling rate of the IED used, starting time of data captured, etc.

### **4.3. Power system models**

Two representations of power networks are in use simultaneously by different applications. Node-breaker or real-time model represents actual connections between nodes, breakers and isolator switches. Bus-branch or planning model is a less detailed model where power network is represented by buses (combination of several nodes connected by closed circuit breakers) and branches connecting them [57].

### **4.4. Integration of data and model**

The basic idea of integration of substation data is to collect all the IED data and SCADA data in a substation database and use it for extracting information automatically

and then utilizing the extracted information for several power system applications. The functional diagram for substation data flow is shown in Figure 4.3.

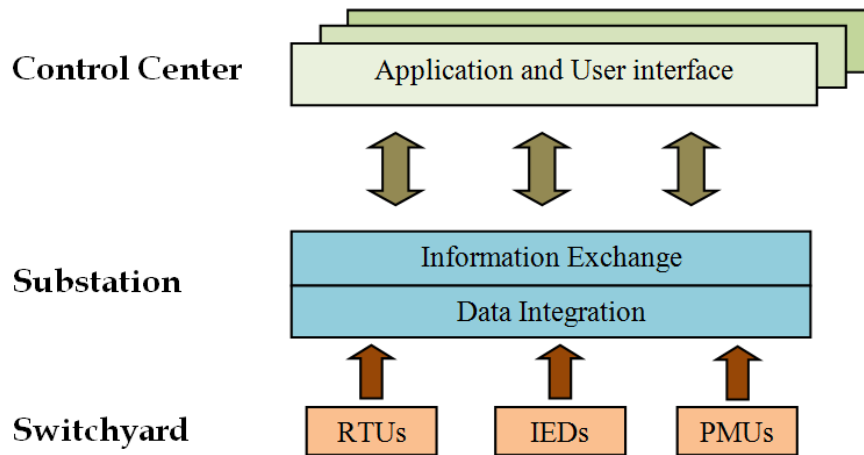


Figure 4.3 Functional diagram for substation data flow.

To import all the measured data into the central repository requires means of data format conversion and communication among different IEDs. In addition to the automatically retrieved IED and RTU data, the database should contain several other data and model, such as:

- Static system model containing description of the system components and their connections (i.e. topology)
- State estimation scans (SCADA PI historian data) which may be used to tune the static system model with real time data



- Substation interpretation data that allows one to correlate the naming convention of recording devices and of the static system model and with PI Historian data.

Although, integrating a huge amount of data provides improved information by exploiting redundancy, the quality of data is also a major concern. Distortion in magnitude and phase angle of current and voltage signal is introduced in each stage of the measurement chain. Ideally the output waveform should be an exact replica of the input signal, but the error introduced in several data processing stages makes the output distorted. Thus the quality of data depends largely on the performance of devices used in the measurement chain. The performance of these devices and the information extraction schemes are discussed elaborately in [58]. In that report we have done an extensive survey of performance of different IEDs in present day substations. The accuracy characteristics of the total measurement chain for a typical substation data is presented in that report. The issues related to extracting useful information from raw data and integrating that information to enhance the substation database are also covered there.

#### **4.5. Standards used to describe data and model**

Several standards, either in use or proposed for data description and exchange purposes, are prepared by both IEEE and IEC. [59]-[60]. The Smart Grid Interoperability Panel also has defined a catalog of standards to achieve interoperability in the proposed smart grid [61]. Related standards for data and model representation are [51], [62]-[74]. Table 4.1 lists related standards used to describe data and model interpretation and exchange. Figure 4.4 shows the layers 3-4 of GWAC stack with related standards.

Table 4.1 Standards to describe data and model interpretation and exchange

<b>Standard No.</b>	<b>Standard Name</b>	<b>Purpose</b>
IEEE C37.2-2008	IEEE Standard for Electrical Power System Device Function Numbers, Acronyms, and Contact Designations	Device numbering scheme
IEEE C37.111-1999	IEEE Standard Common Format for Transient Data Exchange (COMTRADE) for Power Systems	Exchange of transient data captured in IEDs to applications
IEEE C37.118-2005	IEEE Standard for Synchrophasors for Power Systems	Measurement requirements and data format for PMU measurements and communication between PMU and PDC
IEEE C37.118.1-2011	Standard for Synchrophasor Measurements for Power Systems	Measurement requirements and data format for PMU measurements
IEEE C37.118.2-2011	Standard for Synchrophasor Data Transfer for Power Systems	Communication of phasor measurements
IEEE C37.232-2007	IEEE Recommended Practice for Naming Time Sequence Data Files	Naming convention of time sequence data files
IEEE C37.239-2010	IEEE Standard Common Format for Event Data Exchange (COMFEDE) for Power Systems	Common data format for event data exchange
IEC 61850-6	Communication networks and systems for power utility automation - Part 6: Configuration description language for communication in electrical substations related to IEDs	Specify data format for IEDs. Describes substation equipments and configuration in details
IEC 61850-90-5	Communication networks and systems for power utility automation Part 90-5: Use of IEC 61850 to transmit synchrophasor information according to IEEE C37.118	Integration of PMU (data expressed as in IEEE C37.118) into IEC 61850 environment
IEC 61970	Energy management system application program interface (EMS-API)	Application program interfaces to integrate EMS applications by exchanging information. The semantics for this API is called CIM
IEC 61968	Application integration at electric utilities - System interfaces for distribution management	Same as IEC 61970 but applied to distribution management
IEC 61588 Ed.2 (2009-02) (IEEE 1588-2008)	Precision Clock Synchronization Protocol for Networked Measurement and Control Systems	Synchronization requirements of PMU measurements
IEEE C37.238-2011	IEEE Standard Profile for Use of IEEE 1588 Precision Time Protocol in Power System Applications	Profile for application of IEEE 1588 to power applications

Syntactic interoperability needs understanding of the syntax for data exchange. Common data formats for IEDs are described in IEEE C37.111 [63] and those of PMUs are described in IEEE C37.118 [64] (also in new IEEE C37.118.1 standard [65]). IEEE C37.239 [68] describes common data formats for event data exchange. SCL (IEC 61850-6 [69]) provides description for substation equipment and their configuration as well as data formats for IEDs. IEEE C37.118.2 [65] covers the communication issues of synchrophasor measurements. IEC TC57 added a new standard IEC 61850-90-5 [70] with IEC 61850 which defines PMU as a logical node in the 61850 environment and cover the communication issues of synchrophasor measurements. IEC 61850-90-5 and IEEE C37.118.2 are complementary standards.

Semantic understanding requires interpreting exchanged data. CIM (combined IEC 61968 & 61970) contains semantics for data modeling and information sharing across control center applications. SCL has the semantics of data modeling and sharing inside a substation. IEEE C37.2 [62] and IEEE C37.232 [67] help understanding naming convention of devices and time sequence data files respectively. IEC 61588 (IEEE 1588) [73] helps understanding the synchronization requirements for time-tagged measurements. IEEE C37.238 [74] describes a common profile for Precision Time Protocol (PTP) for power system applications (extension of IEEE 1588).

Among those standards, we will primarily use three of them to represent data and models.

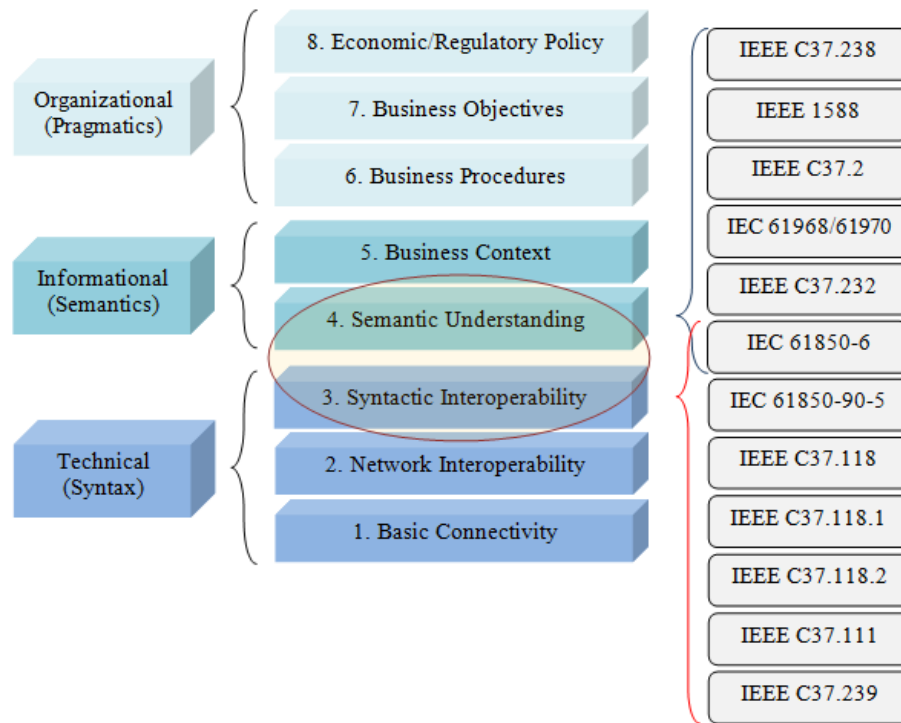


Figure 4.4 GWAC Stack with related standards.

#### 4.5.1. Common information model (CIM) [71]

CIM (IEC 61970) is an abstract model representing all objects in an electric utility typically contained in EMS information model [71]. CIM represents common semantics for classes and attributes for these objects as well as their relationships which are defined using object-oriented modeling techniques (unified modeling language, UML). CIM has been implemented in eXtensible Markup Language (XML) to provide a comprehensive power system data exchange format within control center. CIM consists of several interrelated packages of models. Each package contains a number of defined classes and one or more class diagrams showing their relationships graphically. Descriptions of class

packages which are relevant to this project (to develop a CIM profile to describe power system model) are shown in Table 4.2.

Table 4.2 Packages of common information model

Package	Class		
	Name	Description	Base Class
<b>Core:</b> Contains definition of the parent classes which are inherited in classes defined in other packages.	IdentifiedObject	Provides common naming attributes to the classes needing that.	
	BaseVoltage	Collection of base voltages is presented in this class.	IdentifiedObject
	GeographicalRegion and SubGeographicalRegion	Represents a geographical region and a subset of geographical region.	IdentifiedObject
	PowerSystemResource	It can be equipment, a collection of equipments or an organizational entity.	IdentifiedObject
	ConnectivityNodeContainer	A base class for all objects that may contain ConnectivityNodes or TopologicalNodes (in topology package).	
	Equipment and ConductingEquipment	Equipments are parts of the power system that are physical devices and ConductingEquipments are those that carry current.	Equipments, PowerSystemResource
	Terminal	This is an electrical connection point to a piece of conducting equipment.	ConductingEquipment
	EquipmentContainer	A modeling construct to provide a root class for all Equipment classes.	
	Substations, Bays and Voltage Levels	They are used to model aggregation of equipments.	EquipmentContainer
<b>Topology:</b> Defines how the equipments are electrically connected in the network.	ConnectivityNode	These are points where terminals of conducting equipments are connected together with zero impedance.	IdentifiedObject

Table 4.2 Continued

Package	Class		
	Name	Description	Base Class
<b>Wires:</b> Defines all pieces of equipments electrically connected in the network.	Line	They represent part of the power system extending between adjacent substations.	EquipmentContainer
	Conductor	These are combination of conducting materials with consistent electrical characteristics.	ConductingEquipment
	ACLineSegment	These are used to carry alternating currents.	Conductor
	PowerTransformer	A device consisting of two or more coupled windings.	Equipment
	TransformerWindings	They represent winding at each terminal of a power transformer.	ConductingEquipment
	Switch	They close or open one or more electric circuits.	ConductingEquipment
	Breaker and Disconnecter	They close or open one or more electric circuits.	Switch
	BusbarSection	They connect with other conducting equipment within a substation.	ConductingEquipment
	RegulatingControl	Set of equipments work together to control a power system quantity.	PowerSystemResouce
	RegulatingCondEq	They are conducting equipment which regulate a power system quantity.	ConductingEquipment
	SynchronousMachine	They operate synchronously within a power system.	RegulatingCondEq
EnergyConsumer	Point of energy consumption.	ConductingEquipment	
<b>Generation:</b> Contains different types of generators in two packages: Production and GenerationDynamics.	GeneratingUnit	Single or set of synchronous machines.	Equipment
<b>Meas:</b> Defines measurements taken from a particular power system resource.	Measurement	Represents any measured or calculated or non-measured or non-calculated quantity.	IdentifiedObject
	MeasurementValue	Represents value of measurement.	Measurement

#### 4.5.2. Substation configuration language (SCL) [69]

SCL (IEC 61850-6) is a standard to describe substation configuration allowing semantic interpretation of substation data. This is also expressed in XML but the data model is not defined using UML. Substation functions are modeled into different logical nodes (LN) which are grouped under different logical devices (LD). Data exchanged between LNs are modeled as data objects, which consist of data attributes. The different components of SCL are described in Table 4.3.

Table 4.3 Contents of substation configuration language

Section	Object
<b>Substation section:</b> describes functional structure of substation in terms of LNs and IEDs associated.	<b>Substation</b> <b>VoltageLevel:</b> electrically connected part of substation having same voltage level. <b>Bay:</b> part or subfunction of substation within same voltage level. <b>ConductingEquipment</b> <b>SubEquipment</b> <b>ConnectivityNode</b> <b>Terminal</b> <b>Function</b> <b>Subfunction</b> <b>PowerTransformer</b> <b>TransformerWinding</b>
<b>Communication section:</b> communication connections between IEDs	Not used
<b>IED section:</b> describes configuration of IEDs and LNs associated	<b>IED</b> <b>Server:</b> Communication entity within an IED <b>LDevice:</b> LD contained in server of IED <b>LNode:</b> LN contained in LD of IED <b>DO:</b> Data contained in LN
<b>Data Type section:</b> describes data objects contained in LNs defined for IEDs	Not used

The following files types are the components of SCL:

- **System Specification Description (SSD):** single line diagram of substation and logical nodes.
- **IED Capability Description (ICD):** capabilities of an IED.
- **Substation Configuration Description (SCD):** complete substation configuration.
- **Configured IED Description (CID):** an instantiated IED with all configuration parameters relevant to that IED.

#### 4.5.3. *IEEE standard common format for transient data exchange (COMTRADE) [51]*

COMTRADE describes syntax of the following files extracted from the raw measurements captured by substation IEDs:

- **Configuration files (\*.cfg):** information for interpreting the allocation of measured data to the equipment (input channels) for a specific substation.
- **Data files (\*.dat):** analog and digital sample values for all input channels (described in configuration file) in substation.

## 4.6. Conclusions

This section addresses interoperability issues in smart grid context. Different types of power system data and model used for smart grid applications implementation are discussed. Data exchange standards used to interpret data and model are discussed while some key standards are explored. These discussions are important for understanding interoperable implementation of fault location algorithms, which allows any algorithm developed in the future to be seamlessly integrated with the available data.



## 5. UNIFIED REPRESENTATION OF DATA AND MODEL FOR TRANSMISSION LINE FAULT LOCATION

### 5.1. Background

This section addresses the need of unified representation of data and model for improving smart grid applications like fault disturbance monitoring and fault location.

Power system components exposed to different weather, as well as human and animal contacts are subject to several types of faults which are caused by random and unpredictable events. Therefore a power system operator should always remain alert by monitoring disturbances caused by faults. Fault disturbance monitoring consists of the following stages:

1. **Detection of event:** An event is a disturbed power system condition which can be triggered by several causes and can be of different types (fault is one of them).
2. **Measurement and alarm (M&A) processing:** A major disturbance can trigger numerous alarms and most of them may be redundant or false. Alarm processors analyze alarm messages and extract information explaining events. It also uses measurements of analog waveforms to draw final conclusions.
3. **Fault detection:** From the information extracted from the alarm processor, the faulted region is detected by cause-effect analysis of alarms and measurements.

4. **Fault location:** An exact location of fault is required to help the maintenance crew find and repair the faulted equipment as soon as possible. It is calculated using samples from the transient waveforms.

A fault disturbance monitoring scheme requires adequate information (measurements data as well as power system modeling information) to perform all these four steps successfully.

Figure 5.1 shows the data & information flow in an advanced fault disturbance monitoring implementation. It is evident that all four applications need to communicate with all databases and models and also between them which sometimes results in duplicate information extraction and exchange. As the substations are generally modeled in a detailed node-breaker model while the power system static model is a less detailed bus-branch model, the names and numeric designations of the same power system components described in those two models may become different due to different nomenclature used by various utility groups that maintain given models and data acquisition devices. Nomenclature used in IED database follows that of substation model while nomenclature used in SCADA database follows the similar yet less-detailed static system model expressed in bus-branch. It requires nomenclature correlation tables to correlate between them, which is a very cumbersome process as for each substation separate nomenclature correlation tables are required. Therefore, a significant number of mappings between all types of data and model are required to create a unified correlation between the nomenclatures. Sometimes the mapping has to be done manually or semi-automatically resulting in longer operating time.

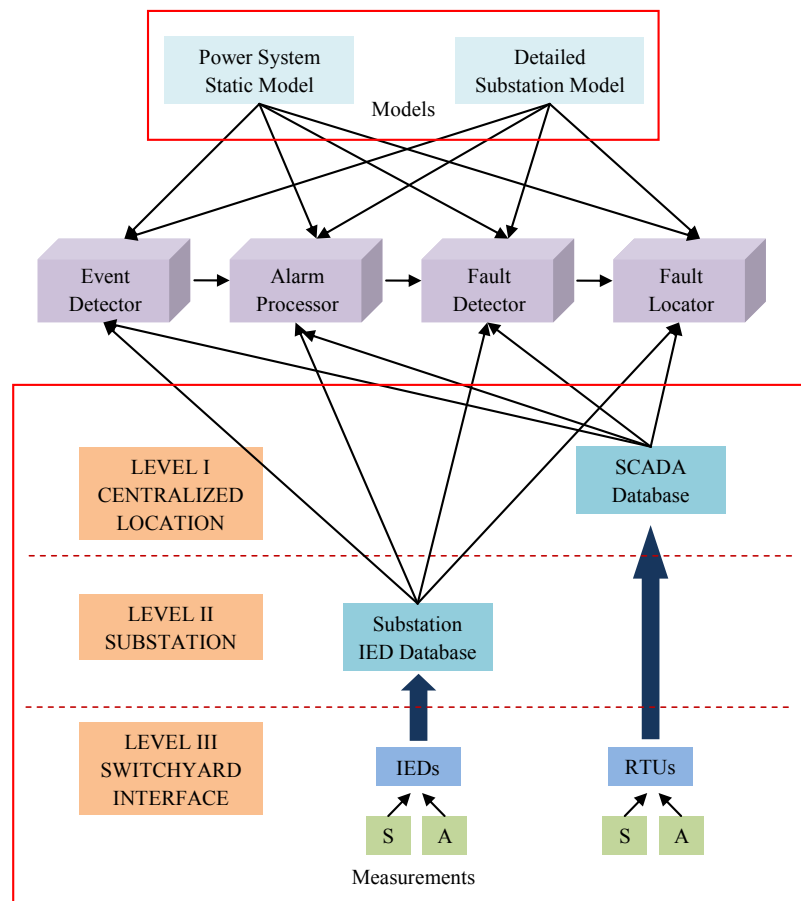


Figure 5.1 Data and information flow for fault disturbance monitoring.

As a result, the following issues are hindering interoperability and integration of data and model for this application:

- Field data collected from various IEDs from different vendors has different data format and information contents.
- Sampling rates and techniques for IED data and SCADA Historian archived data sampling are different.

- The names and numeric designations are different for the same power system components.

Such differences need to be reconciled when interoperability of data and model are sought, and this has to happen at both the semantic and syntactic levels.

Therefore to speed up system restoration under fault disturbances a scheme to represent data and model used in this application in a unified form is required which should have the following features:

- Reduce number of mappings between data and model.
- Correlate different types of data and model without any user intervention.

A unified representation of data and model is proposed which will resolve interoperability issues by using standardized representation of data and models and correlating automatically using several intuitive steps.

## **5.2. Unified representation of data and model**

Data exchange standards play a major role in automatic exchange of data and information through different applications and within a database. To achieve unified representation of data and models data exchange standards are needed to interpret and exchange data captured in several IEDs and RTUs (from different vendors, having different sampling rates and different naming and nomenclature designations for power system components) and correlating proprietary defined power system models. Although an all-encompassing standard (which may include all the features) is almost impossible to create, we can still unify all related standards (by unifying complementary data models and

harmonizing overlapping standard semantics) to expedite automation of fault disturbance monitoring from data and information integration interoperability perspective.

A unified representation of data and model is shown in Figure 5.2. The proposed solution [75]-[78] uses standard formats of data and model (CIM for describing power system model and SCADA data; SCL for describing substation model and COMTRADE for describing event data triggered by IEDs) all expressed in node-breaker representation and by using simple rules for representing those data and models interoperability can be achieved.

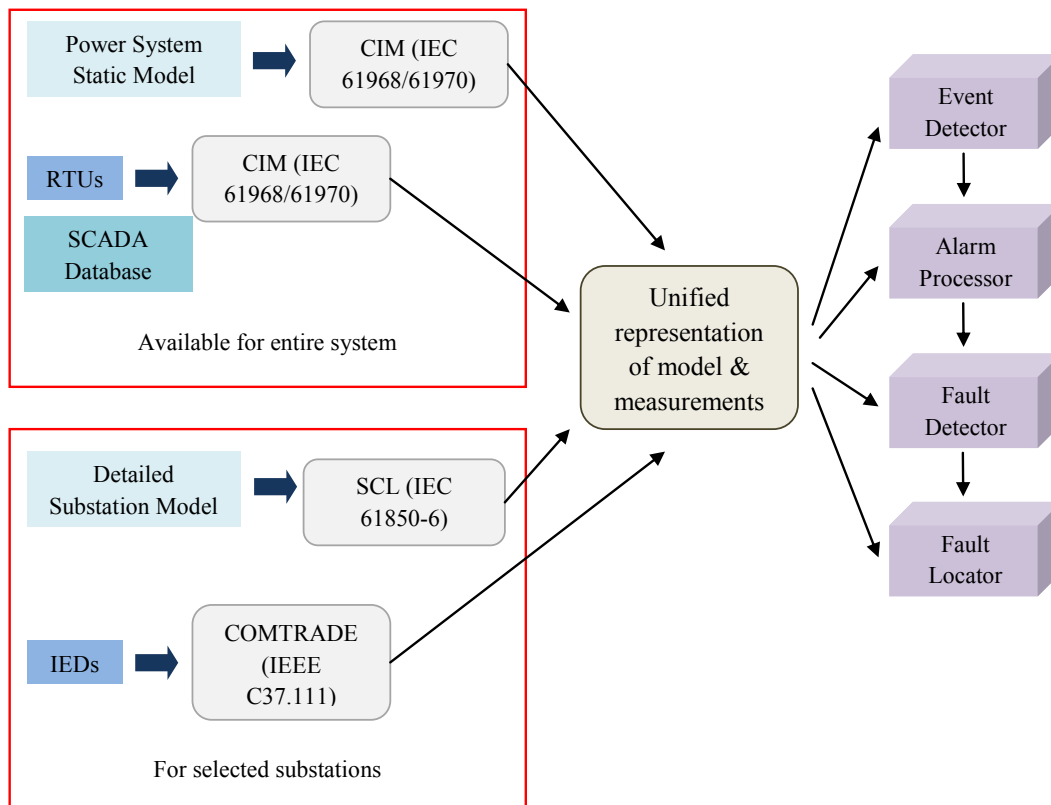


Figure 5.2 Unified representation of data and model.

Correlation of COMTRADE files with SCL is easy as they correspond to same substation model. Mapping is required only to correlate between the model and measurements represented in CIM and that of SCL to obtain a uniform representation. Though both CIM and SCL are described in node-breaker model and most of the objects are modeled in a similar way and share same name, some discrepancies are also present.

Several harmonization efforts to properly use CIM and SCL standards can be found in literature [79]-[82]. Formal integration of CIM and SCL by bi-directional mapping between them is addressed in [79]. Mapping for topology processing application is proposed in [80]. Harmonizing these two standards to develop a unified semantic model is discussed in EPRI report [81]. In [82] mismatches between those two standards are addressed and solutions for all types of mismatches are proposed without modifying the original CIM and SCL information model.

The correlation between CIM profile and SCL profiles of different substations is done using the following simple rules:

- **For similar objects:** Common data structure is used to represent those objects present in both standards.
- **For dissimilar objects:** Some objects are defined in either of the standards, for those no mapping is needed. Separate data structures for each model are used.

By using the very simple rules mentioned above, data and models used in this fault location application are represented in a unified way. That way automatic correlation can be achieved. Besides, the information extracted from the data and model representation can be used properly in the application.

### 5.3. Illustration of unified representation

#### 5.3.1. Data and model for the test case

The unified representation of data and model is implemented on a small power system model for simplicity of description. As there are no standard test cases available for both CIM model and SCL model, we have used the following model data and took some assumptions to artificially generate a fault case:

A small power system network (expressed in CIM model) is chosen, which is obtained from a sample system used in [83]. The detailed node-breaker representation of the power system network is shown in Figure 5.3.

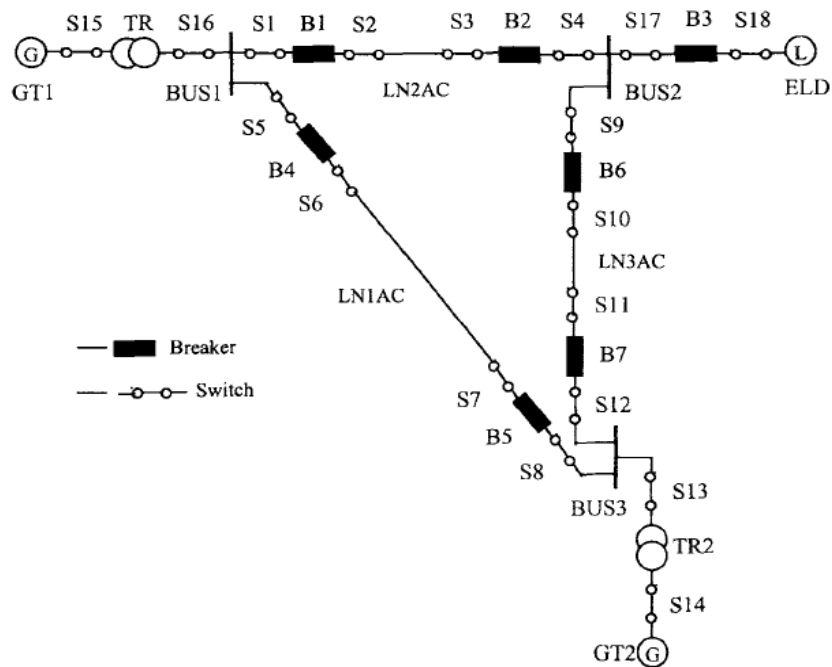


Figure 5.3 Node-breaker representation of small power network [83].

Several faults on the line between Bus-2 and Bus-5 are considered. We are assuming that DFR installed on Bus-4 is triggered due to the fault. Figure 5.4 shows the bus-branch representation of the faulted power system network.

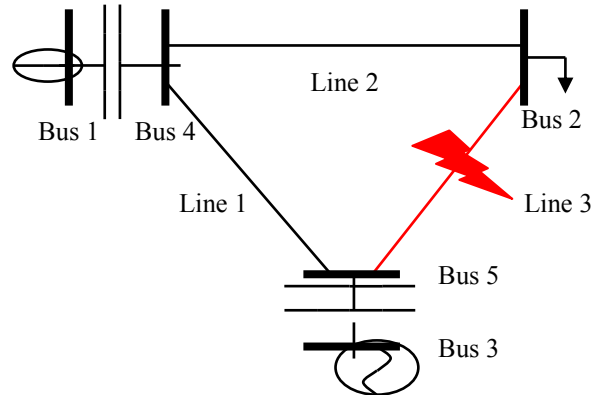


Figure 5.4 Bus-branch representation of small power network.

The fault is simulated in ATP [38] and the pre-fault, during-fault and post-fault voltage and current signals at Bus-4 are recorded and converted to COMTRADE format using the Output Processor [84].

As no corresponding SCL models are available for the substation 1 (Bus-4), example from IEC 61850-6 standard is used. The detailed node-breaker diagram for the substation is shown in Figure 5.5.



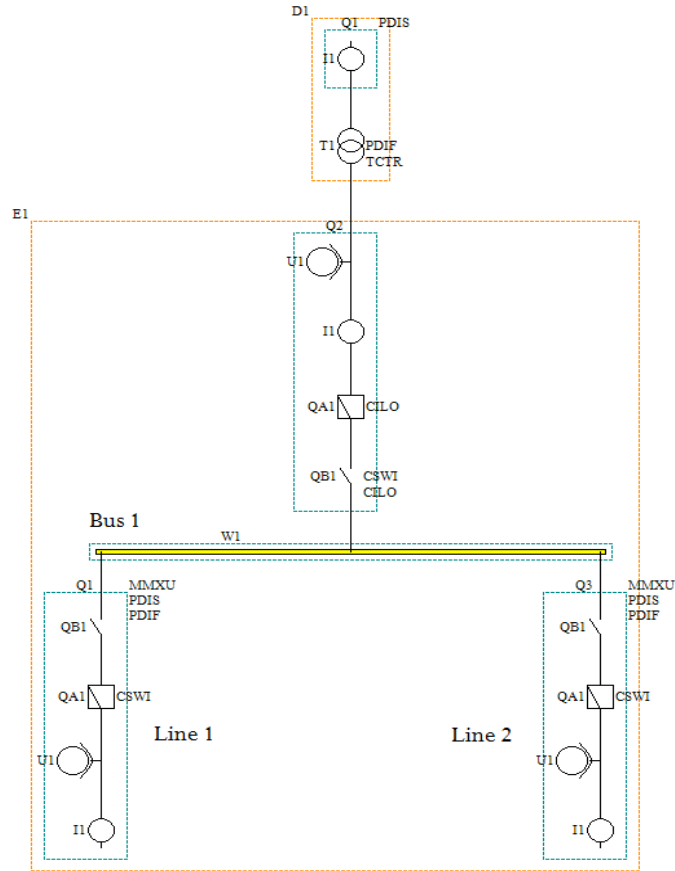


Figure 5.5 Node breaker representation of Substation-1.

The following changes are made in the above models for uniformity:

- a. As the voltage levels in CIM model and SCL models were different we have changed the voltage level in SCL model to that of CIM.
- b. In SCL a switch and breaker combination (QB1 & QA1) is present between Busbar (W1) and transformer (T1) while in CIM only a switch (S16) is present between Bus1 and TR1. For uniformity we have added a breaker (B8) between S16 and TR1 in substation -1 in CIM xml file.

### 5.3.2. *Implementation procedure*

The detailed implementation procedure is discussed in brief:

#### ***Representation of power system static model***

A CIM profile of power system objects needed to model static power system is chosen. All the equipments (generator, load, line, transformer, breaker, disconnecter etc.) have one or two terminals. Connectivity nodes are points where terminals of conducting equipments are connected together with zero impedance. In CIM connectivity and topology of power network can be determined by terminals and connectivity nodes and switch status. Topology of the system changes with change of switching status of breakers and disconnectors.

Power system static model in base case for the small network expressed in CIM XML file [83] is processed in the following steps:

1. The XML file is parsed and all the objects with same nomenclature with the XML file are assigned with the values obtained from the XML file.
2. *Topological node for base case determination:* Topological Node is a set of connectivity nodes that, in the current network state, are connected together through any type of closed switches, including jumpers. Topological nodes can change as the current network state changes (i.e., switches, breakers, etc. change state). A topological node corresponds to *bus* in equivalent bus-branch model. All topological nodes for the base case are determined using the algorithm presented in [85]. The algorithm starts from primary equipment (i.e. generator, transformer, load, line) and scans through all closed switches and

groups the connectivity nodes associated in a single topological node and stops when another primary equipment is found. The node-breaker representation of the static power system model is shown in Figure 5.6 (all of the switches are closed). Small black dots represent terminals and large black dots represent connectivity nodes. Bus-branch model of the same network by creating topological nodes (in box with dash lines) is shown in Figure 5.7.

3. *Selection of pNode:* A primary node (pNode) is selected [57]. In the topological node determination algorithm, the 1<sup>st</sup> connectivity node in a topological node is usually a primary equipment; therefore the 1<sup>st</sup> connectivity node in a topological node is selected as pNode. The other connectivity nodes in that topological node point that pNode which corresponds to bus in equivalent bus-branch model. The pNodes in all the topological nodes are shown in Figure 5.7.
4. *Extraction of PSS/E data:* As our fault location method uses short circuit program in PSS/E, the PSS/E raw data (expressed in bus branch representation) is extracted [85]-[86] where the bus names are actually the connectivity node names and therefore no nomenclature correlation between node-breaker model and bus-branch model is required.

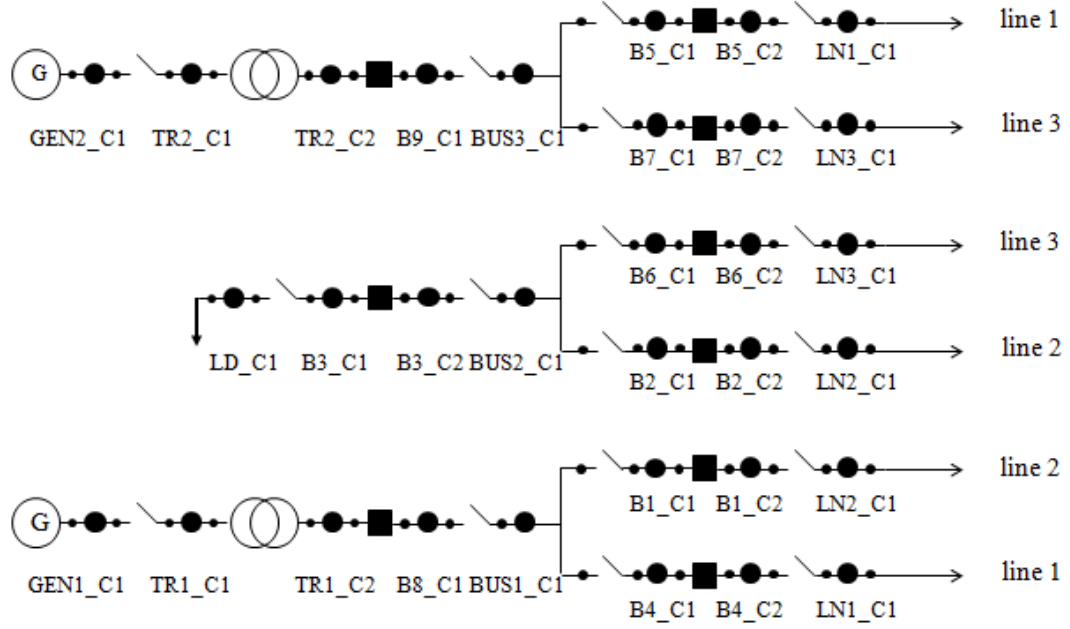


Figure 5.6 Node-breaker representation with terminals and connectivity nodes

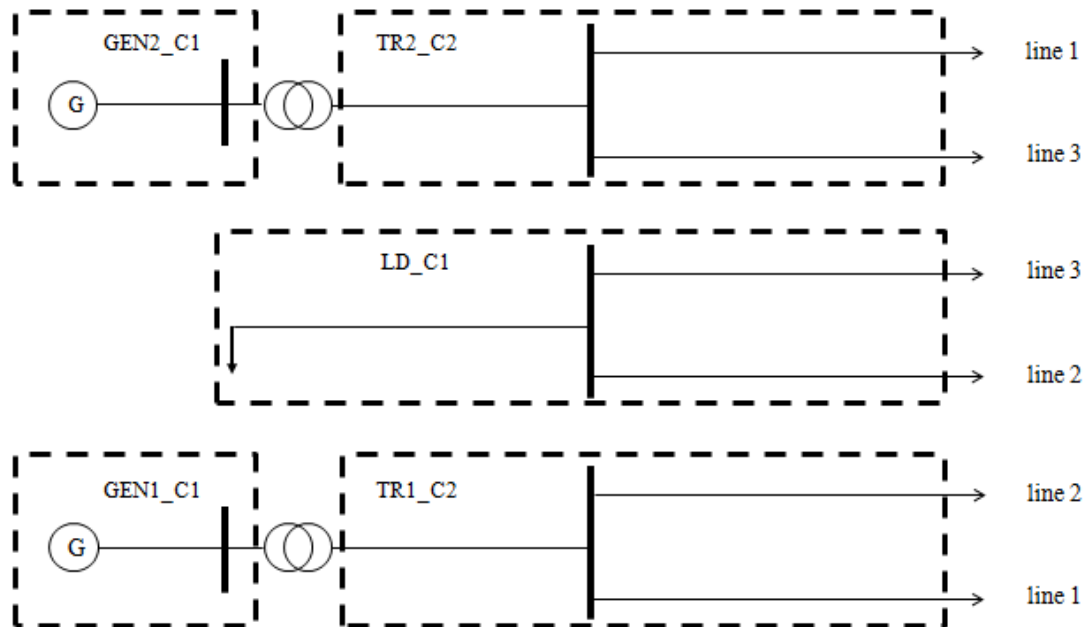


Figure 5.7 Bus-branch representation with topological nodes

### ***Tuning static system model***

Power system static model should be updated with the pre-fault conditions (switching changes and load/generation changes). CIM dynamic file [87] consists of measurement data with time stamps. As we don't have this, a model of the small power system in ATP is used to generate measurements. Breaker and disconnector status updates are used to perform incremental topology processing [57] where topological nodes are recreated with changed switch status.

### ***Representing substation model in SCL***

In SCL substation functions are modeled into different logical nodes (LN) which are grouped under different logical devices (LD). All the logical nodes are associated to IEDs. Data exchanged between LNs are modeled as data objects, which consist of data attributes. SCL file for a selected substation is processed using the following steps:

1. The XML file is parsed and all the objects with same nomenclature with the XML file are assigned with the values obtained from the XML file.
2. For objects present in CIM (i.e. power transformer, voltage level etc.) both CIM and SCL names are stored so that no naming correlation required later. (discussed in next section).
3. The IED names correspond to the logical nodes for measurement purpose are stored which helps finding the COMTRADE file for the recorder.

## ***Representing event data in COMTRADE***

The raw measurement captured in DFR present in the substation are processed with the knowledge obtained from the configuration file (\*.cfg) of the data (\*.dat) in COMTRADE.

### ***Unified representation***

The unified representation of data and model is achieved using the following rules:

1. Common data structures are used for similar objects. For example both of the models have substation object in common. Figure 5.8 shows the CIM representation and Figure 5.9 shows the SCL representation.

```
<cim:Substation rdf:ID="_ID_SUBSTATION1">
  <cim:IdentifiedObject.name>Substation1</cim:IdentifiedObject.name>
  <cim:IdentifiedObject.localName>Substation1</cim:IdentifiedObject.localName>
  <cim:Substation.Region rdf:resource="#_ID_SubGeographicalRegion"/>
</cim:Substation>
<cim:VoltageLevel rdf:ID=" ID SUB1 VLevel 220KV EF4559BF7EB">
<cim:VoltageLevel rdf:ID=" ID SUB1 VLevel 15KV EEF4559BF7EB">
```

Figure 5.8 Substation object in CIM

```
<Substation name="S12" desc="Substation1">
  <Text />
  <VoltageLevel sxy:x="10" sxy:y="10" name="D1" xmlns:sxy="http://www.iec.ch/61850/2003/SCLcoordinates">
  <VoltageLevel sxy:x="10" sxy:y="185" name="E1" xmlns:sxy="http://www.iec.ch/61850/2003/SCLcoordinates">
</Substation>
```

Figure 5.9 Substation object in SCL

A class substation defined in our program has the following description:

```
Substation.name.cim="Substation1"
```

```
Substation.name.scl="S12"
```

```
Substation.VoltageLevel.high.name.cim="Substation-1 220KV"
```

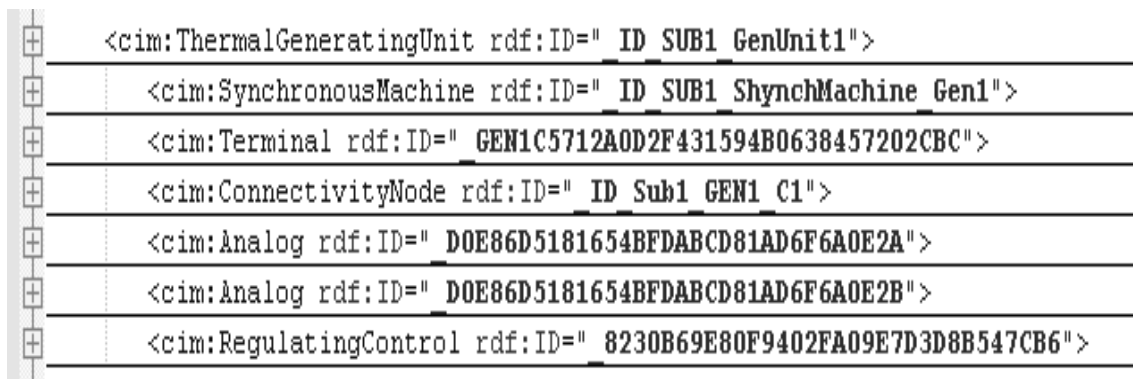
```
Substation.VoltageLevel.low.name.cim="Substation-1 15KV"
```

```
Substation.VoltageLevel.high.name.scl="E1"
```

```
Substation.VoltageLevel.low.name.scl="D1"
```

The other objects inside Substation object are defined in same fashion.

2. Separate data structures for each model for dissimilar objects. For example CIM has ThermalGeneratingUnit but SCL doesn't. Figure 5.10 shows the CIM representation.



```
<cim:ThermalGeneratingUnit rdf:ID=" ID SUB1 GenUnit1">  
  <cim:SynchronousMachine rdf:ID=" ID SUB1 ShynchMachine Gen1">  
    <cim:Terminal rdf:ID=" GEN1C5712A0D2F431594B0638457202CBC">  
      <cim:ConnectivityNode rdf:ID=" ID Sub1 GEN1 C1">  
        <cim:Analog rdf:ID=" DOE86D5181654BFDABCD81AD6F6A0E2A">  
          <cim:Analog rdf:ID=" DOE86D5181654BFDABCD81AD6F6A0E2B">  
            <cim:RegulatingControl rdf:ID=" 8230B69E80F9402FA09E7D3D8B547CB6">
```

Figure 5.10 ThermalGeneratingUnit object in CIM

A class ThermalGeneratingUnit within substation is defined in our program has the following description:

Substation.ThermalGeneratingUnit.name="GEN1"

3. In some cases both similar and dissimilar objects are present which represent same electrical equipment. Both common and separate data structures within the object are used. For example both CIM and SCL have PowerTransformer object while SCL also include IED associated to that (TCTR i.e. current transformer LN here). Figure 5.11 shows the CIM representation and Figure 5.12 shows the SCL representation of PowerTransformer.

```
<cim:PowerTransformer rdf:ID=" ID PowerXfr TR1">
  <cim:TransformerWinding rdf:ID=" ID TR1 W1">
    <cim:Terminal rdf:ID=" T1W1C5712A0D2F431594B0638457202CBC">
      <cim:ConnectivityNode rdf:ID=" ID TR1 W1 C1">
    <cim:TransformerWinding rdf:ID=" ID TR1 W2">
      <cim:Terminal rdf:ID=" T1W2C5712A0D2F431594B0638457202CBC">
        <cim:ConnectivityNode rdf:ID=" ID TR1 W2 C1">
```

Figure 5.11 PowerTransformer object in CIM

```
<PowerTransformer sxy:x="386" sxy:y="95" name="T1">
  <Text />
  <LNNode lnInst="1" lnClass="PDIF" iedName="D1Q1BP2" ldInst="F1">
  <LNNode lnInst="1" lnClass="TCTR" iedName="D1Q1SB1" ldInst="C1">
  <TransformerWinding name="W1">
  <TransformerWinding name="W2">
</PowerTransformer>
```

Figure 5.12 PowerTransformer object in SCL



A class PowerTransformer within substation defined in our program which has the following description:

```
Substation.PowerTransformer.name.cim="TR1"
```

```
Substation.PowerTransformer.name.scl="T1"
```

```
Substation.PowerTransformer.Lnode.iedname="D1Q1SB1"
```

4. SCADA measurements are updated in the following classes:

```
Substation.VoltageLevel.high.Meas.value
```

```
Substation.VoltageLevel.high.Meas.type
```

```
Substation.VoltageLevel.high.Meas.accuracy
```

5. Name and corresponding measurement channels for IEDs are located from SCL. If an IED is triggered, corresponding COMTRADE files (configuration and data) can be located from the database using the name of the IED. Figure 5.13 shows a part of SCL corresponding to triggered IED.

A class within Substation.VoltageLevel.high is defined which corresponds to measurements (as MMXU corresponds to measuring unit LN in SCL). For the measuring unit corresponding IED name and analog measurement channel are also stored. The class and subclasses are shown below:

```
Substation.VoltageLevel.high.mmxu.iedname="E1Q1SB1"
```

```
Substation.VoltageLevel.high.mmxu.iedname.CTR.name="I1"
```

```

<VoltageLevel sxy:x="10" sxy:y="185" name="E1" xmlns:sxy="http://www.iec.ch/61850/2003/SCLcoord"
  <Text />
  <Voltage unit="V" multiplier="k">220000</Voltage>
  <Bay sxy:x="10" sxy:y="320" name="Q1">
    <Text />
    <LNode lnInst="1" lnClass="MXU" iedName="E1Q1SB1" ldInst="C1">
    <LNode lnInst="1" lnClass="PDIS" iedName="E1Q1BP3" ldInst="F1">
    <LNode lnInst="1" lnClass="PDIF" iedName="E1Q1BP2" ldInst="F1">
    <ConductingEquipment sxy:x="183" sxy:y="75" name="QA1" type="CBR">
    <ConductingEquipment sxy:x="183" sxy:y="15" name="QB1" type="DIS">
    <ConductingEquipment sxy:x="183" sxy:y="135" name="U1" type="VTR">
    <ConductingEquipment sxy:x="183" sxy:y="195" name="I1" type="CTR">
    <Text />
    <Terminal connectivityNode="S12/E1/Q1/L3" substationName="S12" voltageLevelName="E1" bay
    <Terminal connectivityNode="S12/E1/Q1/L4" substationName="S12" voltageLevelName="E1" bay
    <SubEquipment name="A" phase="A">
      <Text />
      <LNode desc="CT phase Line1" lnInst="1" lnClass="TCTR" iedName="E1Q1SB1" ldInst="C1">
        <Text />
      </LNode>
    </SubEquipment>

```

Figure 5.13 Part of SCL corresponding to triggered IED

By using the rules mentioned above, correlation between data and models are achieved automatically. After correlation of data and model, required information (voltage and current phasors for pre-fault and faulted network for each of the monitored channel mentioned in COMTRADE configuration file, status of the breakers from COMTRADE data file, relay trip signals from COMTRADE data file, SCADA measurements) are extracted as in [24].

#### 5.4. Conclusions

This section explores barriers to implementation of fault disturbance monitoring applications. A unified representation of data and model is proposed, which uses

standardized representation of data and model and uses simple but intuitive schemes to correlate data and models thereby achieve interoperability in implementation. Seamless integration of power system data and model information for effective fault location implementation is demonstrated in this section. This allows future expansions of the ways how data and fault location algorithms are integrated.

## 6. CONCLUSIONS

### 6.1. Contributions

The main achievements and contributions of this research are summarized as:

- *Two end synchronous sampling based transmission line fault detection, classification and location method:* A simple yet efficient fault analysis method to detect, classify and locate transmission line faults using synchronized samples of voltage and current from both (all) transmission line ends is proposed. The proposed method is setting-free and transparent to fault resistance, different transmission line layouts, applicable to high resistance faults; detect, classify and locates fault with a very high accuracy while using moderate sampling rate for voltage and current measurement waveforms.
- *Sparse measurement based transmission line fault location method with fault resistance sensitivity corrections:* An efficient scheme for reducing the impact of fault resistance on the sparse measurement fault location algorithm for transmission line is proposed. Sparse measurement based fault location method [23] is applicable when none of the transmission line ends recorded measurements but the accuracy is influenced by the fault resistance. The proposed fault resistance correction scheme estimates least sensitive pair of fault resistance and fault location using variance based sensitivity analysis. The proposed method can be applied with limited measurements while it is still being transparent to fault resistance impacts.

- *An interoperable implementation using unified representation of data and model:* A unified representation of data and model is proposed which uses standardized representation of data and model (using node-breaker representation) and uses simple but intuitive schemes to correlate data and models. Seamless integration of data and model is achieved thereby enabling interoperability in fault location implementation

## **6.2. Conclusions**

The following conclusions were observed while implementing main contributions of this dissertation:

1. Two-end synchronous sampling based fault analysis method:
  - It detects and classifies faults very accurately and quickly. Using pre and post event samples it can detect whether the disturbance is a fault within  $\frac{1}{2}$  of nominal frequency cycle of event inception.
  - It is suitable for online fault analysis including fault detection, classification and location in the cases relay operation needs to be classified in real time.
  - It does not require elaborate parameter settings for detection thresholds.
  - It is transparent to the effects of fault resistance and the use of transmission line models, which makes it very easy to implement.
  - The method depends on accurate representation of a transmission line model and as a result produces very accurate fault location results.

- Due to the presence of modern circuit breakers opening in less than two cycles, limited post fault waveform signal is available to be captured by the recorders, and this method is applicable in that situation.
  - The method is tested for several fault cases varying fault distance, fault resistance, and fault inception angle simulated in an IEEE test case, and accurate fault detection, classification and location is demonstrated.
  - The method can successfully detect and classify which line is faulted in case of parallel lines and even can detect cross-line faults. For the location part, only the transmission line that is faulted is used to estimate the location.
  - The method can discriminate load level changes from fault cases, and it can be used to validate relay trip decisions.
2. Sparse measurement based fault location method with fault resistance sensitivity correction:
- It can estimate fault location and fault resistance value even if the measurement from the ends of the faulty line are unavailable.
  - A correction scheme to reduce the impact of fault resistance which is an unpredictable parameter in fault location estimation procedure is proposed.
  - To achieve better accuracy, this method takes advantage of waveform data recorded by IEDs and archived data measured by SCADA RTUs.
  - The fault resistance compensation process is automated to allow practical use in actual power network application.

### 3. Unified representation of data and model:

- Extracting useful information from both operational data (data captured continuously by RTUs and stored in SCADA) and non-operational data (data captured upon occurrence of an event by IEDs) in an automated way, which significantly enhances situational awareness, is achieved.
- It is shown how to update static power system model with pre-fault conditions using information from both SCADA and IED data.
- The proposed approach performs seamless translation between bus-branch and node-breaker model representation of power system and correlate data captured with power system model without any user intervention to achieve interoperability.
- The approach reduces significant number of mappings and data exchanges (sometimes redundant) between several data and models which simplify software design tremendously and make future updates easier.

## REFERENCES

- [1] M. Kezunovic, B. Perunicic, "Fault Location," Wiley Encyclopedia of Electrical and Electronics Terminology, Wiley Encyclopedia of Electrical and Electronics Engineering, John Wiley, New York, Vol.7, pp. 276-285, 1999.
- [2] M. Kezunovic, et al, "IEEE Guide for Determining Fault Location on the Transmission and Distribution Lines," IEEE C37.144-2004.
- [3] M. Kezunovic, "Smart Fault Location for Smart Grids," IEEE Transactions on Smart Grid, Vol. 2, No. 1, pp 11-22, Mar. 2011.
- [4] T. Takagi, Y. Yamakoshi, J. Baba, K. Uemura, T. Sakaguchi, "A New Algorithm of an Accurate Fault Location for EHV/UHV Transmission Lines: Part I-Fourier Transformation Method," IEEE Transactions on Power Apparatus and Systems, Vol. 100, No. 3, pp. 1316–1323, Mar. 1981.
- [5] T. Takagi, Y. Yamakoshi, M. Yamaura, R. Kondow, T. Matsushima, "Development of a New Type Fault Locator Using the One-Terminal Voltage and Current Data," IEEE Transactions on Power Apparatus and Systems, Vol. 101, No. 8, pp. 2892-2898, Aug. 1982.
- [6] L. Eriksson, M. M. Saha, G. D. Rockefeller, "An Accurate Fault Locator with Compensation for Apparent Reactance in the Fault Resistance Resulting from Remote End Infeed," IEEE Transactions on Power Apparatus and Systems, Vol. 104, No. 2, pp. 423-436, Feb. 1985.



- [7] M. T. Sant, Y. G. Paithankar, "On line digital fault locator for overhead transmission line," IEE proceedings, Vol. 126, No. 11, pp. 1181-1185, Nov. 1979.
- [8] Y. Liao, S. Elangovan, "Digital distance relaying algorithm for first-zone protection for parallel transmission lines," IEE Proceedings- Generation, Transmission and Distribution, Vol. 145, No. 5, pp. 531-536, Sep. 1998.
- [9] J. Izykowski, E. Rosolowski, M. M. Saha, "Locating faults in parallel transmission lines under availability of complete measurements at one end," IEE Proceedings- Generation, Transmission and Distribution, Vol. 151, No. 2, pp. 268-273, Mar. 2004.
- [10] Edmund O. Schweitzer, III, "Evaluation and development of transmission line fault locating techniques which use sinusoidal steady- state information," Proceedings of the 9th Annual Western Protective Relay Conference, Spokane, WA, Oct. 1982.
- [11] B. Jeyasurya, M. A. Rahman, "Accurate fault location of transmission lines using microprocessors," 4th International Conference on developments in power protection, pp. 13-17, Apr. 1989.
- [12] M. S. Sachdev, R. Agarwal, "A technique for estimating line fault locations from digital impedance relay measurements," IEEE Transactions on Power Delivery, Vol. 3, No. 1, pp. 121-129, Jan. 1988.
- [13] D. A. Tziouvaras, J. B. Roberts, G. Benmouyal, "New multi-ended fault location design for two- or three-terminal lines," 7th International Conference on Developments in Power System Protection, Amsterdam, Netherlands, pp. 395-398. Apr. 2001.

- [14] A. T. Johns, S. Jamali, "Accurate fault location technique for power transmission lines," IEE Proceedings- Generation, Transmission and Distribution, Vol. 137, Pt. C, No. 6, pp. 395-402, Nov. 1990.
- [15] D. Novosel, D.G. Hart, E. Udren, J. Garitty, "Unsynchronized two-terminal fault location estimation," IEEE Transactions on Power Delivery, Vol. 11, No. 1, pp.130-138, Jan. 1996.
- [16] A. A. Gigris, D. G. Hart, and W. L. Peterson, "A new fault location technique for two- and three-terminal lines," IEEE Transactions on Power Delivery, Vol. 7, No. 1, pp. 98-107, Jan. 1992.
- [17] M. Kezunovic, B. Perunicic, J. Mrkic, "An accurate fault location algorithm using synchronized sampling," Electric Power Systems Research Journal, Vol. 29, No. 3, pp. 161-169, May 1994.
- [18] A. Gopalakrishnan, M. Kezunovic, S. M. McKenna, and D. M. Hamai, "Fault location using distributed parameter transmission line model," IEEE Transactions on Power Delivery, Vol. 15, No. 4, pp. 1169–1174, Oct. 2000.
- [19] S. M. Brahma, A. A. Gigris, "Fault location on a transmission line using synchronized voltage measurements," IEEE Transactions on Power Delivery, Vol. 19, No. 4, pp. 1619-1622, Oct. 2004.
- [20] L. Lewis, "Travelling Wave Relations Applicable to Power-System Fault Locators," AIEE Transactions, Vol. 70, No. 2, pp. 1671-1680, Jul. 1951.

- [21] P. F. Gale, P. A. Crossley, B. Xu, Y. Ge, B. J. Cory, J. R. G. Barker, "Fault location based on travelling waves," 5th International Conference on Developments in Power System Protection, pp. 54-59, Mar. 1993.
- [22] F. Gale, J. Stokoe, P. A. Crossley, "Practical experience with travelling wave fault locators on Scottish Power's 275 & 400 kV transmission system," 6th International Conference on Developments in Power System Protection, pp. 192-196, Mar. 1997.
- [23] M. Kezunovic, Y. Liao, "Fault location estimation based on matching the simulated and recorded waveforms using genetic algorithms," 7th International Conference on Development in Power System Protection, pp. 399-402, Apr. 2001.
- [24] M. Kezunovic, P. Dutta, "Fault location using sparse wide area measurement," CIGRE Study Committee B5 Annual Meeting and Colloquium, Jeju, South Korea, Oct. 2009.
- [25] M. S. Sachdev, M. A. Baribeau, "A new algorithm for digital impedance relays," IEEE Transactions on Power Apparatus and Systems, Vol. 98, No. 6, pp. 2232-2240, Nov. 1979.
- [26] A. A. Girgis, "A new Kalman filtering based digital distance relay," IEEE Transactions on Power Apparatus and Systems, Vol. 101, No. 9, pp. 3471-3480, Sep. 1982.
- [27] M. Kezunovic, I. Rikalo, D. J. Sobajic, "High Speed Fault Detection and Classification with Neural Nets," Electric Power Systems Research Journal, Vol. 34, No. 2, pp. 109-116, Aug. 1995.

- [28] N. Zhang, M. Kezunovic, "Coordinating Fuzzy ART Neural Networks to Improve Transmission Line Fault Detection and Classification," IEEE Power & Energy Society General Meeting, San Francisco, California, Jun. 2005.
- [29] B. Das, J. V. Reddy, "Fuzzy Logic Based Fault Classification Scheme for Digital Distance Protection," IEEE Transactions on Power Delivery, Vol. 20, No. 2, pp. 609-616, Apr. 2005.
- [30] O. A. S. Youssef, "Combined Fuzzy-Logic Wavelet-Based Fault Classification Technique for Power System Relaying," IEEE Transactions on Power Delivery, Vol. 19, No. 2, pp. 582-589, Apr. 2004.
- [31] B. Mahamedi, "A Novel Setting-Free Method for Fault Classification and Faulty Phase Selection by Using a Pilot Scheme," 2nd International Conference on Electric Power and Energy Conversion Systems (EPECS), Nov. 2011.
- [32] M. Kezunovic, B. Perunicic, "Automated transmission line fault analysis using synchronized sampling at two ends," IEEE Transactions on Power Systems, Vol. 11, No. 1, pp. 441-447, Feb. 1996.
- [33] N. Zhang, M. Kezunovic, "A Real Time Fault Analysis Tool for Monitoring Operation of Transmission Line Protective Relay," Electric Power Systems Research Journal, Vol. 77, No. 3-4, pp. 361-370, Mar. 2007.
- [34] J. -A. Jiang, J. -H. Yang, Y. -H. Lin, C. -W. Liu, J. -C. Ma, "An adaptive PMU based fault detection/location technique for transmission lines. I. Theory and algorithms," IEEE Transactions on Power Delivery, Vol. 15, No. 2, pp. 486-493, Apr. 2000.

- [35] Y. -H. Lin, C. -W. Liu, C. -S. Chen, "A new PMU-based fault detection/location technique for transmission lines with consideration of arcing fault discrimination-part I: theory and algorithms," IEEE Transactions on Power Delivery, Vol. 19, No. 4, pp. 1587-1593, Oct. 2004.
- [36] Mathworks Inc., "Cubic spline data interpolation," Sep. 2013. [Online]. Available: <http://www.mathworks.com/help/matlab/ref/spline.html>
- [37] P. S. Barnett, "The analysis of travelling waves on power system transmission lines," PhD Thesis, University of Canterbury. Electrical Engineering, 1974.
- [38] EMTP, "Alternative Transients Program," Dec. 2010. [Online]. Available: <http://www.emtp.org/>
- [39] V. V. Terzija, H. -J. Koglin. "On The Modeling of Long Arc in Still Air And Arc Resistance Calculation," IEEE Transactions on Power Delivery, Vol. 19, No. 3, pp. 1012 - 1017, Jul. 2004.
- [40] M. B. Djuric, Z. M. Radojevic, V. V. Terzija. "Time Domain Solution Of Fault Distance Estimation And Arcing Faults Detection On Overhead Lines," IEEE Transactions on Power Delivery, Vol. 14, No. 1, pp. 60-67, Jan. 1999.
- [41] G. Preston, Z. M. Radojević, C. H. Kim, V. V. Terzija, "New settings-free fault location algorithm based on synchronised sampling," IET Generation, Transmission & Distribution, Vol. 5, No. 3, pp. 376 - 383, Mar. 2011.
- [42] R. Zivanovic, "Evaluation of transmission line fault-locating techniques using variance based sensitivity measures," 16th Power System Computation Conference, Glasgow, Scotland, Jul. 2008.

- [43] R. Zivanovic, H. B. Ooi, "A Systematic Approach for Testing Transmission Line Fault-Locating Techniques," Electricity 2007 Conference, The Electric Energy Society of Australia (EESA), Melbourne, Australia, Aug. 2007.
- [44] A. Phadke, et. al., "Synchronized Sampling and Phasor Measurements for Relaying and Control," IEEE Transactions on Power Delivery, Vol. 9, No. 1, pp. 442-452, Jan. 1994.
- [45] OSISoft, "PI Historian." [Online]. Available: <http://www.osisoft.com/>
- [46] PSS<sup>TM</sup>E Load Flow ©Siemens Power Transmission & Distribution, Inc., PTI, Schenectady, NY, USA.
- [47] D. E. Goldberg, Genetic Algorithms in Search, Optimization and Machine Learning, Addison Wesley, Reading, MA, 1989.
- [48] Papiya Dutta, Mladen Kezunovic, "Fault Resistance Sensitivity of Sparse Measurement Based Transmission Line Fault Location," 43rd North American Power Symposium (NAPS 2011), Boston, USA, Aug. 2011.
- [49] R. L. Eubank, Nonparametric Regression and Spline Smoothing, Marcel Dekker, N.Y., Basel, 1988.
- [50] I. M. Sobol, "Sensitivity Analysis for Non-linear Mathematical Models," Mathematical Modeling & Computational Experiment, Vol. 1, No. 4, pp. 407-414, 1993.
- [51] IEEE Standard Common Format for Transient Data Exchange, IEEE Standard C37.111-1999, Mar. 1999.

- [52] Test Laboratories International, Inc. “DFR Assistant - Software for Automated Analysis and Archival of DFR records with Integrated Fault Location Calculation.” [Online]. Available: <http://www.tli-inc.com>
- [53] IEEE, “IEEE Standard Computer Dictionary: A Compilation of IEEE Standard Computer Glossaries,” New York, 1990.
- [54] The GridWise Architecture Council, “Introduction to Interoperability and Decision Maker’s Interoperability Checklist, v1.5,” Aug. 2010. [Online]. Available: [http://www.gridwiseac.org/pdfs/gwac\\_decisionmakerchecklist\\_v1\\_5.pdf](http://www.gridwiseac.org/pdfs/gwac_decisionmakerchecklist_v1_5.pdf)
- [55] The GridWise Architecture Council, “GridWise® Interoperability Context-Setting Framework,” Mar. 2008. [Online]. Available: [http://www.gridwiseac.org/pdfs/interopframework\\_v1\\_1.pdf](http://www.gridwiseac.org/pdfs/interopframework_v1_1.pdf)
- [56] Grant Gilchrist, “An Overview of Smart Grid Standards,” (PPT) Nov. 2008. [Online]. Available: [http://cio.nist.gov/esd/emaildir/lists/t\\_and\\_d\\_interop/pdf00001.pdf](http://cio.nist.gov/esd/emaildir/lists/t_and_d_interop/pdf00001.pdf)
- [57] S. Grijalva, “Integrating Real-Time Operations and Planning using Same-Format Power System Models,” IEEE Power & Energy Society General Meeting, Florida, Jun. 2007.
- [58] M. Kezunovic, T. Overbye, C. Davis, J. Tate, P. Dutta, “Integration of Substation IED Information into EMS Functionality,” PSERC Report #08-08, Aug. 2008.
- [59] IEEE, “Approved & Proposed IEEE Smart Grid Standards,” [Online]. Available: <http://smartgrid.ieee.org/standards/ieee-approved-proposed-standards-related-to-smart-grid>

- [60] IEC, “Core IEC Standards,” [Online]. Available:  
<http://www.iec.ch/smartgrid/standards/>
- [61] SGIP, “SGIP Catalog of Standards.” [Online]. Available:  
<http://collaborate.nist.gov/twiki-sggrid/bin/view/SmartGrid/SGIPCatalogOfStandards>
- [62] IEEE Standard for Electrical Power System Device Function Numbers, Acronyms, and Contact Designations, IEEE Standard C37.2-2008, Oct. 2008.
- [63] IEEE Standard Common Format for Transient Data Exchange, IEEE Standard C37.111-1999, Mar. 1999.
- [64] IEEE Standard for Synchrophasors for Power Systems, IEEE Standard C37.118-2005, Mar. 2006.
- [65] IEEE Standard for Synchrophasor Measurements for Power Systems, IEEE Standard C37.118.1-2011, Dec. 2011.
- [66] IEEE Standard for Synchrophasor Data Transfer for Power Systems, IEEE Standard C37.118.2-2011, Dec. 2011.
- [67] IEEE Recommended Practice for Naming Time Sequence Data Files, IEEE Standard C37.232-2007, Aug. 2007.
- [68] IEEE Standard Common Format for Event Data Exchange (COMFEDE) for Power Systems, IEEE Standard C37.239-2010, Nov. 2010.
- [69] IEC, “Communication networks and systems for power utility automation - Part 6: Configuration description language for communication in electrical substations related to IEDs,” IEC Standard 61850-6.



- [70] IEC, “Communication networks and systems for power utility automation - Part 6: Use of IEC 61850 to transmit synchrophasor information according to IEEE C37.118,” IEC Standard 61850-90-5.
- [71] IEC, “Energy management system application program interface (EMS-API) ,” IEC Standard 61970.
- [72] IEC, “Application integration at electric utilities - System interfaces for distribution management,” IEC Standard 61968.
- [73] IEEE Standard for a Precision Clock Synchronization Protocol for Networked Measurement and Control Systems, IEC Standard 61588: 2009(E), Feb. 2009.
- [74] IEEE Standard Profile for Use of IEEE 1588 Precision Time Protocol in Power System Applications, IEEE Standard C37.238-2011, Jul. 2011.
- [75] P. Dutta, M. Kezunovic, “Unified representation of data and model for sparse measurement based fault location,” Proceedings of IEEE PES General Meeting 2012, San Diego, Jul. 2012.
- [76] M. Kezunovic, S. Grijalva, Papiya Dutta, Ayusman Roy, “The Fundamental Concept of Unified Generalized Model and Data Representation for New Applications in the Future grid,” Proceedings of the 45th HICCS Hawaii International Conference on System Sciences, Hawaii, pp. 2096-2103, Jan. 2012.
- [77] Mladen Kezunovic, Papiya Dutta, “The Role of Data Exchange Standards in Developing Automated Fault Disturbance Monitoring,” 6th International Workshop on Deregulated Electricity Market Issues in South-Eastern Europe (DEMSEE 2011), Bled, Slovenia, Sep. 2011.

- [78] M. Kezunovic, Papiya Dutta, S. Grijalva, Ayusman Roy, “The Smart Grid Needs: Model and Data Interoperability, and Unified Generalized State Estimator,” PSERC Report #12-22, Aug. 2012.
- [79] T. Kostic, O. Preiss, C. Frei, “Towards the Formal Integration of Two Upcoming Standards: IEC 61970 and IEC 61850,” 2003 Large Engineering Systems Conference on Power Engineering, pp. 24-29, May 2003.
- [80] Y. Pradeep, P. Seshuraju, S.A. Khaparde, V.S. Warriar, S. Cherian, “CIM and IEC 61850 integration issues: Application to power systems,” IEEE Power & Energy Society General Meeting, Calgary, Canada, Jul. 2009.
- [81] EPRI, “Harmonizing the International Electrotechnical Commission Common Information Model (CIM) and 61850 Standards via a Unified Model: Key to Achieve Smart Grid Interoperability Objectives,” EPRI, Palo Alto, CA, Report #1020098, May 2010.
- [82] R. Santodomingo, J.A. Rodríguez-Mondéjar, M.A. Sanz-Bobi, “Solving the Mismatches between the Electric System Ontologies,” The International IFIP Working Conference on Enterprise Interoperability, Estocolmo, Suecia. Mar. 2011.
- [83] M. Shahidehpour, Y. Wang, Communication and Control in Electric Power Systems: Applications of Parallel and Distributed Processing, Wiley-IEEE Press, pp. 149-163, Jun. 2003.
- [84] PQSoft, “TOP, The Output Processor,” [Online]. Available: <http://www.pqsoft.com/top/>

- [85] A. W. McMorran, G. W. Ault, I. M. Elders, C. E. T. Foote, G. M. Burt, J. R. McDonald, "Translating CIM XML Power System Data to a Proprietary Format for System Simulation," IEEE Transactions on Power Systems, Vol. 19, No. 1, pp. 229-235, Feb. 2004.
- [86] EPRI, "Common Information Model Primer," EPRI, Palo Alto, CA, Report #1024449, USA, Nov. 2011.
- [87] Y. Pradeep, P. Seshuraju, S. A. Khaparde, R. K. Joshi, "CIM-Based Connectivity Model for Bus-Branch Topology Extraction and Exchange," IEEE Transactions on Smart Grid, Vol. 2, No. 2, pp. 244-253, Jun. 2011.

## APPENDIX A

### Journal papers:

1. Papiya Dutta, Ahad Esmaeilian, Mladen Kezunovic, "Transmission Line Fault Analysis Using Synchronized Sampling," Accepted for publication in IEEE Transactions on Power Delivery.
2. C. Pang, P. Dutta, M. Kezunovic, "BEVs/PHEVs as Dispersed Energy Storage for V2B Uses in the Smart Grid," IEEE Transactions on Smart Grid, Special Issue on Transportation Electrification and Vehicle-to-Grid Applications, Vol. 3, No. 1, pp 473-482, March 2012.

### Conference papers:

1. Ahmad Abdullah, Ahad Esmaeilian, Gurunath Gurralla, Papiya Dutta, Tomo Popovic, Mladen Kezunovic, "Test Bed for Cascading Failure Scenarios Evaluation," International Conference on Power System Transients-IPST 13, Vancouver, Canada, July 2013.
2. P. Dutta, M. Kezunovic, "Unified representation of data and model for sparse measurement based fault location," Proceedings of IEEE PES General Meeting, San Diego, July 22-26, 2012.
3. M. Kezunovic, S. Grijalva, Papiya Dutta, Ayusman Roy, "The Fundamental Concept of Unified Generalized Model and Data Representation for New Applications in the Future grid," Proceedings of the 45th HICCS Hawaii International Conference on System Sciences, Hawaii, January 4-7, 2012.

4. Mladen Kezunovic, Papiya Dutta, "The Role of Data Exchange Standards in Developing Automated Fault Disturbance Monitoring," 6th International Workshop on Deregulated Electricity Market Issues in South-Eastern Europe (DEMSEE 2011), Bled, Slovenia, Sept. 2011.
5. Papiya Dutta, Mladen Kezunovic, "Fault Resistance Sensitivity of Sparse Measurement Based Transmission Line Fault Location," 43rd North American Power Symposium (NAPS 2011), Boston, USA, Aug. 2011.
6. Nikhil Kumar, Papiya Dutta, Le Xie, "Optimal DG Placement for Congestion Mitigation and Social Welfare Maximization," 43rd North American Power Symposium (NAPS 2011), Boston, USA, Aug. 2011.
7. C. Pang, P. Dutta, S. Kim, M. Kezunovic, I. Damnjanovic, "PHEVs as Dynamically Configurable Dispersed Energy Storage for V2B Uses in the Smart Grid," 7th Mediterranean Conference on Power Generation, Transmission Distribution and Energy Conversion (MedPower 2010), Cyprus, Nov. 2010.
8. M. Kezunovic, Papiya Dutta, "Fault location using sparse wide area measurements," CIGRE Study Committee B5 Annual Meeting and Colloquium, Jeju, Korea, Oct. 2009.
9. P. Dutta, Y. Guan, M. Kezunovic "Use of Substation IED Data for Improved Alarm Processing and Fault Location," 40th North American Power Symposium (NAPS 2008), Calgary, Canada, Sept. 2008.

## APPENDIX B

IEEE 118 bus test system fault cases:

1. Case 2

Table B.1 Summary of fault detection, classification and location (IEEE 118 bus test system: Case 2)

Fault Type	Fault Location (mi)	Fault Resistance ( $\Omega$ )	Fault Inception Angle (degree)	Actual Fault Inception Time (s)	Detected Fault Type	Calculated Fault Inception Time (s)	Time to detect (ms)	Calculated Fault Location (mi)	Fault Location % Error
ag	6.25 (5%)	0	0	0.02	ag	0.0248	4.8	10.23	3.18
	25.02 (20%)				ag	0.0252	5.2	27.79	2.21
	62.55 (50%)				ag	0.0250	5	62.93	0.31
	6.25 (5%)	20	0	0.02	ag	0.0249	4.9	10.48	3.38
	25.02 (20%)				ag	0.0251	5.1	27.88	2.29
	62.55 (50%)				ag	0.0250	5	62.97	0.34
	6.25 (5%)	100	0	0.02	ag	0.0253	5.3	10.09	3.07
	25.02 (20%)				ag	0.0253	5.3	27.77	2.20
	62.55 (50%)				ag	0.0250	5	62.98	0.35
ab	6.25 (5%)	0	0	0.02	ab	0.0230	3	10.27	3.22
	25.02 (20%)				ab	0.0226	2.6	27.84	2.26
	62.55 (50%)				ab	0.0225	2.5	62.99	0.36
abg	6.25 (5%)	0	0	0.02	abg	0.0239	3.9	10.27	3.22
	25.02 (20%)				abg	0.0239	3.9	27.84	2.26
	62.55 (50%)				abg	0.0239	3.9	62.99	0.36
	6.25 (5%)	20	0	0.02	abg	0.0239	3.9	8.75	2.00
	25.02 (20%)				abg	0.0239	3.9	27.49	1.98
	62.55 (50%)				abg	0.0239	3.9	63.02	0.38
	6.25 (5%)	100	0	0.02	abg	0.0239	3.9	-	-
	25.02 (20%)				abg	0.0239	3.9	25.94	0.74
	62.55 (50%)				abg	0.0239	3.9	63.04	0.39

Table B.1 Continued

Fault Type	Fault Location (mi)	Fault Resistance ( $\Omega$ )	Fault Inception Angle (degree)	Actual Fault Inception Time (s)	Detected Fault Type	Calculated Fault Inception Time (s)	Time to detect (ms)	Calculated Fault Location (mi)	Fault Location % Error
abc	6.25 (5%)	0	0	0.02	abc	0.0247	4.7	15.09	7.06
	25.02 (20%)				abc	0.0239	3.9	32.40	5.91
	62.55 (50%)				abc	0.0250	5	65.58	2.42
	6.25 (5%)	20	0	0.02	abc	0.0252	5.2	16.36	8.08
	25.02 (20%)				abc	0.0251	5.1	39.46	11.55
	62.55 (50%)				abc	0.0249	4.9	-	-
	6.25 (5%)	100	0	0.02	abc	0.0255	5.5	-	-
	25.02 (20%)				abc	0.0255	5.5	-	-
	62.55 (50%)				abc	0.0255	5.5	-	-

2. Case 3

Table B.2 Summary of fault detection, classification and location (IEEE 118 bus test system: Case 3)

Fault Type	Fault Location (mi)	Fault Resistance ( $\Omega$ )	Fault Inception Angle (degree)	Actual Fault Inception Time (s)	Detected Fault Type	Calculated Fault Inception Time (s)	Time to detect (ms)	Calculated Fault Location (mi)	Fault Location % Error
ag	1.81 (5%)	0	0	0.02	ag	0.0262	6.2	-	-
	7.24 (20%)				ag	0.0257	5.7	7.41	0.47
	18.10 (50%)				ag	0.0256	5.6	18.07	0.07
	1.81 (5%)	20	0	0.02	ag	0.0245	4.5	-	-
	7.24 (20%)				ag	0.0245	4.5	7.44	0.55
	18.10 (50%)				ag	0.0251	5.1	18.07	0.08
	1.81 (5%)	100	0	0.02	ag	0.0255	5.5	-	-
	7.24 (20%)				ag	0.0256	5.6	7.35	0.33
	18.10 (50%)				ag	0.0257	5.7	17.91	0.50

Table B.2 Continued

Fault Type	Fault Location (mi)	Fault Resistance ( $\Omega$ )	Fault Inception Angle (degree)	Actual Fault Inception Time (s)	Detected Fault Type	Calculated Fault Inception Time (s)	Time to detect (ms)	Calculated Fault Location (mi)	Fault Location % Error
ab	1.81 (5%)	0	0	0.02	ab	0.0269	6.9	-	-
	7.24 (20%)				ab	0.0245	4.5	7.83	1.63
	18.10 (50%)				ab	0.0243	4.3	18.80	1.94
abg	1.81 (5%)	0	0	0.02	abg	0.0269	6.9	-	-
	7.24 (20%)				abg	0.0254	5.4	7.83	1.63
	18.10 (50%)				abg	0.0243	4.3	18.80	1.94
	1.81 (5%)	20	0	0.02	abg	0.0241	4.1	-	-
	7.24 (20%)				abg	0.0241	4.1	8.56	3.67
	18.10 (50%)				abg	0.0241	4.1	19.77	4.62
	1.81 (5%)	100	0	0.02	abg	0.0258	5.8	5.93	11.40
	7.24 (20%)				abg	0.0258	5.8	10.97	10.31
	18.10 (50%)				abg	0.0256	5.6	20.84	7.57
abc	1.81 (5%)	0	0	0.02	abc	0.0285	8.5	-	-
	7.24 (20%)				abc	0.0269	6.9	-	-
	18.10 (50%)				abc	0.0285	8.5	12.09	16.58
	1.81 (5%)	20	0	0.02	abc	0.0241	4.1	-	-
	7.24 (20%)				abc	0.0241	4.1	-	-
	18.10 (50%)				abc	0.0241	4.1	19.57	4.08
	1.81 (5%)	100	0	0.02	abc	0.0260	6	-	-
	7.24 (20%)				abc	0.0258	5.8	-	-
	18.10 (50%)				abc	0.0259	5.9	-	-



### 3. Case 4

Table B.3 Summary of fault detection, classification and location (IEEE 118 bus test system: Case 4)

Fault Type	Fault Location (mi)	Fault Resistance ( $\Omega$ )	Fault Inception Angle (degree)	Actual Fault Inception Time (s)	Detected Fault Type	Calculated Fault Inception Time (s)	Time to detect (ms)	Calculated Fault Location (mi)	Fault Location % Error
ag	0.88 (5%)	0	0	0.02	ag	0.0315	11.5	-	-
	3.54 (20%)				ag	0.0239	3.9	3.74	1.19
	8.85 (50%)				ag	0.0240	4	8.99	0.81
	0.88 (5%)	20	0	0.02	ag	0.0229	2.9	-	-
	3.54 (20%)				ag	0.0228	2.8	3.69	0.87
	8.85 (50%)				ag	0.0228	2.8	8.97	0.70
	0.88 (5%)	100	0	0.02	ag	0.0230	3	-	-
	3.54 (20%)				ag	0.0231	3.1	3.69	0.88
	8.85 (50%)				ag	0.0230	3	8.92	0.40
ab	0.88 (5%)	0	0	0.02	ab	0.0253	5.3	-	-
	3.54 (20%)				ab	0.0247	4.7		
	8.85 (50%)				ab	0.0247	4.7	10.41	8.83
abg	0.88 (5%)	0	0	0.02	abg	0.0246	4.6	-	-
	3.54 (20%)				abg	0.0242	4.2	4.20	3.76
	8.85 (50%)				abg	0.0244	4.4	8.97	0.73
	0.88 (5%)	20	0	0.02	abg	0.0214	1.4	-	-
	3.54 (20%)				abg	0.0210	1	3.90	2.09
	8.85 (50%)				abg	0.0214	1.4	8.72	0.72
	0.88 (5%)	100	0	0.02	abg	0.0214	1.4	-	-
	3.54 (20%)				abg	0.0274	7.4	4.02	2.76
	8.85 (50%)				abg	0.0273	7.3	8.48	2.06

Table B.3 Continued

Fault Type	Fault Location (mi)	Fault Resistance ( $\Omega$ )	Fault Inception Angle (degree)	Actual Fault Inception Time (s)	Detected Fault Type	Calculated Fault Inception Time (s)	Time to detect (ms)	Calculated Fault Location (mi)	Fault Location % Error
abc	0.88 (5%)	0	0	0.02	abc	0.0367	16.7	-	-
	3.54 (20%)				abc	0.0252	5.2	-	-
	8.85 (50%)				abc	0.0267	6.7	8.87	0.14
	0.88 (5%)	20	0	0.02	abc	0.0228	2.8	-	-
	3.54 (20%)				abc	0.0229	2.9	-	-
	8.85 (50%)				abc	0.0233	3.3	9.23	2.18
	0.88 (5%)	100	0	0.02	abc	0.0272	7.2	-	-
	3.54 (20%)				abc	0.0272	7.2	-	-
	8.85 (50%)				abc	0.0355	15.5	9.47	3.53

4. Case 5

Table B.4 Summary of fault detection, classification and location (IEEE 118 bus test system: Case 5)

Fault Type	Fault Location (mi)	Fault Resistance ( $\Omega$ )	Fault Inception Angle (degree)	Actual Fault Inception Time (s)	Detected Fault Type	Calculated Fault Inception Time (s)	Time to detect (ms)	Calculated Fault Location (mi)	Fault Location % Error
ag	7.71 (5%)	0	0	0.02	ag	0.0240	4	7.22	0.32
	30.86 (20%)				ag	0.0238	3.8	32.43	1.02
	77.15 (50%)				ag	0.0240	4	83.28	3.98
	7.71 (5%)	20	0	0.02	ag	0.0236	3.6	7.54	0.11
	30.86 (20%)				ag	0.0239	3.9	24.76	3.95
	77.15 (50%)				ag	0.0241	4.1	71.38	3.74
	7.71 (5%)	100	0	0.02	ag	0.0240	4	7.64	0.04
	30.86 (20%)				ag	0.0241	41	24.77	3.94
	77.15 (50%)				ag	0.0243	4.3	83.60	4.18

Table B.4 Continued

Fault Type	Fault Location (mi)	Fault Resistance ( $\Omega$ )	Fault Inception Angle (degree)	Actual Fault Inception Time (s)	Detected Fault Type	Calculated Fault Inception Time (s)	Time to detect (ms)	Calculated Fault Location (mi)	Fault Location % Error
ab	7.71 (5%)	0	0	0.02	ab	0.0260	6	-	-
	30.86 (20%)				ab	0.0250	5	29.31	1.00
	77.15 (50%)				ab	0.0248	4.8	77.52	0.24
abg	7.71 (5%)	0	0	0.02	abg	0.0260	6	10.20	1.62
	30.86 (20%)				abg	0.0232	3.2	29.31	1.00
	77.15 (50%)				abg	0.0232	3.2	77.52	0.24
	7.71 (5%)	20	0	0.02	abg	0.0230	3	10.63	1.90
	30.86 (20%)				abg	0.0232	3.2	31.77	0.59
	77.15 (50%)				abg	0.0233	3.3	76.46	0.44
	7.71 (5%)	100	0	0.02	abg	0.0242	4.2	6.63	0.70
	30.86 (20%)				abg	0.0244	4.4	31.76	0.59
	77.15 (50%)				abg	0.0249	4.9	74.15	1.94
abc	7.71 (5%)	0	0	0.02	abc	0.0254	5.4	-	-
	30.86 (20%)				abc	0.0240	4	32.56	1.10
	77.15 (50%)				abc	0.0238	3.8	74.77	1.54
	7.71 (5%)	20	0	0.02	abc	0.0235	3.5	-	-
	30.86 (20%)				abc	0.0236	3.6	32.64	1.16
	77.15 (50%)				abc	0.0239	3.9	76.39	0.49
	7.71 (5%)	100	0	0.02	abc	0.0245	4.5	-	-
	30.86 (20%)				abc	0.0246	4.6	32.65	1.16
	77.15 (50%)				abc	0.0249	4.9	74.00	2.04